Development of Innovative Mix Design for Road Construction in Hot Regions

by

Aioub GUHA

MANUSCRIPT-BASED THESIS PRESENTED TO ÉCOLE DE TECHNOLOGIE SUPÉRIEURE IN PARTIAL FULFILLMENT FOR THE DEGREE OF DOCTOR OF PHILOSOPHY
PH.D

MONTREAL, MAY 12, 2022

ÉCOLE DE TECHNOLOGIE SUPÉRIEURE
UNIVERSITÉ DU QUÉBEC

BOARD OF EXAMINERS

THIS THESIS HAS BEEN EVALUATED

BY THE FOLLOWING BOARD OF EXAMINERS

Mr. Gabriel Assaf, Thesis Supervisor
Department of Construction Engineering, École de Technologie Supérieure

Mr. Kamal Al-Haddad, President of the Board of Examiners
Department of Electrical Engineering, École de Technologie Supérieure

Mr. Constantine Katsanis, Member of Jury
Department of Construction Engineering, École de Technologie Supérieure

Mr. Luc Pellecuer, Member of External Jury
Department of Geography and Environmental Management, University of the West of England

Mr. Adnan SHIYAB, External Evaluator
Consultant Engineer

THIS THESIS WAS PRENSENTED AND DEFENDED

IN THE PRESENCE OF A BOARD OF EXAMINERS AND PUBLIC

ON MARCH 31ST, 2022

AT ÉCOLE DE TECHNOLOGIE SUPÉRIEURE

ACKNOWLEDGMENT

I would like to express my sincere gratitude to all who have helped me directly and indirectly in conducting this research. The contributions and support from the following people and institutions have been very valuable.

I am particularly grateful to my supervisor, Dr. Gabriel Assaf, for his help, support, and encouragement, upholding me through the journey of this dissertation. Also, I would like to thank the president of the board of examiners, Dr. Kamal Al-Haddad, and express my special gratitude to Dr. Constantine Katsanis, Dr. Adnan Shiyab and Luc Pellecuer the external members of the jury.

I would like to express my sincere thanks and indebtedness to my friends and colleagues in the construction engineering department at École de Technologie Supérieure, such as Fathi Madwi and Talal Emhadi. I would also like to thank all the École de Technologie Supérieure asphalt lab technicians, especially Mr. Francis Bilodeau and Mr. Sylvain Bibeau, for their wise advice and unlimited help.

Finally, I would also like to express my sincere thanks to my mom, wife, and the rest of my family for their continued support, encouragement, and patience throughout the duration of this study. This work was only possible because of the kindness and assistance of the many individuals mentioned above and more.

Développement d'une conception de mélange innovante pour construction de route dans les zones chaudes

Aioub GUHA

RÉSUMÉ

La déformation permanente des enrobés bitumineux se manifeste principalement sous la forme d'ornières, et représente un des problèmes majeurs affectant les chaussées flexibles, particulièrement dans les pays chauds. Elle est grave car elle met en cause la sécurité des usagers. Elle est conditionnée par la résistance et la déformation ou la viscosité des liants bitumineux constitutifs utilisés aux températures élevées qui prévalent. Elle est accentuée dans les pays très chauds où la température de l'air peut dépasser 45°C et l'enrobé atteindre 70ºC. Le recours au bitume à pénétration 60/70 (B60/70), qui est un bitume relativement dur, ne se comporte pas bien aux températures élevées sur les routes subissant le passage répété des poids lourds. Ceci est principalement dû au fait que le B60/70 est basé sur la résistance à la déformation du bitume à 25°C et non à 45ºC voire plus. Par ailleurs, les chaussées souples dans ces régions chaudes développent aussi des bourrelets causés également par le trafic, une viscosité insuffisante du bitume aux températures de service et/ou une angularité des agrégats qui est déficiente et une granulométrie trop fine. Dans plusieurs pays d'Afrique du Nord et d'Afrique subsaharienne tels que la Libye, mais aussi l'Algérie, le Mali, le Burkina Faso, le Sénégal, le Tchad, le Bénin, la Mauritanie, le Burundi et le Mozambique, la température en surface des enrobés peut atteindre 70°C, les matériaux disponibles près de l'alignement sont souvent très fins et arrondis par le vent ce qui accentue encore plus ces manifestations, rendant les administrations routières totalement incapables à y faire face à des coûts raisonnables, c'est-à-dire qui permettent de dégager une rentabilité économique.

C'est dans le but de contribuer à solutionner cette problématique que s'inscrit cette recherche notamment en évaluant l'intérêt de recourir à de très petites quantités de ciment Portland ordinaire (OPC) et aux fibres de cellulose (CF) pour améliorer la résistance à la déformation ou la rigidité des enrobés bitumineux à base de bitume B60/70 tout en ayant recours à des granulats fins, non conformes, mais néanmoins aisément accessibles pour la construction de routes. On observe en effet que ce recours à l'OPC et aux CF améliore sensiblement la stabilité et accroît la résistance à la déformation de l'enrobé à ossature fine à des températures élevées. Pour apprécier les effets de l'OPC sur les performances des enrobés fins dans les climats chauds, quatre pourcentages différents d'OPC (0 %, 2 %, 4 % et 6 %) sont utilisés comme substituts au filler dans trois mélanges différents. Par ailleurs, les mélanges CF ont également été testés avec trois pourcentages différents de CF (0,25 %, 0,5 % et 0,75 %) utilisés comme fillers. Les performances des mélanges OPC et CF sont évaluées à l'aide de la presse à compactage giratoire Superpave, l'analyseur d'orniérage de chaussée et l'essai de traction indirecte (ISTM). Les tests ITSM ont été réalisés à - 5°C, 10°C, 25°C pour simuler les conditions les plus défavorables dans des zones désertiques et des hauts plateaux de l'Afrique du Nord, et le test de l'analyseur d'orniérage a été effectué à 60°C pour simuler les températures les plus défavorables observées en Afrique Sub-Saharienne.

Il ressort de ce plan expérimental que les mélanges bitumineux renfermant des pourcentages plus élevés d'OPC, *utilisés à titre de filler*, sont significativement plus résistants à l'orniérage selon l'analyseur d'orniérage, tout en étant plus faciles à poser selon la presse à cisaillement giratoire. Ces résultats expérimentaux prometteurs portent à conclure que le ciment peut représenter une alternative intéressante qui augmente la stabilité du mélange à ossature même fine, sans en affecter la facilité de pose ou la maniabilité, et réduit du fait même l'épaisseur en enrobé qui est requise comme établi à l'aide d'une analyse structurale analytique, en raison du module de rigidité plus élevé qui en résulte. Cela a des implications importantes sur les coûts dans les zones rurales chaudes, avec de rares carrières pour disposer de granulats de bonne qualité puisque des granulats arrondis et non conformes donnent des résultats de performance probants, mais aussi en réduisant l'épaisseur de l'enrobé bitumineux, ramenant du fait même les coûts à des niveaux un peu plus raisonnables, plus proches des économies générées par la réduction des coûts du transport résultant d'une route en meilleur état, plus longtemps.

Mots-clés: Enrobé à chaud, ciment Portland, fibre de cellulose, charge, B60/70, stabilité, rigidité, ornières, compacteur giratoire et analyseur d'orniérage de chaussée, analyse structurale.

Development of Innovative Mix Design for Road Construction in Hot Regions

Aioub GUHA

ABSTRACT

Permanent deformation in the form of rutting and bleeding is one of the major mechanisms of deformation affecting asphalt pavements, with severe safety and comfort consequences and substantial associated economic cost and marginal pollution. This is a serious concern exacerbated in hot countries whereby the resistance to deformation or viscosity of the bitumen binders, at those prevailing extremely hot in-service temperatures, drops multifold. In hot countries, air temperatures can exceed 45°C and the asphalt mix may reach 70°C. Even in the construction of primary roads, bitumen 60/70 (B60/70), which is a relatively low-grade and hard bitumen, continues to be used for Hot Mix Asphalt (HMA) construction because of the lack of availability of Performance Grade Superpave asphalts. Asphalt pavement roads therefore develop extreme deformations in the form of rutting because the B60/70 is primarily based on the resistance to deformation at 25°C. As a result, flexible pavements in hot regions namely those subject to heavy loads, often show substantial rutting and shoving. These distresses are caused by heavy traffic, an inadequate viscosity of bitumen at these in-service temperatures, a poor fine gradation with less coarse aggregates and/or an insufficient aggregate angularity.

In several countries of North Africa and Middle East: 1) the surface temperature of asphalt can reach 70°C, and 2) the materials available near the alignment are often very thin and rounded by wind erosion, which accentuates rutting and shoving. Road agencies have difficulties coping with these issues at a cost that makes economic sense for funding.

This research investigates the use of Ordinary Portland Cement (OPC) and cellulose fiber (CF) as a filler substitute to improve the resistance to deformation or rigidity of asphalt concrete mixes made with B60/70 bitumen and readily available low quality, fine and rounded, aggregates. This amended mixture increases the pavement's stability and resistance to high temperatures. To establish the effects of OPC on the performance of asphalt mixtures in hot climates, four different percentages of OPC (0%, 2%, 4% and 6%) are used as filler substitutes in three different mixes. CF mixes were also tested with three different percentages of CF (0.25%, 0.5%, and 0.75%) used as filler. The performance of the OPC and CF mixes are assessed using the Superpave Gyratory Compactor to ensure easiness to place, the Asphalt Pavement Rutting Analyzer to ensure lack of rutting and The Indirect Tensile Stiffness Modulus (ITSM) to prevent in-service cracking. ITSM tests were conducted at - 5°C, 10°C, 25°C to simulate adverse conditions in desertic or mountainous regions in the Middle East and North Africa and the rutting analyzer test was conducted at 60°C to simulate adverse hot temperatures in the region.

Findings indicate that mixtures containing higher percentages of OPC as a filler are significantly more resistant to rutting as found with the rutting analyzer, while remaining easy to place as found with the gyratory compactor. These experimental results also show that

Portland Cement Filler Asphalts (PCFA) represents a more stable alternative to conventional asphalts that also reduces thickness requirements as demonstrated with mechanistic pavement design model, because of the higher resulting modulus of rigidity. This has important cost implications in hot rural areas with scarce quarries for good quality aggregates, because of the increased stability and therefore performance and the reduced thicknesses, both of which reduce the construction and the maintenance cost of the road, to levels more in line with the savings generated by the reduction in transport cost resulting from a road in better condition.

Keywords: Hot Mix Asphalt, Portland cement, cellulose fiber, filler, B60/70, stability, rigidity, rutting, gyratory compactor and the pavement rutting analyzer, structural analysis.

TABLE OF CONTENTS

Page

INTRODUCTION 1

CHAPITRE 1 BACKGROUND AND LITERATURE REVIEW 3
1.1 Flexible Pavement...3
1.1.1 Flexible Pavements Structure 3
1.2 Improvements of HMA Performance 5
1.2.1 HMA Additives 5
1.2.2 Benefits of Additives in HMA 7
1.3 Cracks in Cement Asphalt Pavements 7
1.4 HMA Designs and Methods...8
1.4.1 The Marshall Method (MM) 8
1.4.2 Hveem Method 9
1.4.3 The Superpave Method (SPM).. 9
1.4.4 LC Method 11
1.5 Transition from Marshall to Superpave Mix Design Methods. 11
1.6 Pavement Performance 13
1.7 Typical Pavement Stresses...15
1.7.1 Stresses Induced by Axle Load 15
1.7.2 Climatic Condition Stress... 16
1.7.3 Bitumen Behaviour at High Temperatures.. 17
1.7.4 HMA Properties and Viscoelasticity 18
1.8 Literature Review of Previous Applications of using additives in HMA 19

CHAPITRE 2 RESEARCH FOCUS AND OBJECTIVES 25
2.1 Introduction...25
2.2 Problem Statement...26
2.3 Research Objectives..27
2.4 Research Methodology 28
2.4.1 introduction 28
2.4.2 Determining the Optimal Ratio of the Fillers.. 29
2.4.2.1 Ordinary Portland Cement 29
2.4.2.2 Cellulose Fiber 29
2.4.3 Methodology Framework 29
2.5 Research Significance...30
2.6 Research Outline..31

CHAPITRE 3 EFFECT OF PORTLAND CEMENT AS A FILLER IN HOT-MIX ASPHALT IN HOT REGIONS...33
3.1 Introduction...34
3.2 Background...34
3.3 Experimental Details and Material 38
3.3.1 Materials 38

3.4 Experimental Procedure 39
3.4.1 Superpave Gyratory Compaction Test (SGC) 39
3.4.2 Rutting Test 40
3.5 Results and Discussion 41
3.5.1 Results of the Gyratory Compaction Test 41
3.5.2 Rutting Test Results 44
3.6 Conclusion 46

CHAPITRE 4 EFFECTS OF DIFFERENT FILLERS ON PAVEMENT DEFORMATION OF HOT MIX ASPHALT IN HOT CLIMATES 47
4.1 Introduction 48
4.2 Background 49
4.3 Experimental Details and Materials 51
4.3.1 Materials 51
4.4 Experimental Procedure 53
4.4.1 Rutting test (Asphalt Pavement Rutting Analyzer Test) 53
4.4.2 The Indirect Tensile Stiffness Modulus Test 54
4.5 Results and Discussion 54
4.5.1 Rutting Test Results 54
4.5.2 Results of ITSM Test Modulus 57
4.6 Conclusion and Limitations 58

CHAPITRE 5 USING CEMENT AS FILLER TO ENHANCE ASPHALT MIXES PERFORMANCE IN HOT REGIONS 61
5.1 Introduction 62
5.2 Background 62
5.3 Experimental Procedure and Material 66
5.3.1 Materials 66
5.3.1.1 Aggregate 66
5.3.1.2 Portland Cement 67
5.3.1.3 Bitumen 68
5.4 Experimental Procedure 68
5.4.1 Wheel Tracking Tester (WTT) 68
5.4.2 The Indirect Tensile Stiffness Modulus (ITSM) Test 69
5.4.3 WinJulea Software 70
5.5 Results and Discussion 70
5.5.1 Results of The Rutting Tests 70
5.5.2 Results of the ITSM Tests 72
5.5.3 Increase of Pavement File 72
5.5.4 Cost Analysis 75
5.5.4.1 Calculate Asphalt Quantity 75
5.5.4.2 Materials Cost 76
5.5.4.3 Costs of Traffic Signs 77
5.6 CONCLUSION 77

CONCLUSION 79

RECOMMENDATIONS 81

APPENDIX I REPRESENTING COLLECTED ROAD CONDITION DATA WITH CHERNOFF FACES FOR EVALUATION OF PAVEMENT CONDITIONS 85

APPENDIX II STRUCTURAL ANALYSIS WITH WINJULEA 103

BIBLIOGRAPHY…..139

LIST OF TABLES

Page

Table 3.1 Chemical composition of ordinary Portland cement 39

Table 3.2 Chemical properties of the binder B60/70 39

Table 3.3 Specifications and limitations according to MTQ 4202, ESG10....40

Table 4.1 Physical and Chemical properties of modified CF 52

Table 4.2 Chemical composition of OPC 52

Table 4.3 Chemical properties of the binder B60/70 53

Table 4.4 Rutting Test Results....55

Table 5. 1 Chemical composition of OPC 67

Table 5. 2 Chemical composition of bitumen B60/70 68

Table 5. 3 Rut depth deformation for each sample....71

Table 5. 4 Elastic modulus for each asphalt concrete mix....73

Table 5. 5 Cost and quantity breakdown for control mix to build 1 km of asphalt materials....76

Table 5. 6 Cost breakdown of road pavement materials using Winjulea Software.....76

Table AI. 1 The levels of quality for each pavement condition factor 87

Table AI. 2 Pavement rating condition based on the PASER scale....93

Table AI. 3 Pavement rating condition ten-point scale....100

Table AII. 1 Mechanistic analysis....103

Table AII. 2 Results Number of allowable repetitions (Nf) in compression for 75 mm of AC....104

Table AII. 3 Number of allowable repetitions (Nf) in compression for 100 mm of AC 105

Table AII. 4 Number of allowable repetitions (Nf) in tension for 75 mm of AC 105

Table AII. 5 Number of allowable repetitions (Nf) in tension for 100 mm of AC 105

LIST OF FIGURES

Page

Figure 1. 1 Cross-section of flexible pavement layers..4
Figure 1. 2 Zone map of required PG in Libya..12
Figure 1. 3 Map of temperature zone for PG in Iraq 13
Figure 1. 4 Conditions affecting HMA performance...14
Figure 1. 5 HMA's stress distribution at critical interface points.................................16
Figure 1. 6 Environmental impact on pavement surfaces...17
Figure 1. 7 Bitumen behaviour at high temperatures..18
Figure 1. 8 Behaviour domains for HMA..19

Figure 2. 1 Flow charts for laboratory works process 30

Figure 3. 1 Aggregate mix gradation 38
Figure 3. 2 French laboratory system 41
Figure 3. 3 Gyratory Compactor (SGC) test for Va...42
Figure 3. 4 Gyratory Compactor (SGC) test for VFA 42
Figure 3. 5 Gyratory Compactor (SGC) test for VMA...43
Figure 3. 6 Analysis of the Gyratory Compactor (SGC) test for Va 43
Figure 3. 7 Analysis of the Gyratory Compactor (SGC) test for VFA 44
Figure 3. 8 Analysis of the Gyratory Compactor (SGC) test for VMA..........................44
Figure 3. 9 Average rut depth for each type of design mix 45

Figure 4. 1 Aggregate Gradation 51
Figure 4. 2 Rutting Test Results 56

Figure 4. 3 The Average rutting depth for each mix....56
Figure 4. 4 Average ITSM tests for each type of cement design mix 58

Figure 5. 1 Aggregate gradation curves of the mix 67
Figure 5. 2 WTT specimen position 69
Figure 5. 3 Rutting tests performed at 60°C, rutting depth values for each mix 71
Figure 5. 4 Average ITSM test results for all cement mixtures....72
Figure 5. 5 Number of allowable repetitions of an 8-ton axle load for all 74
Figure 5. 6 Number of allowable repetitions of an 8-ton axle load for all 74

Figure AI- 1 Examples Chernoff faces....91
Figure AI- 2 Facial variations....91
Figure AI- 3 Example of shapes to each feature according to the factors in Table 3....98
Figure AI- 4 Examples of Chernoff faces showing the factors 99

Figure AII- 1 Asphalt Institute Equation to determine structural....104
Figure AII- 2 Asphalt Institute Equation to determine structural....104

LIST OF SYMBOLS

AASHTO	American association of state highway and transportation officials
ASTM	American society for testing and materials
AC	Asphalt concrete
ACP	Asphalt concrete pavements
APRA	Asphalt pavement rutting analyzer
B60/70	Penetration grade
CEI	Construction energy index
CF	Cellulose fiber
CFM	The Chernoff face method
CFPCS	Chernoff face pavement surface condition scale
DMA	Dynamic mechanical analyzer
E	Dynamic modulus
ESG10	Called semi-grouted asphalt
FAA	Fine aggregate angularity
FRT	French rutting tester
FHWA	Federal Highway administration (US)
GDP	Gross domestic product
GIS	Geographic information system
HMA	Hot mix asphalt
HMAC	Hot mix asphalt concrete
IAPST	Index of aggregate particle shape and texture
IDT	Indirect tensile test
IRI	International roughness index
ITS	Indirect tensile strength
ITSM	Indirect tensile strength modulus
LCPC	Laboratoire Central des Ponts et Chaussées
LSP	Lime stone powder
LVE	Linear viscoelastic
LVRs	Low-volume roads
LTPP	Long-term pavement performance

LPC	Laboratory slab compactor
M-E	Mechanistic-empirical
MEPDG	The mechanical-empirical pavement design approach
MM	Marshall Method
MTQ	Ministère des Transports de Québec
NCHRP	National cooperative highway research program
OPC	Ordinary Portland Cement
OBC	Optimum bitumen content
PCFA	Portland cement filler asphalts
PG	Performance grade
RCA	Recycled aggregate concrete
PCI	Pavement condition index
PEM	Pavement evaluation methods
SEM	Scanning electron microscope
SGC	SUPERPAVE gyratory compaction
SHRP	The strategic highway research program
SIP	Stripping inflection point
SM	Stiffness modulus
SMA	Stone-matrix asphalt
SPM	Superpave Method
SSA	Specific surface area
SUPERPAVE	Superior performing asphalt pavements
TSR	Tensile strength ratio
TTSP	The time-temperature superposition principle
VA	Virgin aggregates
VB	Percent bitumen volume
V_a	Air voids content
VFA	Voids filled with asphalt
VMA	Voids mineral aggregate
UNDP	United nations development programme.

INTRODUCTION

Permanent deformations in the form of rutting and bleeding is one of the major mechanisms of deformation affecting asphalt pavements, with severe safety and comfort consequences and substantial associated economic cost and marginal pollution. This is a serious concern exacerbated in hot countries whereby the resistance to deformation or viscosity of the bitumen binders, at those prevailing extremely hot in-service temperatures, drops multifold. In hot countries, air temperatures can exceed 45°C and the asphalt mix may reach 70°C. Even in the construction of primary roads, bitumen 60/70 (B60/70), which is a relatively low-grade and hard bitumen, continues to be used for Hot Mix Asphalt (HMA) construction because of the lack of availability of Performance Grade Superpave asphalts. Asphalt pavement roads therefore develop extreme deformations in the form of rutting because the B60/70 is primarily based on the resistance to deformation at 25°C. As a result, flexible pavements in hot regions including those in urban cities, often show substantial rutting and shoving. These distresses are mostly caused by traffic, an inadequate viscosity of bitumen at these in-service temperatures, and/or an insufficient aggregate angularity.

Over the last several decades, there have been many techniques to design better-performing asphalt pavement mixtures. A popular method is to add fillers to improve the performance of HMA basically to only regulate the voids content. A low voids content results in bleeding of the expanding bitumen to the surface when subject to high temperatures. Reversely, a high void content results in subsequent compaction and rutting in the wheel paths. In hot and arid countries where temperatures often exceed 45°C, HMA is still often made with B60/70. Although there are better Performance Grade bitumen, these are not always available (Almadwi & Assaf, 2017). Fillers that can improve B60/70 HMA performance and reported in the literature include brick powder, polymers, mineral fibers, and OPC. Without these additive materials, or alternatives such as higher-grade performance bitumen, asphalt concrete in hot climates undergoes permanent deformation, such as rutting and fatigue (Willway *et al.,* 2008). The effects of any given filler depend on the HMA's characteristics and how it relates to climatic conditions and axle loads. Traditionally, mineral fillers have been added to dense-graded HMA paving mixtures to fill and reduce the voids in both the aggregate skeleton and the mix (Prowell, Zhang, & Brown, 2005) . Fillers also have other functions, such as contributing to mixture cohesion; increasing the bitumen density, stability, and toughness; and finally, working as active fillers. Importantly, the pavement's brittleness and tendency to crack while in service grows as the filler content increases (Sterling 2011). Other studies have found that mineral fillers improve the HMA's overall stiffness and strength (Aljassar, Metwali, & Ali, 2004). Likewise, long-term durability and stability are important so that the HMA resists permanent deformations, such as the ones mentioned above (Lesueur, Petit, & Ritter, 2013). In this context, this research investigates the use of OPC and CF as additive materials to HMA made using B60/70 and also with fine, poorly graded and rounded aggregates (between 0 and 10 mm) that are very common and readily available but not suited for road construction.

The present study's overarching aim is to increase HMA stability and resistance to permanent deformation in hot environments with conventional bitumen and poorly graded and round aggregates. HMA was prepared for each of the two fillers, OPC and CF, each with three different filler percentages. The percentages of the two fillers were different for each type of mix. OPC was added to constitute 2%, 4% and 6% of the total weight of the HMA. Conversely, CF was added to make up 0.25%, 0.5% and 0.75% of the mixtures. As a control mixture, there was also HMA control samples that were prepared with no filler. Besides varying filler percentages, the samples were the same. The resulting seven samples were evaluated with the Indirect Tensile Stiffness Modulus Test (ITSM) to assess strength and cracking potential, and the Asphalt Pavement Rutting Analyzer Test (henceforth, the rutting test) to establish the effects of OPC and CF on HMA performance in hot regions.

CHAPITRE 1

BACKGROUND AND LITERATURE REVIEW

1.1 Flexible Pavement

One of the broadest infrastructure materials used in road building is hot mix asphalt (HMA). HMA is a polyphase mixed material made of a viscoelastic asphalt binder, a high volume fraction of uneven rigid aggregate particles namely crushed stone, sand mineral filler, gravel, and sometimes slag, and a minor quantity of air voids (Nega et al., 2013; Gopalakrishnan & Kim 2011). About 95% of the HMA mixture's weight is composed of aggregates and 5% of asphalt binder. These components contribute to HMA's multifaceted performance via their various properties. The binder properties are plastic and viscoelastic, which vary according to diverse conditions, such as load applications, aging, and temperature (With et al., 2001; Nega et al., 2013), which in turn affect the HMA's mechanical behavior.

The performance and mechanical properties of HMA therefore depend on loading intensity and rates, as well as air temperature. Over time and through exposure of the temperature sensitive binder to hot temperatures, HMA can show damage in the form of rutting, which has the potential to self-heal during rest periods from traffic loading (Lytton 2000; Nega 2015) (Kim et al., 1997). HMA's complex behavior under different environmental and traffic loading conditions complicates the process of modelling the properties of an HMA mixture, especially regarding pavement distress, such as cracking and rutting.

1.1.1 Flexible Pavements Structure

This section describes the standard layers of a flexible pavement. The first layer or top layer is directly in contact with the traffic, and its major role is to absorb most of the load before passing it on to the next layer. It is the most expensive, typically consisting of an asphalt binder, a crushed aggregate, and a filler to adjust the voids content. This layer may be composed of two sub-layers, one asphalt wearing course sub-layer and one asphalt base course sub-layer.

The underlying granular base course, approximately 150 to 300 millimeters in thickness, provides for drainage and ensures the transfer of stresses to the lower subbase layer. Traditionally, coarse aggregates are used to create a strong base course, reducing the thickness of the top asphalt surface/s. Having less asphalt concrete and a stronger base course can reduce both the pavement costs and the likelihood of structural rutting damage. However, various recent studies demonstrate that, even more than the surface course, the base course needs special care and design to improve its longevity and endurance against fatigue (Olard 2012) (Garfield 1992). A cross-section showing the layers of an asphalt pavement structure is illustrated in Figure 1.1.

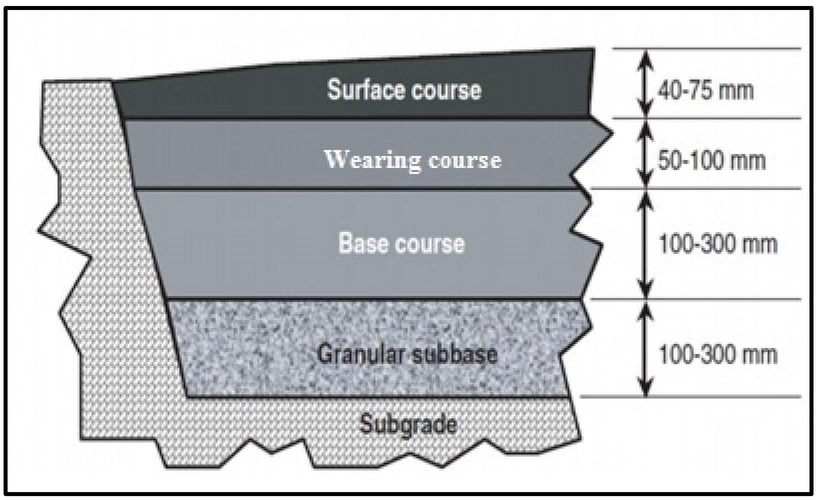

Figure 1. 1Cross-section of flexible pavement layers
Taken from Jenks et al. (2011)

The layer thicknesses of a flexible pavement are calculated using the road's environmental conditions and traffic volume over a specific time period. There are various methods for designing flexible pavements, such as the mechanical-empirical flexible pavements design approach (MEPDG). NCHRP 1-37A introduced this approach based on mechanistic-empirical (M-E) prediction of the pavement response (cracking, rutting, etc.) resulting from the rheological properties of the materials, the projected environmental conditions and the traffic load spectrum over the life of the pavement. Structural responses are obtained from strains, deflections, and stresses that are measured in a laboratory or through field-performance data.

Field performance data relies on the material properties, loading characteristics, and environmental conditions. As a complement, the empirical calibration, between model predictions and real observations considers these structural responses as inputs to calculate performance predictions, such as rutting and fatigue (Madwi 2020). The MEPDG model's accuracy relies on the quality of the input data and the empirical models' calibration, which is based on field performance. Therefore, the MEPDG design is a two-stage process. One directly predicts distress and the other adjusts them to match reality through calibration to field-measured distress (Carvalho and Schwartz 2006).

1.2 Improvements of HMA Performance

Many regions in the world have little access to appropriate pavement materials. One common way to compensate is to use additives to increase or maintain strength and flexibility over time to meet target values with ideal performance-based laboratory tests. These tests simulate in-service performance in order to select the HMA formula that will most likely perform best. Another imperative is to follow proper construction techniques to meet the desired engineering properties established in the laboratory, including for different load applications and temperature ranges.

1.2.1 HMA Additives

To extend pavement lifespans, recent technological advancements in HMA materials have rightly so focused on mitigating pavement distress (e.g., moisture damage, permanent deformation, low-temperature or fatigue cracking) (Preciado et al., 2017). Pavement technologists have developed numerous HMA additives that attempt to mitigate these aforementioned distress types (Kök and Çolak 2011; Preciado et al., 2017). Various studies have recently evaluated modifications to the mix design formula that improves asphalt mixtures' performance (Kök and Çolak 2011; Isacsson and Lu 1995), particularly stiffness, strength, temperature sensitivity and resistance to aging.

Additives can be combined directly within the HMA, either as a binder modifier via a wet method, or mixed with the aggregates using a dry method (Zhu, Birgisson, and Kringos 2014). The most common additives for improving HMA stability, moisture susceptibility, resistance to rutting, and other mechanical properties, are fibres, fly ash, hydrated lime, polymers, brick powder, and OPC. Of the available polymers, elastomer polymers are the most popular choice for improving HMA performance (Preciado et al., 2017).

Moreover, the two most common modifiers used to enhance the fundamental properties of asphalt binders are polymer-based additives which properties are similar to asphalt binders (Kanitpong & Bahia, 2005). Kök and Çolak (2011) show that the overall performance of polymer-modified mixtures is better than those of mixes modified with antistripping additives and mixes that are unaltered. Polymers improve asphalt binders' cohesion, adhesion, and rutting performance (Kanitpong & Bahia, 2005). For many decades, polymer-based additives have been used around the world to bolster HMA performance. It is indeed less common to use fibres to improve resistance to cracking and increase stability (i.e., lessen rutting) in dense-graded HMAs. Porous asphalt mixes and open-graded friction courses perform better with fibres (Watson & Jared 1998; McDaniel, 2015).

Waxes (e.g., sasobit and asphaltan) and fatty amides (e.g., emulsifiers and surfactants) are the typical choices for organic additives, since they reduce the binder's viscosity to above its melting point. Chemical additives, such as Rediset and Evotherm designed by Astec Industries, do not decrease binder viscosity but do enhance the aggregates' coating by lowering the surface energy of the inner friction and the aggregate/binder interface (Caputo et al., 2020; Pereira et al. 2018). Similar to organic additives, binder foaming techniques reduce binder viscosity, but for a shorter time. Foaming techniques are achieved by introducing tiny portions of water to the hot binder (bitumen), resulting in bitumen expansion and sizeable amounts of foam. There are two types of foaming techniques: a) water-based processes that entail the use of injection foaming nozzles; and, b) using water-bearing additives, such as minerals (e.g., zeolites) (Caputo et al., 2020; Diab, et al., 2016).

1.2.2 Benefits of Additives in HMA

HMA additive materials produce various benefits (McDaniel, 2015), including:

- Improvement of the tensile strength leading to better cracking resistance due to fatigue or oxidation,
- Reduction in the air voids percentage leading to lesser rutting in service,
- Increased lateral restraint of the HMA, resulting in improved shear strength and therefore rutting,
- Increased resistance to abrasion,
- Higher asphalt content requirements which increase pavement durability, and
- A longer service life, potentially lowering maintenance and therefore life-cycle costs.

1.3 Cracks in Cement Asphalt Pavements

Pavement that is cement-stabilized has a base course treated with cement. Such pavement also has a bituminous wearing surface with a thickness of approximately 38 mm to 127 mm (1.5 to 5 inches) that is either a hot mix asphalt layer or surface treatment. One or more of the following modes can cause surface cracks:

1. Fatigue cracks at the lowest area of the pavement's surface, which ultimately spread to the top.
2. Cracks due to asphalt aging and thermal cracks that start at the surface, breaking the pavement layer (excluding failure near shrinkage cracks). Extensive fatigue along the soil-cement asphalt wheel path (item 4, below) is rarely an obstacle.
3. Thermal (environmental) cracks and shrinkage deriving from the base made of cement.
4. Fatigue cracks caused during heavy truck traffic loads are established in the cement base (Portland Cement Association (PCA) 2003).

Bituminous surfacing cracks are often linked with fatigue (item 1) and thermal aging and shrinkage (item 2). Notably, there is extant literature on both features of surface cracking on asphalt.

In cemented material, shrinkage cracks are inevitable, either because of change to the ambient temperature or drying. Drying is caused by moisture loss and/or “self-desiccation” (moisture reduction caused by hydration of cement), triggering the cement-stabilized layer to contract. Some have asserted that shrinkage cracking is an untreated soil-cement trait, suggesting that the cement creates a hardened base with considerable tensile and flexural strength. However, if the cracks grow thicker, pavement degradation along the cracks causes local failure, an irregular traveling surface, and layer delamination (For et al. 1999).

Recent studies reinforce the phenomenon of local failure. Dallas Little et al. (1995), for example, studied several heavily stabilized bases’ functioning. They concluded that the sections’ performance was determined based on the shrinkage quantity of soil-cement asphalt. As a crack widens, more water penetrates the pavement, increasing the subsequent draining of the material underneath. Additional cracks develop as the load-induced stresses grow along the edge of the crack, most often down the wheel path longitudinally (For et al. 1999).

1.4 HMA Designs and Methods

Roads are usually designed and constructed to be in use for a minimum of 20 years. To meet these criteria, various HMA design methods are used worldwide, such as Marshall Method (MM), Hubbard’s field, Asphalt Institute Triaxial, Hveem mix design, and Superpave methods. In particular, the Marshall and Superpave mix design methods are the most widely practised.

1.4.1 The Marshall Method (MM)

One of the most widely used mix design methods is the MM. Bruce Marshall developed it in the late 1930s for the Mississippi Highway Department. The MM’s standards provide engineers a procedure for choosing the optimum asphalt content for particular aggregate blends for a mix. This process ensures that the combined blend and mix meet the desired properties of flow, stability, and density. There are clear steps for the preparation procedure that require mixing, compacting, and heating mixtures of asphalt and aggregate. After being prepared, density-void analysis and a stability-flow test are conducted on the samples. The following detailed standards define MM: “ASTM D 1559 Marshall stability and flow of asphalt concrete", "ASTM D2726 Bulk Specific Gravity of Compacted Bituminous Mixtures", and "ASTM D1559-Resistance to Plastic Flow of Bituminous mixtures using Marshall Apparatus".

The MM enables mix designers to choose an Optimum Bitumen Content (OBC) for particular asphalt-aggregate mixture design formulations where stability and flow are met. In most cases, when using the MM, the field specifies the compaction of 95% or greater of the maximum laboratory value. Furthermore, due to the control sample limitations in the lab and the unlimited compactive effort available in the field, reaching a maximum density of over 100% is possible. Unfortunately, if the asphalt concrete is compacted beyond 100%, the air is entirely removed from the pavement. When this happens, the bitumen will bleed upwards when the asphalt expands under hot temperatures due to the lack of air voids.

1.4.2 Hveem Method

Since the 1920s, California has used the Hveem Method, named after F.N. Hveem, who developed it at the California Division of Highways (ASTM D1561). It basically requires the same equipment as the MM to characterize asphalt mixtures. There are three major principles in this method. The first is that the surface of the aggregate determines its stability. The second is that the aggregate's texture, surface area, porosity, and the bitumen's stiffness are all function of the OBC. The third is that, when possible, to preserve sample stability and avoid asphalt bleeding, the mix should have at least 4% air voids in the mix (V_a). Moreover, using a variety of bitumen content, the kneading compaction test (ASTM D1561) helps ready samples to be tested in a lab. Finally, the compaction method simulates density that represents axle loads.

1.4.3 The Superpave Method (SPM)

Superior Performing Asphalt Pavements are referred to as "Superpave." A product of the Strategic Highway Research Program, Superpave is a new and comprehensive asphalt mix design and analysis system (SHRP 1994; 1987). Since 1993, when the SHRP research was completed, most highway agencies and the asphalt industry worldwide have employed significant efforts in using Superpave in their asphalt mixture designs.

Superpave represents various improvements to asphalt mix design. It is an enhanced, performance-based system for specifying mineral aggregates and asphalt binders. It also develops the processes of asphalt mixture design and pavement performance analysis. The system has an asphalt binder specification using physical property tests of the new binder; various aggregate specifications and tests; a design and analysis system for hot mix asphalt (HMA); and computer software that combines the components of the system. As it is standard with all design processes, it is still necessary to obtain field control measurements to ensure the field-produced mixes match the laboratory design. The Superpave binder specification and mix design procedures integrate various design criteria, test equipment and methods. The SHRP-developed specifications, test methods and practices of AASHTO, ASTM, and other test methods are used in the Superpave system (e.g., ASTM D 4123 for ISTM and AASHTO TB 63 for rutting).

Presently, the SPM is geared to meet particular aggregate, volumetric, and asphalt binder properties. Some examples of these properties include 1) aggregate gradation control limits, 2) asphalt binder performance grading (PG) specification, 3) voids filled with asphalt (VFA), 4) gradation distribution ranges, 5) voids in mineral aggregate (VMA), and 6) asphalt mix air voids (V_a). It influences almost each one of the HMA's important properties, including stability, permeability, stiffness, durability, workability, and resistance to fatigue, friction, and moisture damage (Xiao 2009).

A leading consideration in SPM is gradation. In particular, the appropriate gradation of an aggregate ensures that the maximum size of the aggregate is neither too small nor too large and that the grain distribution is within a certain range. Once the VMA requirements are satisfied and a suitable aggregate skeleton is achieved, the SPM can correctly limit aggregate gradations for use in HMA mixes. To improve previous HMA design methods, the SPM has various goals, including 1) recognition of climatic and traffic conditions, 2) enhanced aggregate and asphalt binder selection and evaluation, and 3) superior mix design volumetric approaches (Obadat 2021). The dissimilarities between the MM and the SPM are mainly regarding the materials selection process, the specimen dimensions, the compaction method, the specifications and the void analysis approach. One of SPM's functions is to produce higher quality asphalt mixes by addressing the rutting and transverse cracks that occur when using the Hveem Method and the MM (Kakrasul 2015).

1.4.4 LC Method

The *Ministère des Transports du Québec* developed the LC method, which was later perfected at the *Laboratoire des Chaussées*, explaining its initial name, "*Méthode LC*." LC method's design was informed by both the SPM and France's *Laboratoire Central des Ponts et Chaussées* (LCPC). Notably, the LC method's equipment and trial characteristics are uniquely based on the SPM. Using the LC method for this part of the process results in similar mixtures to those produced by the SPM, but there is usually an undesirably elevated asphalt content. The LC method illustrates how different properties of pavement mixtures can affect the pavement, and how to improve performance via optimized granulometry. This method also provides a practical example of mix design and reviews the volumetric properties (Ministère des Transports de Quebec, 2003). Studies have already been done to establish temperature ranges and to determine the required PG grades in countries with hot and arid conditions.

1.5 Transition from Marshall to Superpave Mix Design Methods.

Some research establishes temperature zones and defines the required performance grades (PG) in hot and arid countries. For instance, Wahhab et al. (1995) studied pavement rutting in the Kingdom of Saudi Arabia (KSA), where they identified the main factors in pavement deformation. They also made traffic and material selection recommendations but did not use Superpave grading in their material recommendations (Wahhab et al. 1995).

Asi (2007) evaluated pavement mixture design methods used in the Kingdom of Jordan. During this study, Asi produced a temperature map for the whole country and carried out tests on samples. In particular, the author used the following tests: indirect tensile strength, resilient modulus, loss of indirect tensile strength, Marshall stability, loss of stability, rutting behaviour, creep performance, and fatigue life. The samples were prepared based on the Marshall and Superpave mix design schemes. The map showed that most of the Kingdom of Jordan qualified for PG64-10, while the northeast, northwest, and southwest of the country qualified for PG70-10. This study showed that Superpave mixtures, which prescribe less bitumen than Marshall mixtures, performed better than Marshall mixtures (Asi 2007).

The predictions of the SHRP equations were more stringent and thus provided a larger buffer against the stresses of extreme heat and uncontrolled axle loading. Such conditions are often found on the roads in countries such as Libya. Uncontrolled axle load is a critical factor that is also mentioned in studies done in other desert countries. (Ahmed, A., & Othman, 2000; Almadwi & Assaf, 2017). Figure 1.2. shows the PG zones in Libya, for the eastern, central and most of the western area of the country (88% of the total area), the suggested grade of asphalt concrete binder is PG76-10; for the northwest corner, the suggested grade is PG70-10; for the southwest corner, PG82-10 is recommended (Almadwi & Assaf, 2017).

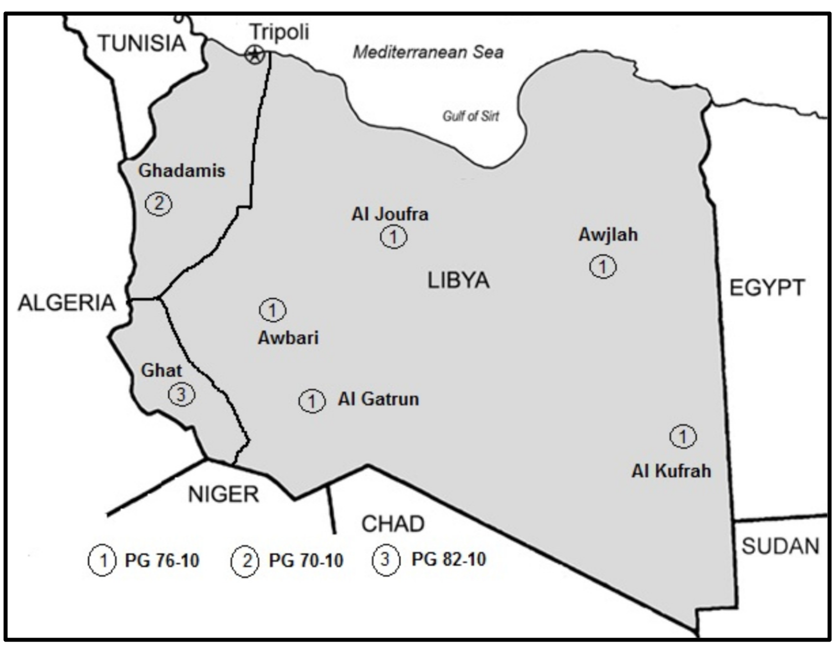

Figure 1. 2 Zone map of required PG in Libya
Taken from Almadwi & Assaf, (2017)

Hamed M. H. Alani (2010) have considered upgrading to PG for road construction in Iraq. They come up with a temperature zoning map for the whole country and suggested classes from PG64-16 (equivalent to the already used PEN 60/70) to PG76-4 for use in the hottest zone (Basra) (Hamed M. H. Alani 2010). The suggested grade of PG asphalt binder for pavement work in the five regions of Iraq is presented in Figure 1.3.

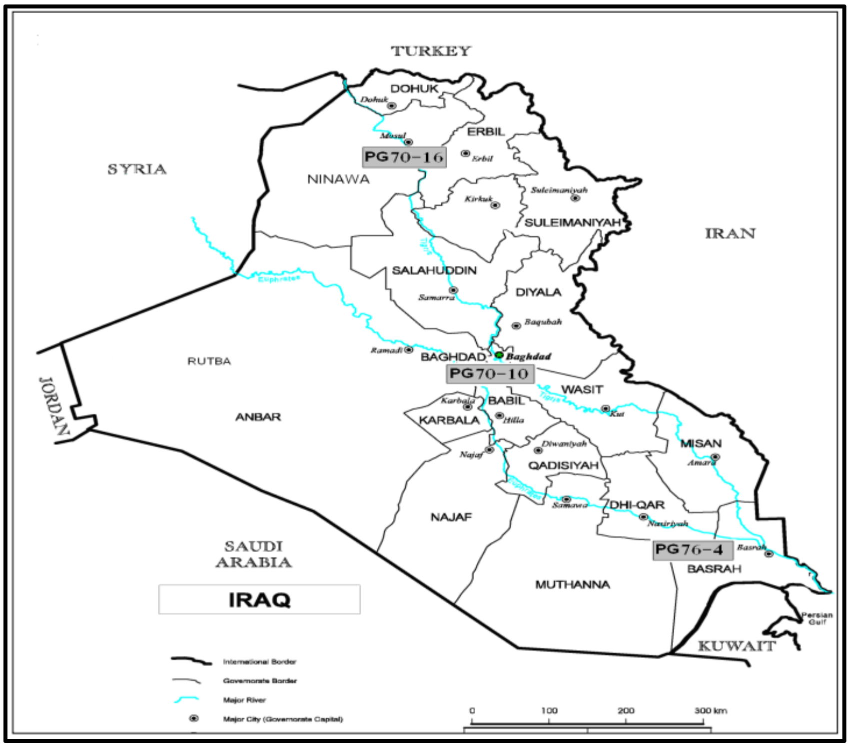

Figure 1. 3 Map of temperature zone for PG in Iraq

Taken from Hamed M. H. Alani (2010)

1.6 Pavement Performance

The AASHTO published a Guide Manual of Practice (MEPDG) in 2008, describing a pavement design methodology based on engineering mechanics. This methodology was nationally calibrated via in-service pavement distress data, such as cracking and rutting (AASHTO 2008). Pavement design to minimize and predict pavement distress in turn makes it feasible to minimize and estimate future maintenance requirements. Implemented recently by many highway agencies through the Mechanistic–Empirical Pavement Design Guide

(MEPDG), the mechanistic-empirical (M-E) approach (Hoeg et al., 2010) provides many improvements over AASHTO (1993). Developed in 2004 under NCHRP 1-37A (Hall et al., 2011), the MEPDG integrates the loading spectrum of the environmental conditions, traffic, and pavement materials (Jannat et al. 2020; Ankit, Kumar, & Rastogi, 2011).

The effect of environmental conditions is well recognized, such as at low temperatures causing embrittlement, thermal contraction, and cracking. Conversely, high temperatures promote softening and permanent deformations, such as rutting (Castelli et al., 2010). Thus, during a project's planning stages, engineers are required to not only consider the HMA's design and construction, but also how to maintain and monitor its performance (AASHTO 2008). Figure 1.4 demonstrates the elements influencing HMA operation.

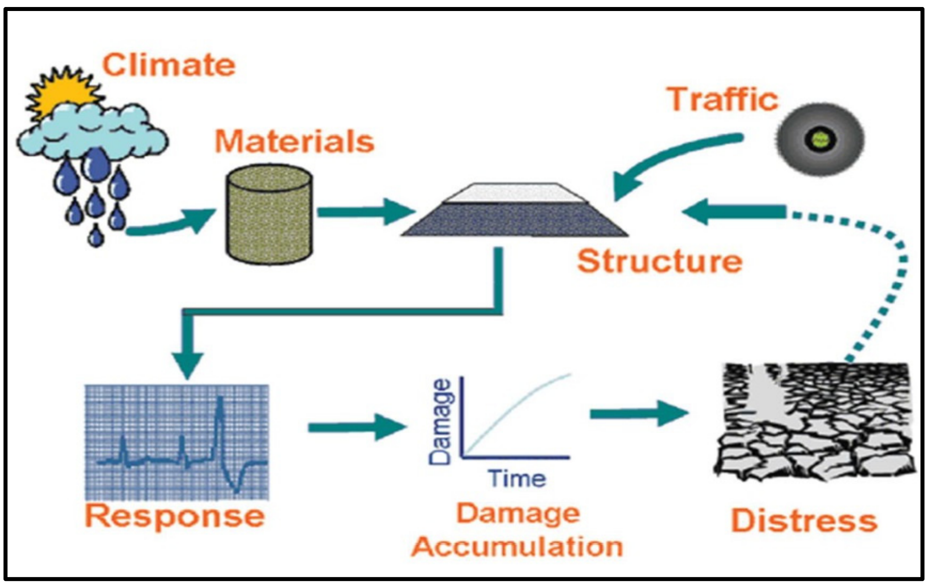

Figure 1. 4 Conditions affecting HMA performance
Taken from Kasperick and Ksaibati (2015)

The rheological behavior of bitumen varies substantially depending on the temperature, affecting the asphalt mix's rheological behavior. At high temperatures, the viscosity of the bitumen and the aggregate adhesion radically decrease. Therefore, the stiffness of the asphalt mix also drops, making it prone to accrued permanent deformation with every repeat loading.

Thus, high-temperature conditions disrupt the asphalt mix in the form of rutting or depressions in the wheel paths.

In hot climates, high temperatures can drastically increase the potential for cracking, aging, and permanent deformation (e.g., rutting) when pavements are not appropriately designed for the environment (Chen, Wei, & Wu, 2009).

1.7 Typical Pavement Stresses

Since pavements are designed to withstand stress, their design relies on a sound knowledge of pavement stress and its quantification. There are various forms of pavement stress, which can be classified as either environmentally induced or load-induced stress (Doré, 2009).

1.7.1 Stresses Induced by Axle Load

Axle loads disperse through pavement layers differently according to whether the pavement is rigid, semi-rigid, or flexible. Specifically, flexible HMA is made to spread the weight exerted on its surface to each successive layer underneath. As a result, they create tensile and compressive strains in several directions. The principal stresses involved in this process can be seen in Figure 1.5. Moreover, Ankit, Kumar, and Rastogi (2011) assert that the factors affecting pavement functioning can be categorized as either tensile or compressive stress. Tensile stress is generated at the interface between the asphalt and subgrade layers. In contrast, compressive stress is exerted from above, passing down through the asphalt and subgrade layers. These types of stress produce fatigue cracking and permanent rutting (Doré 2009).

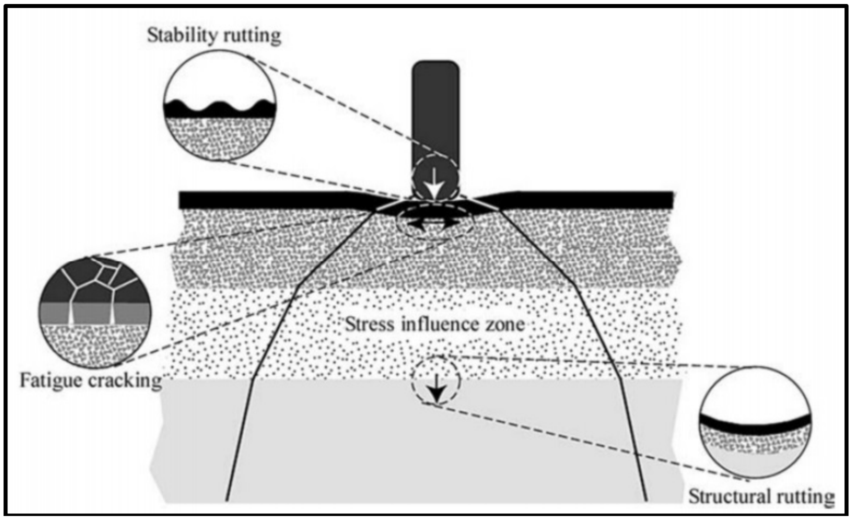

Figure 1. 5 HMA's stress distribution at critical interface points
Taken from Badeli (2018)

1.7.2 Climatic Condition Stress

Climatic stress is produced by environmental conditions such as precipitation, humidity, air pressure and temperature, solar heat, and wind. In hot and arid regions, the most significant forms of environmental stress are hot desert winds and solar heat. Figure 1.6 shows the environmental conditions with the most impact on HMA's surface layer (e.g., changes to stiffness and durability loss). In particular, high-temperature cycles result in a pavement generally diminished durability and stripping distress. Finally, variability in HMA's thermal contraction and expansion makes it subject to other kinds of deformation and stress that lead to cracking (Islam and Tarefder 2015) (Badeli 2018).

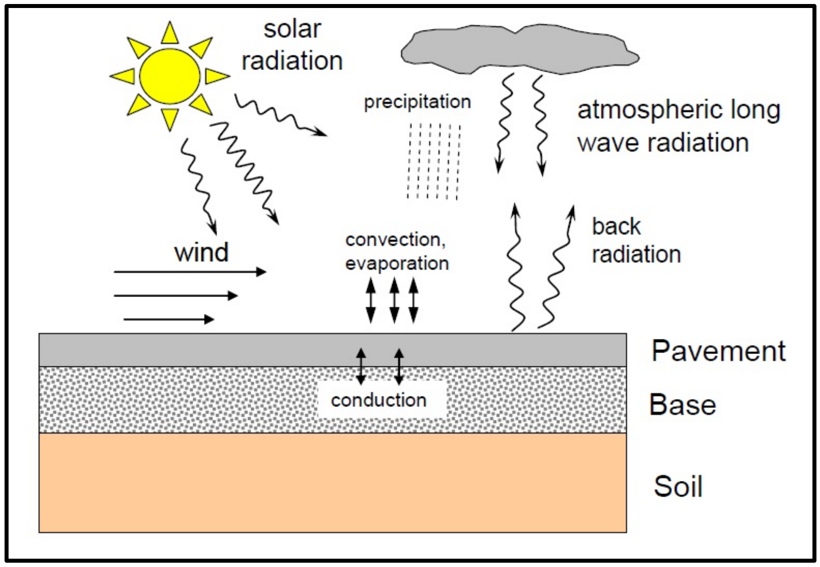

Figure 1. 6 Environmental impact on pavement surfaces
Taken from Herb et al. (2009)

Notably, seasonal changes necessarily affect climatic factors. Therefore, basic HMA design and maintenance must account for such things, including seasonal changes impacting the HMA's resilient modulus and the associated alterations in the resilient modulus of the subgrade. Different pavement layer moduli will show variations in how seasonal changes affect them. As a result, they must be assessed to account for these differences (Ankit et al. 2011).

Daily cycles of heating and cooling of pavement slowly create thermal stress. This stress builds up between fixed pavement layers that cannot contract. Moreover, thermal stress does not grow linearly because environmental forces damage pavement surfaces. Still, HMA has viscoelastic properties that enable some stress release. At particular temperatures and depending on the bitumen binders' properties, asphalt behaves like an utterly elastic material. At this point, thermal stress grows linearly, according to temperature (Doré 2009).

1.7.3 Bitumen Behaviour at High Temperatures

Under heavy traffic loading and at high ambient air temperature, bitumen flows like a viscous liquid. Indeed, viscosity is a liquid's resistance to flow. When viscous liquids do not go back to their original position while flowing, they are called "plastic." Bitumen becomes a plastic viscous liquid in sweltering climates. Specifically, a small portion of HMA's bitumen flows under recurrent axle loads and high heat, resulting in permanent rutting. Rutting is also affected by the aggregate's properties. In other words, HMA has plastic qualities (Madwi 2020) (see Figure 1.7, from the(FH Administration 2008).

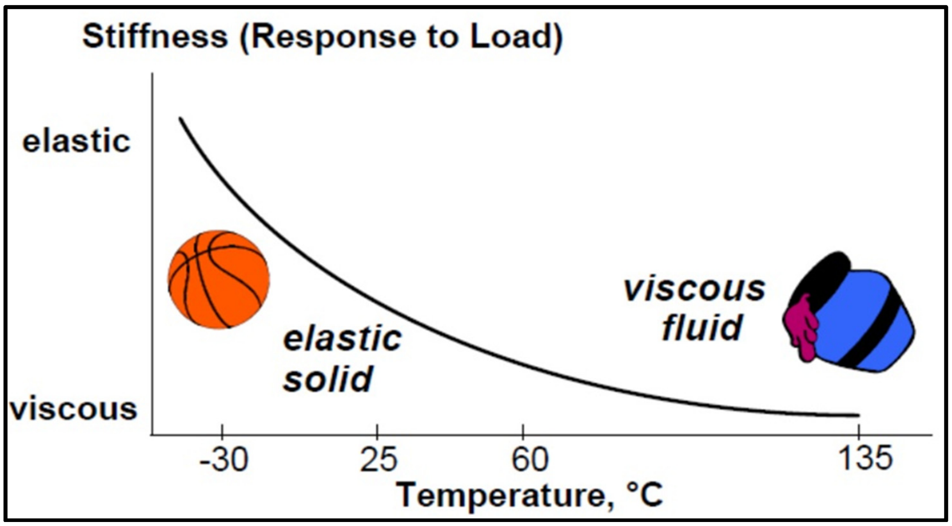

Figure 1. 7 Bitumen behaviour at high temperatures
Taken from FH Administration (2008)

1.7.4 HMA Properties and Viscoelasticity

Figure 1.8 shows the categorization of bitumen mixes by strain volume and the quantity of loads they can endure before failure. When exposed to high strain for a limited cycle count, the bitumen mix acts non-linearly. This behaviour juxtaposes with bitumen under low stress, which can withstand hundreds of cycles before failing, demonstrating its linear viscoelasticity. Then, an HMA's stiffness behaviour is evaluated via complex modulus tests. When strain levels are low, the HMA can survive tens of thousands of cycles before exhibiting fatigue behaviour. Ultimately, a pavement can show plastic distortion when its strain deviator cycles are approaching the rupture threshold (Cardona et al. 2015).

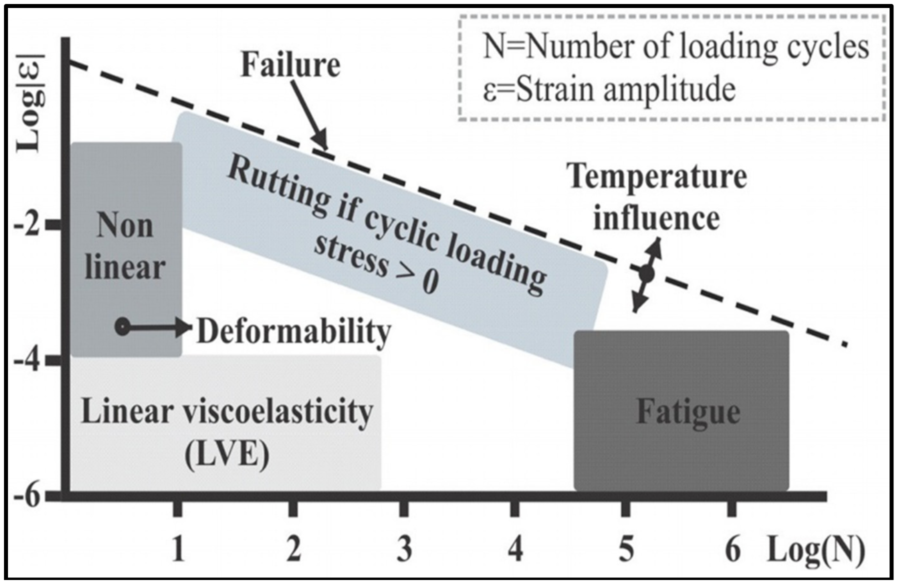

Figure 1. 8 Behaviour domains for HMA

Taken from Cardona et al. (2015)

1.8 Literature Review of Previous Applications of using additives in HMA

When subjected to high temperatures and heavy traffic, roads built according to MM specifications with B60/70 show high rates of permanent deformation, leading to higher repair costs. The challenge, then, is to find a balance between using better quality materials and keeping the total project cost low, particularly in developing countries. This problem has been widely investigated (Willway et al., 2008). Pavement surface deformation, namely rutting and shoving, is substantial in desert regions due to: (a) poor bitumen resistance to deformation at hot temperatures, and (b) the use of readily available rounded sand (Almadwi & Assaf 2017). Zhao and Pang (1998) reported that OPC -asphalt emulsion composites retain the flexible quality of asphalt binders and the strength of OPC. Flexible pavement exhibits rutting when the total stress applied by axle loads is higher than the maximum acceptable weight of the hot mix asphalt. These results are mainly dependent on the viscosity of the bitumen at the prevailing service temperature, the angularity of the aggregates, and the asphalt mixture design. Many studies have investigated how to improve the stability of the HMA by using OPC as a filler substitute.

OPC is often used to avoid binder stripping and improve bitumen coating with wet aggregates in warm-mix asphalt made from recycled aggregates (James & Reid, 1969). Water resistance and dry resilient modulus are improved by adding lime and OPC to HMA (Schmidt & Graf, 1974) and (Oruc, Celik & Aksoy 2006). Head (1974) reports that OPC not only increases the stability of cold-mix asphalt, it also increases its strength. Indeed (Uemura & Nakamori, 1993), found that the addition of only one-percent OPC increases the MM's stability by a percentage between 250% and 300%. Moreover (Al-khateeb & Al-Akha, 2011), demonstrate that combining Portland cement with asphalt binders improves the rotational viscosity of asphalt binders at up to 135 °C and different rotational speeds. They found that a cement-to-asphalt ratio of 0.15 is ideal for achieving a balanced increase in the rotational viscosity. These improvements increased the mixture's overall stiffness and ability to function in high temperatures. Brown and Needham (2000) report that the mechanical properties provided by OPC in cold-mix or asphalt-emulsion mixes are affected by parameters such as void content, curing time, binder grades, and additives such as OPC. They also report that the addition of OPC results in changes in the emulsion droplet convalescence charges, whereby the electronegative charge becomes more positive. Other affected factors include bitumen type, temperature, pressure, and emulsifier level.

Using a binder consisting of an OPC slurry and a small amount of asphalt emulsion (SS-1 and CSS-1), Pouliot, Marchand, and Pigeon (2003) analyzed the microstructures, mechanical properties and hydration process of mortars. They found that the presence of a small amount of asphalt emulsion had a small but notable effect on the Portland cement hydration process. Moreover, mortars using cationic emulsions (CSS-1) had a higher elastic modulus, and therefore increased strength compared to mortars using anionic emulsions (SS-1). In an evaluation of the practical use of polymeric admixtures in asphalt emulsions (Song, Do, & Soh, 2006) found marked improvements by increasing polymer-cement ratios, affecting chloride-ion penetration, carbonation resistance, and waterproofness. They also noted that increasing polymer-cement ratios reduced the compressive strength and reduced the mix's tendency to adhere to the mortar substrate.

The character of the interaction between an OPC-asphalt emulsion and the aggregate is distinct from both the interaction between asphalt and the aggregate, or OPC and the aggregate (Wang & Sha, 2010). In the same study, a microhardness apparatus (MH-5) was used to evaluate the effect of aggregate lithology, fineness, and varieties of Portland cement on variations in hardness found due to the interactions between the aggregate and binders. The study indicated that more Portland cement used with fine mineral filler improved the hardness of the bond; except when the mineral filler was too fine, this advantage was lost. The effects of different asphalt additives on creep strains of heavily loaded asphalt, such as highways, were discussed in (Oruc et al., 2013). In this work, reclaimed cement from factory waste was added as a mineral filler to HMA mixes in various percentages. The MM was used to prepare a cold-mix asphalt emulsion mix course. Oruc, Celik, and Aksoy (2006) report that cement functions in emulsion mixtures as a secondary binder. Permanent deformation and creep resistance were both improved with additional OPC. (Amhadi & Assaf, 2019) investigated how base course layer stabilization in low-volume roads was affected by mixtures of natural sand, manufactured aggregates, and OPC. The authors show how the use of cement for sand base course stabilization is beneficial and how both the chemical and physical properties of OPC improve the characteristics of natural rounded sand. Tests performed indicate that low-grade base materials are stabilized successfully using a mixture of only 30% crushed (manufactured) sand and 70% natural sand (by weight), with the addition of a certain percentage of OPC (e.g., 3%, 5%, 7% of the total mass of the aggregate. The economic advantage of this approach is clearly demonstrated in their paper because manufactured sand has higher transportation costs compared with adding OPC to local materials.

It is well documented that the penetration grade of the bitumen will determine the nature of the final asphalt mix, including properties such as stability, durability, flexibility, and resistance to fatigue and moisture. An excess of bitumen leads to bleeding on the wheel paths and a reduction in pavement’s lifetime performance, and so the properties of the bitumen directly affect the properties of the HMA. Standard B60/70 penetration grade bitumen is routinely used in road projects in hot regions (Almadwi & Assaf 2018). There is a standard test to evaluate the hardness of the bitumen that requires that a specific gauge of needles vertically penetrates a sample repeatedly over the course of 5 sec at 25°C. The day temperature of a road surface in Libya often reaches 70°C, which is well above 49–54°C, which is the softening point of bitumen B60/70. Strategies to resolve this problem include using a polymer-modified asphalt or a harder grade of bitumen such as PG70-10 (Almadwi & Assaf 2019). The extant works reviewed above have, therefore, already established that adding OPC to HMA is a low-cost solution that can be used to increase the stability and strength of roads, even when the MM is used.

In order to make better roadways in hot and dry regions, a lot of research must be conducted on various materials, particularly on how they respond to extreme temperatures. At the same time, it is critical to develop means of inexpensive testing so that the new data can be analyzed and compared with Superpave data (Almadwi & Assaf, 2018). These various additive materials are useful for changing the phase composition and otherwise bettering the physical and chemical properties of an HMA matrix (Ahmedzade, 2013). Typically, the materials used for these fillers are made from organic polymers, but they also include fibers and OPC (Cao & Ji, 2011). Fillers and modifiers are defined as fine or additives materials that work to alter the characteristics of the bitumen binders and the resulting HMA. Both in research and in industrial practice, various modifiers and fillers have been used, including polymer, fly ash, hydrated lime, fiber, clay or mineral particles, brick powder, cellulose, limestone dust, OPC, or used hard bitumen viscosity to resistance at high temperatures. Fillers such as these are not categorized as aggregates, but they are considered to be modifiers that make the HMA more resistant to environmental factors, including temperature variations, thereby improving the durability of the final Asphalt Concrete Pavement (ACP) (Cao & Ji, 2011). For example, mineral fillers such as hydrated lime can also reduce the moisture susceptibility of the ACP (Lesueur et al. 2013). Another study showed that as little as 1–1.5% hydrated lime added to the mix increased the lifespan of the road by 2–10 years (Likitlersuang & Chompoorat, 2016).

Moreover, Almadwi and Assaf (2019) used a weak material to compare the use of two bitumen types, with a fine aggregate mix, including 33% natural desert sand from the local area, as their control. Given the application (i.e., low-volume roads in very hot and arid areas), the mix using bitumen PG70-10 had superior properties to the mix using bitumen B60/70. Furthermore, Chompoorat and Likitlersuang (2016) reported that the use of cement and fly ash together can improve rutting resistance in wet and high-heat environmental conditions, which significantly diminishes the amount of permanent deformation. Ultimately, the findings show that the blend of 1.5% each of cement and fly ash provides the highest rutting resistance. The degree to which the bitumen mix is stiffened by the filler is tied to both its physical properties and its concentration, including factors such as particle shape, size, density, and distribution (Wang et al., 2011). Nonetheless, the exact means by which a given mineral filler will affect HMA rutting is not entirely clear and contradictory results have been published (Faheem et al., 2010). Tayebali, Malpass, and Khosla (1998) found that particle shape was key to controlling permanent deformation. Clearly, as the percentage of a given filler is increased in a mix, its effects are also increased (Kandhal, Lynn, and Parker 1998). It is not a novel concept to use OPC as a filler in hot mix asphalt. For instance, the filler has long been used to prevent the binder from being stripped out of the previously dried aggregate. Furthermore, OPC filler enhances the coating process of wet aggregate with bitumen (Oruc et al. 2006)(Abdel-Wahed & Rashwan 2016). Aljassar et al. (2004) used OPC and pulverized limestone to compare the effects of these fillers on Marshall Stability. The findings indicate that the fillers have the same effects on Marshall Stability, but there is a higher value of retained strength with OPC (Aljassar et al. 2004). Almadwi and Assaf (2021) compared the use of two kinds of additives, Limestone Powder (LSP) and Brick Powder (BP). The additives were taken as a fine aggregate mixture, including 33% natural desert sand. Given the application, the BP mixture had superior properties and performance to the LSP mixture (i.e., low-volume roads in hot regions).

Additionally, Anon (1981) investigated how various filler-asphalt ratios effect the properties of filler-mastic and asphalt paving mixes via five different kinds of fillers (OPC, lime dust stone, hydrated lime, powder of crushed gravel, and sulphate). Furthermore, the filler asphalt ratio's range is influenced by the type of filler used. Moreover, Anon (1981) showed that several locally available materials could be used as filler in asphalt paving mixtures (Abdel-Wahed and Rashwan 2016). Recently, more and more research has tackled various kinds of fillers and how they might affect the properties of the asphalt mix. OPC has shown excellent means of reinforcing HMA (Abiola et al. 2014) because it increases the tensile strength of a mix, resulting in higher strain energy (Jaskuła, Stienss & Szydłowski, 2017). With the higher strain energy, the HMA is more resistant to permanent deformation. This is of great importance for projects in hot climates. Also, using fillers such as OPC and Cellulous Fiber (CF) as alternative materials in road construction could offer many advantages, such as improving the performance of asphalt pavements, reducing the costs of creating and maintaining roads and highways, and being environmentally friendly.

CHAPITRE 2

RESEARCH FOCUS AND OBJECTIVES

2.1 Introduction

Pavement agencies in hot areas face the daunting challenge of preserving their pavements in a fair to good condition to increase their lifespan. This challenge is due to the high occurrence of permanent pavement deformation via rutting, which is one of the major distress factors influencing pavements. This is a particularly serious issue in hot and arid countries which are closely associated with various aggravating factors. These aggravating factors include the choice of bitumen binder viscosity, the type of bitumen, the available low-quality materials, and the high environmental temperatures. Ultimately, poor performance will show within the first few years of service as permanent deformations such as rutting, shoving, and depressions.

All designed asphalt pavements are typically made according to a specific “design life.” This design life is defined by AASHTO standards as the period from the pavement’s initial serviceability (Kucukvar et al. 2014). The Marshall mix design method is used by the majority of developing countries to achieve homogenous asphalt road mixtures. Unfortunately, this method is an empirical design method that cannot reproduce the effects of the asphalt binder characteristics, the region’s hot and arid climates, and field compaction (Ahmad et al. 2014). While newer mix design methods, such as the Superpave mix design method, are available such methods are costly and difficult.

There are various ways to improve pavement performance, as determined by the manifestation of surface distress over time. Performance improvements can include enhanced ability to deform without rupturing, increased rigidity, reduced sensitivity to high temperatures and rates of load applications, and so on. All of these parameters may be improved with additives such as polymers, crumb rubber, fiber, and cement. It is also possible to improve performance under hot climates and heavy traffic by using innovative compaction methods and optimized mix designs (Sol-Sánchez et al. 2015).

2.2 Problem Statement

In the Sahara region, where pavement surface temperatures can go as high as 70°C, rutting is the major form of distress affecting asphalt pavement durability. Aggravating factors to pavement endurance include; the type of bitumen, the bitumen binder viscosity used, the high environmental temperatures, and unavailable good-quality materials. Moreover, even when designing primary roads, B60/70, which is a relatively low-grade and soft bitumen, is still used in pavement construction. Therefore, Libyan asphalt pavements develop extreme deformation in the form of rutting.

This rutting occurs because the majority of hot and dry countries rely on the Marshall method. This method does not meet the requirements of hot and arid climate conditions, which are exacerbated under very heavy loads. Newly constructed asphalt pavements in hot climates, such as those found in the Middle East and Libya, show poor to very poor performance with substantial distress over its first few years of service. Whereas, this pavement distress rapidly reappears after maintenance. This reappearing damage demonstrates the need to address the root causes of the distress, which is achieved by adding fillers to designed asphalt to resist hot temperatures and heavy loads.

In desert regions, low-grade material is often overlooked as a problem that reduces pavement durability. Low-quality materials can compromise pavement stiffness, strength, durability, and stability. The resulting pavement is unable to resist permanent deformations, such as the ones mentioned above. In hot countries such as Libya, there is a need to develop a mix design for asphalt that would account for materials and weather to produce asphalt mixes with greater stability.

2.3 Research Objectives

The overarching goal of this research is to increase the performance of HMA in hot regions whilst using poorly graded and round aggregates to reduce costs and save on good quality quarry materials.

The main objective of this research is to determine the benefit and proportions of OPC and CF as filler substitutes in order to improve the performance of HMA made with lower quality and round aggregates in hot regions.

The specific objectives of this research are:

- To improve the performance of HMA against rutting and shoving deformation in hot regions, even with the recourse to poorly graded and round aggregates;
- To enhance the use of low-quality materials by using additives as filler to improve HMA durability and performance.
- To reduce the final cost by reducing the thickness of the asphalt concrete as a result of the higher stiffness from OPC and CF.

2.4 Research Methodology

2.4.1 introduction

The primary research objective of the present study is to evaluate the effects of hot and arid environments on pavement performance. The Superpave mix design method was used to conduct the lab work. The materials used for this study were natural desert sand (NDS) and crushed aggregate (CA), bitumen binder (B60/70), and two fillers; ordinary Portland cement (OPC) and cellulose fiber (CF). The materials were prepared based on the specifications and standards for road works published by the American Society for the American Association of State Highway and Transportation Officials (AASHTO), Testing and Materials (ASTM), and the Ministère des Transports de Québec (LC). The materials were designed to be used as a guide for obtaining lab work and materials for performing road work circumstances in hot and dry conditions.

The materials used in this study—bitumen (B60/70) and NDS—were sourced from Libya. Laboratory investigation showed the behavior of the asphalt mixes when fillers from the site were added. The asphalt was also exposed to similar weather conditions and traffic loads to the study area throughout the service life. The lab work consisted of two series of tests; the first was conducted before mixing, and the second was carried out on prepared samples.

The first series of tests were sieve analysis and the determination of the specific gravity of the aggregates (CA and NDS). The aggregate obtained from the resources was sieved to separate it by size. Additionally, the chemical and physical properties of bitumen binders and fillers were also investigated. The second series consisted of a mix design, in which a total of 128 samples were made. Mix and compaction temperatures were considered when preparing the samples, and the optimal bitumen content was determined.

Notably, the following specimen tests were carried out: rutting analyzer, Marshall, Superpave gyratory compactor (SGC), and Indirect Tensile Stiffness Modulus (ITSM). These tests provided useful information on the deformation behavior of asphalt during service and were conducted in the Pavement Laboratory of the Higher School of Technology (ETS) at the University of Quebec.

2.4.2 Determining the Optimal Ratio of the Fillers

2.4.2.1 Ordinary Portland Cement

Some tests were carried out with 8% OPC content, and they showed that the amount of OPC was more stringent and created problems in terms of the quality of the final mixture. However, the project goal was to find the maximum number of OPCs that work, so more tests were conducted. The following tests used 2%, 4%, and 6%. At 4%, the resulting pavement performed well, but at 2%, the tests showed much deformation. As a result, the OPC content of 6% by weight was chosen for the samples in this research.

2.4.2.2 Cellulose Fiber

Tests were conducted with 0.10% CF content by weight, which showed that the amount of CF was not a problem in terms of the mix quality. Nonetheless, since the project's main objectives were to find a workable amount of CF, more tests were conducted using 0.25%, 0.50%, and 0.75% CF content by weight. At 0.50%, the resulting pavement samples showed good performance, but at 0.75%, the tests showed much deformation. The best results came from a CF content of 0.25%, which was chosen for the samples in this study.

2.4.3 Methodology Framework

Figure 1 shows the laboratory work process undertaken to achieve this study's research objectives, and analysis for the laboratory works were discussed in the Chapters 3, 4, and 5.

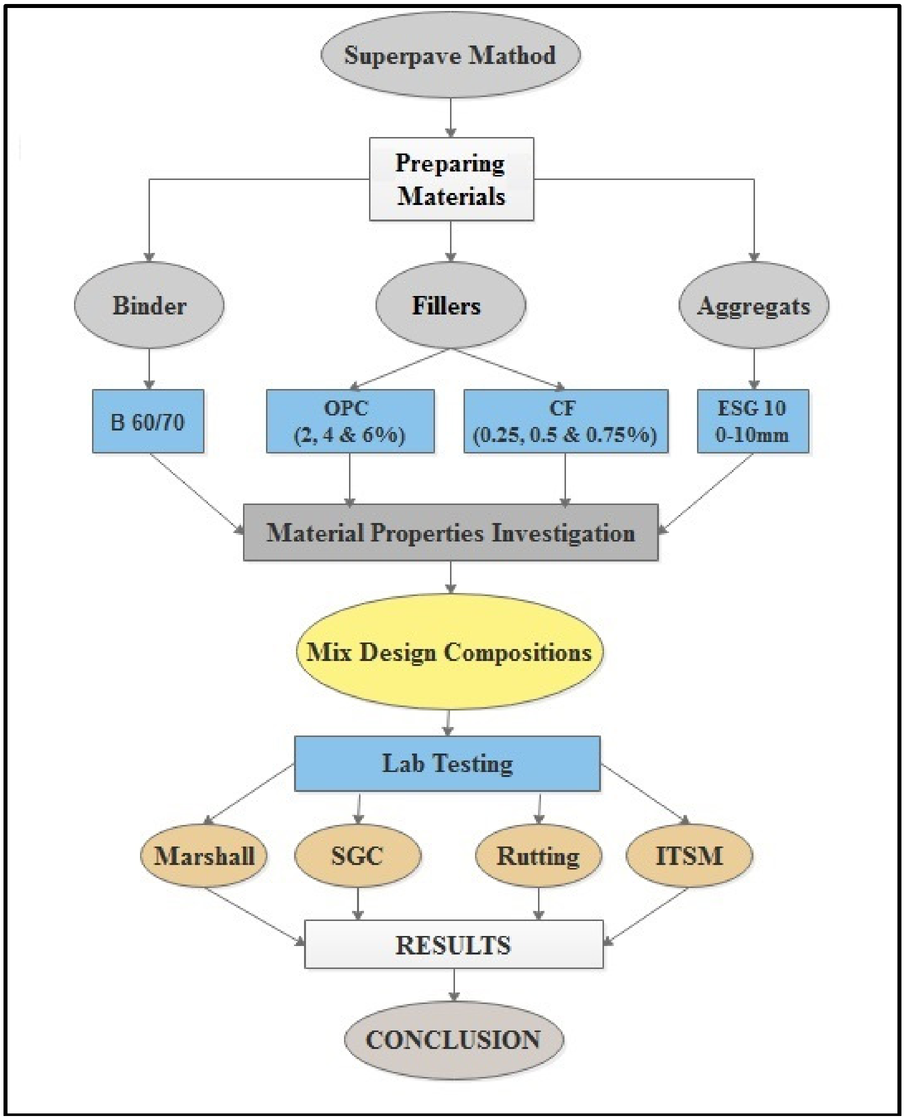

Figure 2. 1 Flow charts for laboratory works process

2.5 Research Significance

The present study also evaluated the OPC filler effects on asphalt binder composition and resistance against permanent deformation. Findings show that cement can be used successfully to produce bituminous concrete mixtures for highway construction. These mixtures should provide long-lasting, economical, and environmentally friendly solutions for constructing asphalt pavement.

2.6 Research Outline

This Ph.D. thesis is a manuscript-based thesis separated into different sections, including an introduction and conclusion. Chapter (1) is the literature review, emphasizing the effects of OPC as filler in HMA. Next, the study's problem statement, objectives and outline are explained in Chapter (2). Chapter (3) explains the effects of Portland cement as a filler in hot-mix asphalt in hot regions. The paper that this chapter is based on is already published in the Journal of Building Engineering (Elsevier). Conversely, Chapter (4) demonstrates the effects of different fillers on pavement deformation of hot mix asphalt in hot climates. This chapter is based on a paper published in the Journal of Construction and Building Materials (Elsevier). Chapter (5) demonstrates the use of cement as filler to enhance asphalt mixes' performance in hot regions. The paper that Chapter (5) is based on is still present under review with the journal of Engineering Failure Analysis (Elsevier).

CHAPITRE 3

EFFECT OF PORTLAND CEMENT AS A FILLER IN HOT-MIX ASPHALT IN HOT REGIONS

Aioub H. Guha [1], Gabriel J. Assaf [2]

[1], [2] Construction Engineering Department Ecole de Technologies Superieure,
1100 Notre-Dame West, Montreal, Quebec H3C 1K3, Canada.

Paper published in Journal of construction and building materials, 29 October 2019

ABSTRACT

Flexible pavement in hot regions often shows significant signs of distress, like rutting and shoving. This distress is mostly caused by traffic, an inadequate viscosity of bitumen, and/or an insufficient aggregate angularity. At present, the conventional bitumen viscosity of 60/70 (B60/70) has many disadvantages in hot countries like Libya, where road-surface temperatures can reach up to 70 °C. This paper reports on the use of Ordinary Portland Cement (OPC) as a filler substitute to improve the rigidity of asphalt concrete mixes made with B60/70 bitumen and low-quality aggregates. This new mixture increases the pavement's stability and resistance to high temperatures. To establish the effects of OPC on the performance of asphalt mixtures in hot climates, four different percentages of OPC (0%, 2%, 4% and 6%) are used as filler substitutes in three different mixes. The performance of the three mixes are assessed using the Superpave Gyratory Compactor and the Asphalt Pavement Rutting Analyzer. Findings indicate that mixtures containing higher percentages of OPC as a filler are significantly more resistant to rutting. These experimental results show that Portland Cement Filler Asphalts (PCFA) represents a more stable alternative to conventional asphalt that also reduces thickness requirements, because of the higher resulting modulus of rigidity. This is equally important in hot rural areas like those found in Libya, where they have very few quarries and aggregates are very costly to transport.

Keywords: Portland cement, Hot Mix Asphalt, shoving, rutting, Gyratory Compactor.

3.1 Introduction

In hot countries and geographical regions such as Libya, road surface temperatures can reach up to 70 °C (Salem, Uzelac, and Matic 2014). However, Hot Mix Asphalt (HMA) pavement design still employs conventional bitumen penetration grade asphalt binders (e.g., B60/70) and other materials that result in substantial rutting and shoving. Making matters worse, current road construction in Libya uses the “Marshall Method,” (MM) which is an older test dating back to 1939 (Zumrawi & Sheikh Edrees, 2016). This test was once widely used but is now almost exclusively employed for roads in moderate climates, making it unsuitable for roads in Libya.

The present study uses the “Superpave Method” (SPM) developed between 1987 and 1993 by the Strategic Highway Research Program (SHRP) (Swami, Mehta & Bose, 2004), since it has become increasingly popular over the last few decades (Almadwi & Assaf 2017). One of the SPM’s approaches consists of using different types of additives, such as fibers, polymers, or Portland cement, as a way to increase the performance of asphalt-concrete mixtures. The current study, however, focuses on the implementation of OPC to improve the performance of asphalt mixtures using B60/70 bitumen. This mixture is accomplished by compensating for the soft performance of B60/70 bitumen, which is classified based on resistance to deformation at only 25 °C, and by the use of readily available, low-cost materials.

3.2 Background

When subjected to high temperatures and heavy traffic, roads built according to MM specifications with B60/70 show high rates of permanent deformation, leading to higher repair costs. The challenge, then, is to find a balance between using better quality materials and keeping the total project cost low, particularly in developing countries. This problem has been widely investigated (Willway et al. 2008)(Montanelli & Srl, 2013). Pavement surface deformation, namely rutting and shoving, is substantial in desert regions due to; (a) poor bitumen resistance to deformation at hot temperatures, and (b) the use of readily available rounded sand (Almadwi & Assaf 2017).

Zhao and Pang (1998) reported that OPC-asphalt emulsion composites retain the flexible quality of asphalt binders and the strength of OPC. Flexible pavement exhibits rutting when the total stress applied by axle loads is higher than the maximum acceptable weight of the hot mix asphalt. These results are mainly dependent on the viscosity of the bitumen at the prevailing service temperature, the angularity of the aggregates, and the asphalt mixture design. Many studies have investigated how to improve the stability of the HMA by using OPC as a filler substitute.

OPC is often used to avoid binder stripping and improve bitumen coating with wet aggregates in warm-mix asphalt made from recycled aggregates (James & Reid 1969). Water resistance and dry resilient modulus are improved by adding lime and OPC to HMA (Schmidt & Graf, 1974) and (Oruc et al. 2006a). Head (1974) reports that OPC not only increases the stability of cold-mix asphalt, it also increases its strength. Indeed (Uemura & Nakamori, 1993), found that the addition of only one-percent OPC increases the MM's stability by between 250% and 300%.

Moreover Al-Khateeb and Al-Akhras (2011), demonstrate that combining Portland cement with asphalt binders improves the rotational viscosity of asphalt binders at up to 135 °C and different rotational speeds. They found that a cement-to-asphalt ratio of 0.15 is ideal for achieving a balanced increase in the rotational viscosity. These improvements increased the mixture's overall stiffness and ability to function at high temperatures. Brown and Needham (2000) report that the mechanical properties provided by OPC in cold-mix or asphalt-emulsion mixes are affected by parameters such as void content, curing time, binder grades, and additives such as OPC. They also report that the addition of OPC, results in changes in the emulsion droplet convalescence charges, whereby the electronegative charge becomes more positive. Other affected factors include bitumen type, temperature, pressure, and emulsifier level.

Using a binder consisting of an OPC slurry and a small amount of asphalt emulsion (SS-1 and CSS-1) (Pouliot et al. 2003), analyzed the microstructures, mechanical properties, and hydration process of mortars. They found that the presence of a small amount of asphalt emulsion had a small but notable effect on the Portland cement hydration process. Moreover, mortars using cationic emulsions (CSS-1) had a higher elastic modulus, and therefore increased strength compared to mortars using anionic emulsions (SS-1).

In an evaluation of the practical use of polymeric admixtures in asphalt emulsions (Song et al. 2006), found marked improvements by increasing polymer-cement ratios, affecting chloride-ion penetration, carbonation resistance, and waterproofness. They also noted that increasing polymer-cement ratios reduced the compressive strength and reduced the mix's tendency to adhere to the mortar substrate.

The character of the interaction between an OPC-asphalt emulsion and the aggregate is distinct from both the interaction between asphalt and the aggregate, or OPC and the aggregate (Wang & Sha, 2010). In the same study, a microhardness apparatus (MH-5) was used to evaluate the effect of aggregate lithology, fineness, and varieties of Portland cement on variations in hardness found due to the interactions between the aggregate and binders. The study indicated that more Portland cement and fine mineral filler improved the hardness of the bond; except when the mineral filler was too fine, this advantage was lost.

The effects of different asphalt additives on creep-strain for pavements with heavy use, such as highways, were discussed in (Oruc et al. 2013). In this work, reclaimed cement from factory waste was added as a mineral filler to HMA mixes in various percentages. The MM was used to prepare a cold-mix asphalt emulsion mix course. The extant literature indicates that cement functions in emulsion mixtures as a secondary binder. Permanent deformation and creep resistance were both improved with additional OPC (Amhadi & Assaf, 2019). Investigated how base course layer stabilization in low-volume roads was affected by mixtures of natural sand, manufactured aggregates, and OPC. It was common to use a mix of sand and cement for base-course stabilization because both the chemical and physical properties of OPC improve the characteristics of natural sand. Tests indicate that low-grade base materials are stabilized successfully using a mixture of 30% crushed (manufactured) sand and 70% natural sand (by weight), with the addition of a certain percentage of OPC (e.g., 3%, 5%, 7% of the total mass of the aggregate. The economic advantage of this approach is clear because manufactured sand has higher transportation costs compared with adding OPC to local materials.

The penetration grade of the bitumen of the chosen aggregate will determine the nature of the final asphalt mix, including properties such as stability, durability, flexibility, and resistance to fatigue and moisture. An excess of bitumen leads to bleeding on the wheel paths and a reduction in pavement’s lifetime performance, and so the properties of the bitumen directly affect the properties of the HMA. Standard B60/70 penetration grade bitumen is routinely used in road projects in hot regions (Almadwi and Assaf 2018). There is a standard test to evaluate the hardness of the bitumen that requires that a specific gauge of needles vertically penetrate a sample repeatedly over the course of 5 s at 25 °C. The day temperature of a road surface in Libya often reaches 70 °C, which is well above 49–54 °C, which is the softening point of bitumen B60/70. Strategies to resolve this problem include using a polymer-modified asphalt or a harder grade of bitumen such as PG70-10 (Almadwi & Assaf, 2019).

The extant works reviewed above have, then, already established that adding OPC to HMA is a low-cost solution that can be used to increase the stability and strength of roads, even when the MM is used. This is a valuable finding because roadwork in these regions also often use low-quality materials. Due to this, the main goal of this study is to assess whether Ordinary Portland Cement (OPC) as a substitute filler can improve the rigidity of asphalt-concrete mixtures made with B60/70 bitumen and low-quality aggregates. Note that OPC was selected because it allows for the use of substandard binders and aggregates, keeping the total cost of a project lower than many other options while still providing an HMA with good levels of rigidity and resistance to rutting. Using such a mix will increase the HMA’s stability or resistance to shear failure at high temperatures. The Superpave mix design methods used in the current study are new to many developing, hot, and arid countries, such as Libya. However, these new designs are shown to have better results than the MM, that has been the most popular mix design method there to date. Here, the performance of the three mixes are assessed using the Superpave Gyratory Compactor and the Asphalt Pavement Rutting Analyzer. To establish the effect of OPC on the performance of asphalt mixes in hot climates, four different percentages of OPC (0%, 2%, 4% and 6%) are used as filler substitutes in three different mixtures.

3.3 Experimental Details and Material

3.3.1 Materials

To ensure a low-cost intervention, some sand is added to the mix (making up 20% of the mix) as well as two types of manufactured fine aggregate (granite), between 0 to 5 mm and 5–10 mm, making up the other 74%. The aggregate gradation used here is from 0 mm to 10 mm and is presented in Fig. 1, respectively showing the grading of the aggregate mix. Table 1 presents the properties of the OPC additive material, while Table 2 shows the properties of the binder used here (B60/70).

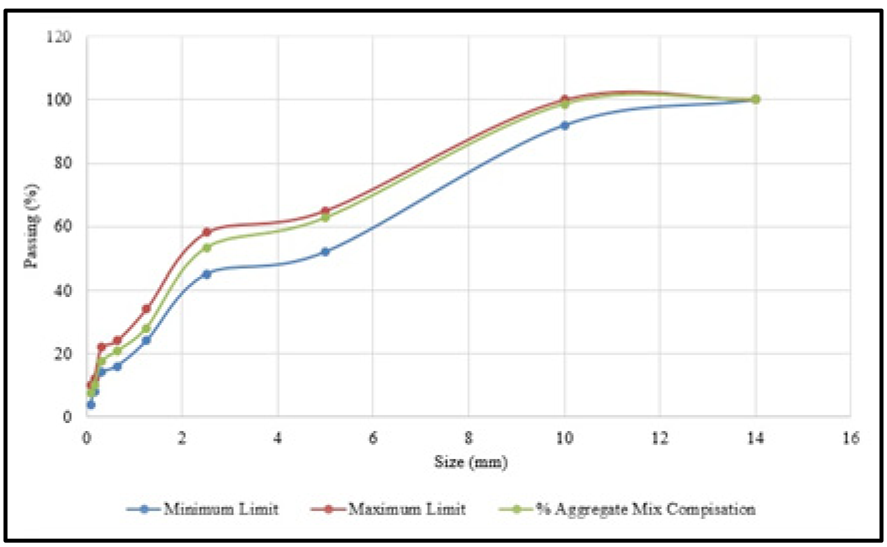

Figure 3. 1 Aggregate mix gradation

Table 3.1 Chemical composition of ordinary Portland cement

Compound	%
Loss on Ignition (LOI)	7.91
SiO_2	20.6
CaO	62.8
MgO	2.0
Al_2O_3	4.3
Fe_2O_3	3.15
Na_2O	0.81
K_2O	0.29
SO_3	2.65
Materials not solvent	1.02

Table 3.2 Chemical properties of the binder B60/70

Binder Properties	Specification	Samples Result
		B60/70
Specific Gravity	T228	1.03
Flash point, °C	T48	302
Mass Loss, %	T240	0.07
Penetration at 25°C, dmm	T316	64.7
Ductility at 25°C, cm	T51	143
Softening point, °C		51.7

3.4 Experimental Procedure

3.4.1 Superpave Gyratory Compaction Test (SGC)

According to the Ministry de Transport de Quebec (MTQ 2016), the SGC base turns at a constant of 30 gyrations per minute for the compaction period, while also applying a constant vertical stress of 600 kPa with the shear stress of 3,000 kPa. Where the mould is set at an angle of compaction of 1.25°. A specimen's height plays an important role in the tests. The density of the specimen is estimated throughout compaction, using: (1) the material's mass in the mould, (2) the mould's inside diameter of 100–150 mm and, (3) the height of the specimen. Height measurements are taken using the ram's position during the test period. These measurements are used to determine the compaction characteristics of a specimen at all gyrations from 0 to 200. Each gyration produces compacted specimens with volumetric properties, voids in mineral aggregate (VMA), voids filled with asphalt (VFA), and air void (Va). Based on the Superpave system, there are important levels for the volumetric properties of the asphalt mix, as shown in Table 3.

Table 3.3 Specifications and limitations according to MTQ 4202, ESG10

Design ESALs	**Properties**	**Specification**		
< 0.3	Va	$N_{initial}$	N_{design}	$N_{maximum}$
		≥11%	≥4-7%	≥2%
	VMA	15%		
	VFA	70-80%		

3.4.2 Rutting Test

For the test, a tire repeatedly passes over the sample's center at a rate of two times per second. Sample loading is achieved by applying a load of 500-N and tire pressure of 600 kPa. Slab dimensions of 500 x 180 x 50–100 mm. The samples are kept at a temperature of 60 °C throughout the tests to reflect hot climate. These were compacted and tested with the French laboratory system Fig. 2 according to MTQ (MTQ 2016).

Figure 3. 2 French laboratory system

After mix design tests and analysis were completed, two slabs were made for each mix design, i.e. two samples for each cement percentage (0%, 2%, 4%, 6%). To define what counts as deformation, 15 measurements are taken and used to find the average rut depth. Three measurements are made using the specimen width at five points along the slab's length. The first sample measurement is made following 1,000 cycles in ambient room temperature; while the subsequent measurements are made after 1,000, 3,000, 10,000 and 30,000 cycles at a consistent temperature of 60 °C. The depth was established by loading samples at all repetitions and checking them against the same specifications and standards.

3.5 Results and Discussion

3.5.1 Results of the Gyratory Compaction Test

Gyratory Compaction is performed with the identical material for every sample. Only the percentage of cement (0%, 2%, 4%, 6%) is different. The gyration numbers for the current study are 200, 100, 80 and 10 gyrations, as seen in Fig. 3, 4, and 5. The Gyratory test results are in Fig. 6, 7 and 8, that shows that samples with 6% cement had a lower Va% than samples with 4%, 2%, and 0%. The VFA test exceeded the acceptance limits, and the test for VFA exceeded the limits set for tests with 2% and 4%. The VMA test also exceeded the acceptance limits with 2% and 4% mixtures.

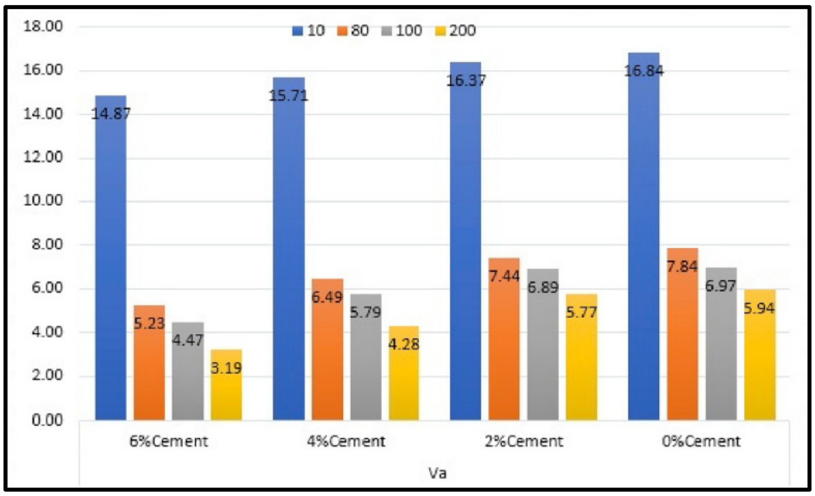

Figure 3. 3 Gyratory Compactor (SGC) test for Va

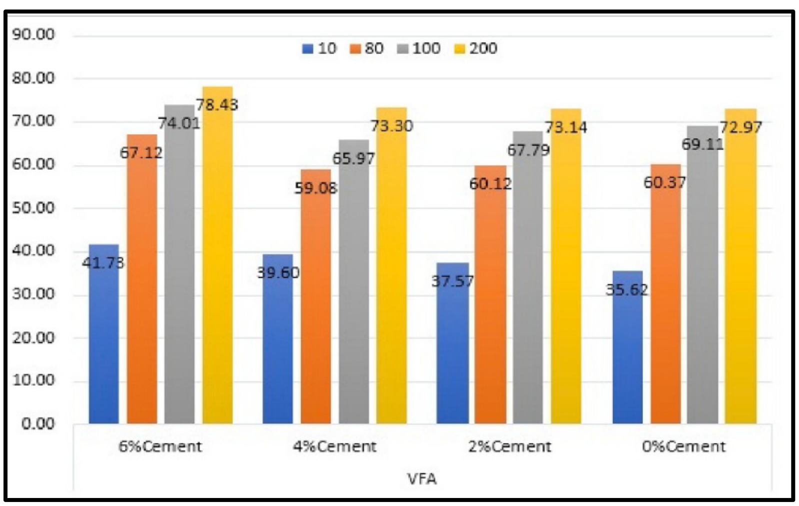

Figure 3. 4 Gyratory Compactor (SGC) test for VFA

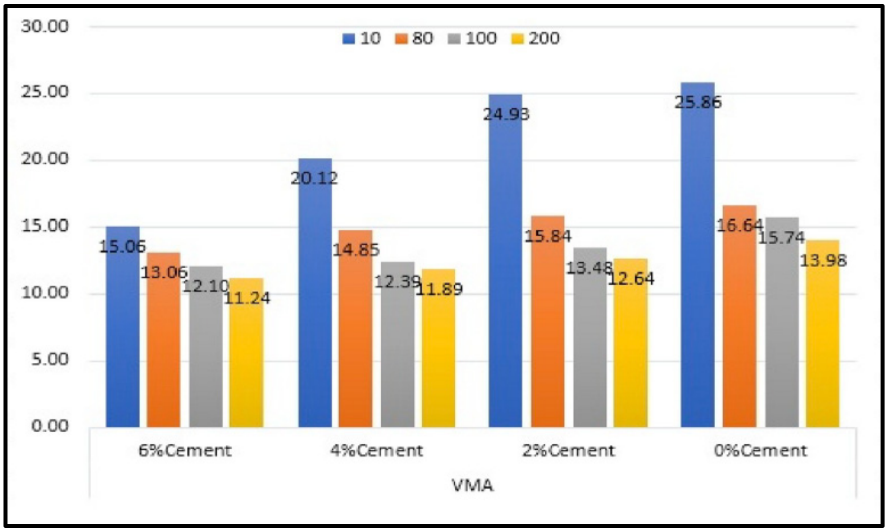

Figure 3. 5 Gyratory Compactor (SGC) test for VMA

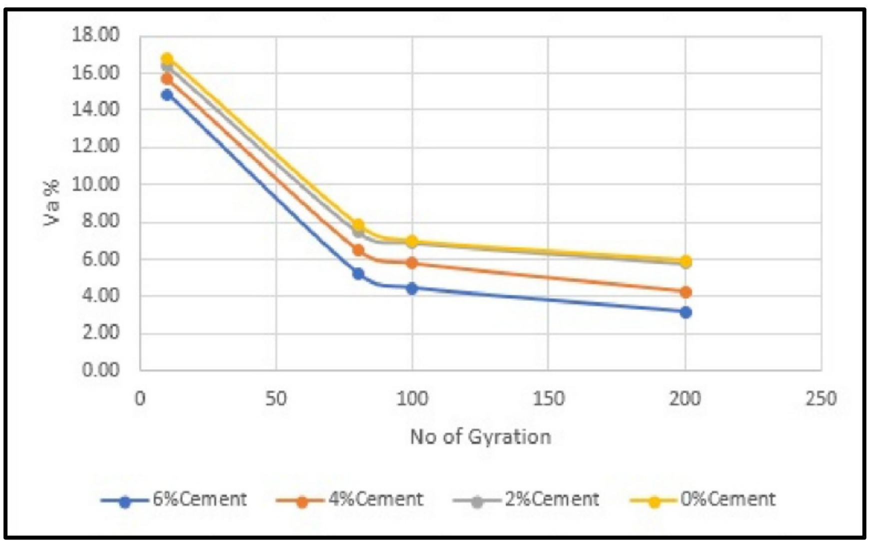

Figure 3. 6 Analysis of the Gyratory Compactor (SGC) test for Va

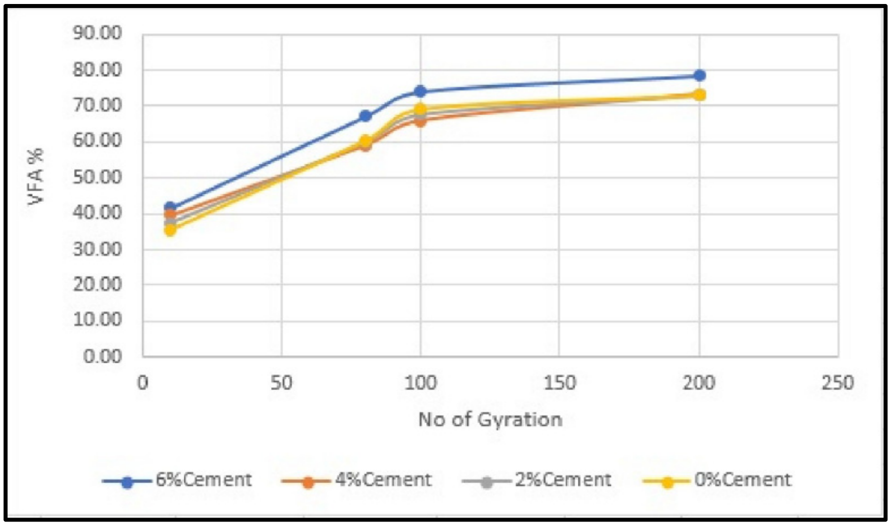

Figure 3. 7 Analysis of the Gyratory Compactor (SGC) test for VFA

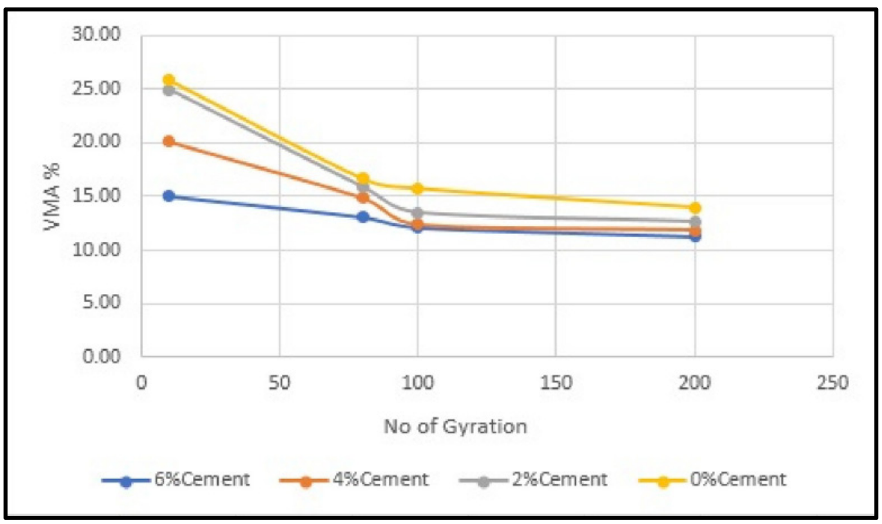

Figure 3. 8 Analysis of the Gyratory Compactor (SGC) test for VMA

3.5.2 Rutting Test Results

The test evaluated six samples with two slabs for each mix percentage. Rutting depths for all samples were determined at 1,000, 3,000, 10,000 and 30,000 passes. The total compressive energy applied to each sample can be calculated as the product force (80 kN standard axle load), number of repetitions (30,000), and distance covered (500 mm; length of the sample). It can be observed from Table 4 that rut depths are lower for asphalt mixes with a higher percentage of cement when compared to samples containing lower percentages of cement. The loading system for the average of different materials determines the rutting depth after the test. After 30,000 repetitions, the 2% cement mixture had the most rutting, while the 6% cement mixture had the smallest amount of rutting. Furthermore, the rutting test made the influence of the OPC ratio on the rutting performance mixture very clear. For the different percentages of OPC (0%, 2%, 4% and 6%) as filler, the rut depth was reduced with a corresponding reduction in the asphalt filler.

Average rut depth values were calculated for all of the samples, and the results of the rutting tests were done according to the MTQ standard. This standard requires that a sample must not have more than 10% rutting over 1,000–3,000 cycles, from its original height, as shown in Fig. 9. From this data it can be seen that there is less rutting with increased amounts of cement, and that these asphalt samples with higher cement percentages have lower rutting depths.

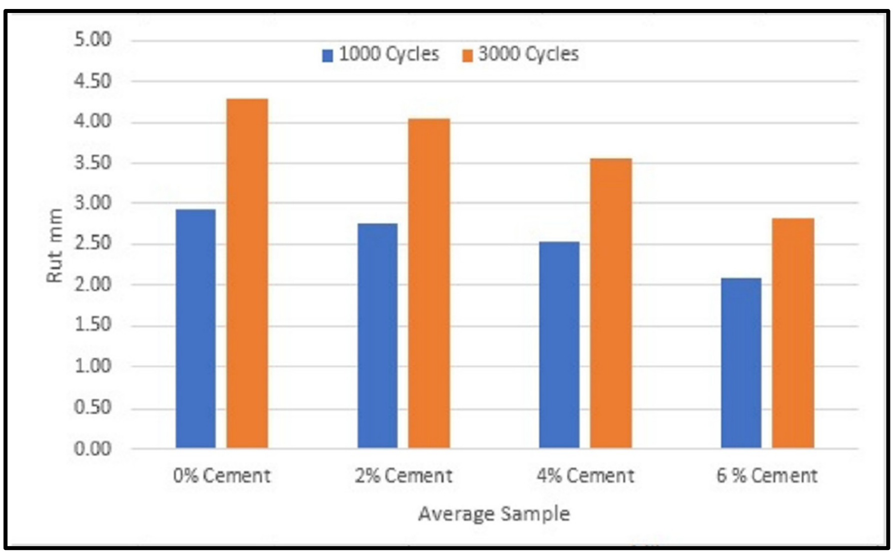

Figure 3. 9 Average rut depth for each type of design mix

3.6 Conclusion

The purpose of this paper is to evaluate the use of Ordinary Portland Cement in Hot Mix Asphalt, and to determine the range of properties for pavement performance. Laboratory tests were performed on different HMA with different percentages of OPC incorporated into the HMA (0 %, 2 %, 4 %, and 6 %). Percentages were determined by total weight and then used to determine the feasibility of incorporating OPC as an additive in HMA. The influence of such an additive can be discussed as follows:

1. Rutting is reduced to an increase in OPC, as determined by the rutting test. 6% mixtures of OPC show superior performance and are recommended for hot regions where the most common type of pavement distress is rutting.

2. OPC as an additive to HMA creates better stability and decreases flow, leading to less rutting and improving the overall strength of the final mix.

3. The 6% cement mixes have a lower air-void percentage and result in less moisture damage when compared with mix percentages of 4% and 2%.

4. These conclusions are based on the figure analysis, all showing that 6% OPC content is recommended for use in modifying the HMA in hot and arid countries like Libya. It is a low-cost way to improve pavement in these regions.

The limitations of this study are that, in order to keep the project costs down, it only used aggregates from 0 to 10 mm. Likewise, the study only used bitumen 60/70 because this is the most common bitumen used in Libya at present. Future research could consider other additives to the HMA, such as fly ash, fiber, polymer, and other recycled materials.

CHAPITRE 4

EFFECTS OF DIFFERENT FILLERS ON PAVEMENT DEFORMATION OF HOT MIX ASPHALT IN HOT CLIMATES

Aioub H. Guha [(a)] & Gabriel J. Assaf [(b)]

[(a)], [(b)] Construction Engineering Department Ecole de Technologies Superieure,
1100 Notre-Dame West, Montreal, Quebec H3C 1K3, Canada.

Paper published in Journal of construction and building materials, 2 July 2020

ABSTRACT

Permanent deformation in the form of rutting is one of the major distresses affecting asphalt pavements. This is a serious issue in hot countries that is associated with the viscosity of the bitumen binders used. In many hot countries, with temperatures exceeding 45°C, bitumen 60/70 (B60/70), a relatively low-grade and soft bitumen at these temperatures, continues to be used in Hot Mix Asphalt (HMA) on primary roads. Libyan asphalt pavements therefore develop deformations in the form of rutting and shoving.

This study evaluates the effect of adding cellulose fiber (CF) and Ordinary Portland Cement (OPC) on the mechanical and volumetric performance of HMA subject to these temperatures. CF and OPC were added to a conventional B60/70 HMA mix according to novel SuperPave mix design specifications. Three percentages of OPC (2%, 4%, and 6%) and three different percentages of CF (0.25%, 0.5%, and 0.75%) were used as filler in a fine-graded HMA; there was also a control mix with no filler (0%). Mix performance was assessed with the Rutting Analyzer and The Indirect Tensile Stiffness Modulus (ITSM). ITSM tests were conducted at -5 °C, 10 °C, 25 °C to simulate lowest temperatures observed in North Africa, and the rutting test was conducted at 60°C to simulate temperatures observed in the region plus a margin to account for heat absorption. Mixes using CF performed better than those with OPC. The results suggest potential savings by using inexpensive additives instead of more expensive binders.

Keywords: Hot mix asphalt, OPC, CF, Stability, Filler, Rutting, and B60/70.

4.1 Introduction

Numerous methods were developed to improve the performance of asphalt pavements. A popular technique is to add fillers to reinforce Hot Mix Asphalts (HMA). In hot and arid countries where temperatures often exceed 45°C, HMA are still often made with bitumen 60/70 (B60/70). Although there are higher grades of bitumen available (Almadwi & Assaf, 2017), numerous studies have concluded that fillers also improve the performance of B60/70 HMA; these fillers include polymers, fibers, and OPC. Without these additive materials, or alternatives such as higher-grade bitumen, HMA in hot climates undergoes permanent deformation such as rutting (Willway et al. 2008). The effects of any given filler depend on the characteristics of the HMA and how it relates to climatic conditions and axle loads. Traditionally, mineral fillers have been added to dense-graded HMA paving mixtures to fill and reduce the voids in both the aggregate skeleton and the mix (Brian et al., 2005). Fillers also have other functions, such as contributing to mixture cohesion, increasing the bitumen density, stability, and toughness, and finally, they may also work as active fillers. Importantly, the pavement's brittleness and tendency to crack while in-service grows as the filler content increases (Sterling, 2011).

Earlier work by Guha and Assaf (2020a) reported that the use of OPC as a filler improves HMA rigidity when using B60/70 bitumen and generally low-grade aggregate obtained predominantly from round-shaped desert sand. OPC Filler Asphalts (PCFA) resulted in a stable HMA, allowing a reduction in the required thickness of the pavement while maintaining the modulus of rigidity. Other studies have found that mineral fillers improve the overall stiffness and strength the HMA (Aljassar et al., 2004). Likewise, long-term durability and stability are important so that the HMA resists permanent deformations such as shoving or rutting (Lesueur et al., 2013).

This study focuses on the use of OPC and CF as additive materials to the HMA made using B60/70 and fine desert aggregates (between 0 and 10 mm). The objective is to increase the HMA stability and resistance to permanent deformation such as rutting and fatigue cracking. HMA was prepared for each of the two fillers, OPC and CF, each with three percentages of filler; one HMA sample was prepared with no filler. The percentages of the two fillers were different for each type. OPC was added in 2%, 4% and 6% of the total weight of the HMA; CF was added in 0.25%, 0.5% and 0.75% of the total weight of the HMA. The resulting seven samples were evaluated with the Indirect Tensile Stiffness Modulus Test (ITSM) and the Asphalt Pavement Rutting Analyzer Test (rutting test) to establish the effects of OPC and CF on HMA performance in hot regions. ITSM tests were conducted at -5 °C, 10 °C, 25 °C to simulate lowest temperatures observed in North Africa, and the rutting test was conducted at 60°C to simulate temperatures observed in the region plus a margin to account for heat absorption.

4.2 Background

In order to improve pavement performance in hot and dry regions, investigations must be conducted on locally available materials, such as desert sands for instance, in order to assess how they respond to extreme temperatures when mixed with conventional or modified binders. At the same time, it is equally important to develop protocols for testing so that the mix design procedures are practical and readily available (Almadwi & Assaf, 2018). Various additive materials may be assessed to change the chemical or physical characteristics of an HMA matrix so that it is suitable under prevailing operating conditions (Ahmedzade, 2013). Typically, the materials used for these fillers are made from organic polymers, but they also include fibers and OPC (Cao & Ji, 2011).

Fillers and modifiers are defined as fine or additives materials that work to alter the characteristics of the bitumen binders and the resulting HMA. Both in research and in industrial practices, various modifiers and fillers have been used, including polymer, fly ash, hydrated lime, fiber, clay or mineral particles, brick powder, cellulose, limestone dust, OPC, or used hard bitumen viscosity to resistance a high temperature. Fillers such as these are not categorized as aggregates, but they are considered to be modifiers that make the HMA more resistant to environmental factors, including temperature variations, thereby improving the durability of the final HMA (Cao & Ji, 2011). For example, mineral fillers such as hydrated lime can also reduce the moisture susceptibility of the HMA (Lesueur et al. 2013). Another study showed that as little as 1–1.5% hydrated lime added to the mix increased the working life of the road by 2–10 years (Likitlersuang & Chompoorat, 2016).

Almadwi and Assaf (2019) used a weak material to compare the use of two bitumen types, with a fine aggregate mix, including 33% natural desert sand from the local area, as their control. Given the application (i.e., low-volume roads in very hot and arid areas), the mix using bitumen PG70-10 had superior properties to the mix using bitumen B60/70. Furthermore, Chompoorat and Likitlersuang (2016) reported that the use of cement and fly ash together can improve rutting resistance in wet and high-heat environmental conditions, which significantly diminishes the amount of permanent deformation. Ultimately, the findings show that the blend of 1.5% each cement and fly ash provide the highest rutting resistance.

The degree to which the bitumen mix is stiffened by the filler is tied to both its physical properties and its concentration, including factors such as particle shape, size, density, and distribution (Wang et al., 2011). Nonetheless, the exact means by which a given mineral filler will affect HMA rutting is not entirely clear and contradictory results have been published (Faheem et al., 2010). Tayebali *et al.* (1998) found that particle shape was key to controlling permanent deformation. Clearly, as the percentage of a given filler is increased in a mix, its effects are also increased (Kandhal et al., 1998).

OPC has often be used as a filler in HMA. For instance, the filler has long been used to prevent the binder from being stripped out of the previously dried aggregate. Furthermore, OPC filler enhances the coating process of wet aggregate with bitumen (Oruc et al. 2006a)(Abdel-Wahed & Rashwan 2016). Aljassar et al., (2004) used OPC and pulverized limestone to compare the effects of these fillers on Marshall Stability. The findings indicate that the fillers have the same effects on Marshall Stability, but there is a higher value of retained strength with OPC (Aljassar et al. 2004). Additionally, Al-Qaisi (1981) investigated how various filler-asphalt ratios affect the properties of filler-mastic and asphalt paving mixes via five different kinds of fillers (OPC, lime dust stone, hydrated lime, powder of crushed gravel, and sulphate).

Al-Qaisi (1981) showed that several locally available materials can be used to replace OPC as filler in HMA (Abdel-Wahed & Rashwan 2016). Abiola has also established that OPC is an excellent means of reinforcing HMA (Abiola et al. 2014) because it increases the tensile strength of a mix, resulting in higher strain energy (Jaskuła et al. 2017). With the higher strain energy, the HMA is more resistant to permanent deformation. This of great importance for HMA in hot climates. Fillers such as OPC and CF improve the performance of HMA, reducing the costs of providing sustainable roads.

4.3 Experimental Details and Materials

4.3.1 Materials

To reduce construction costs, natural desert sand at a ratio of 20% of the total HMA weight, was used; the remainder of the aggregate was crushed fine granite aggregate, between 0 and 10mm. Figure 1, shows the grain distribution of the aggregate skeleton. Table 1 provides the characteristics of the modified CF. Table 2 shows the characteristics of the OPC. Table 3 shows the characteristics of the bitumen binder B60/70, used for all the mixes.

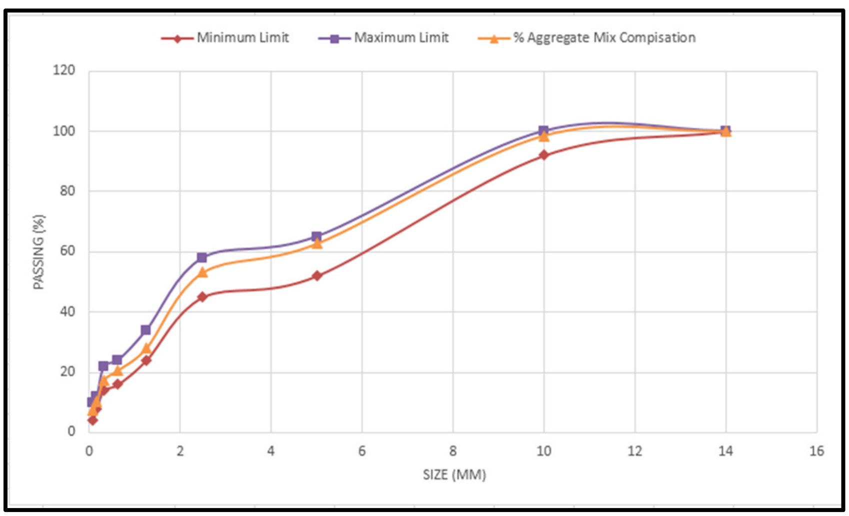

Figure 4. 1 Aggregate Gradation

Table 4.1 Physical and Chemical properties of modified CF

Content	**%**
Fiber length	6 mm Max
Fiber diameter	40 micron
Ash	18.0 % - 5.0 %
Moisture	< 5%
pH	7.5 - 1.0

Table 4.2 Chemical composition of OPC
Taken from Guha & Assaf (2020)

Compound	**%**
SiO_2	20.6
Al_2O_3	4.3
Fe_2O_3	3.15
CaO	62.8
MgO	2.0
Na_2O	0.81
SO_3	2.65
K_2O	0.29
Loss on Ignition (LOI)	7.91
Materials not solvent	1.02

Table 4.3 Chemical properties of the binder B60/70

Binder Properties	Samples result B60/70	Specification
Flash point, °C	302	AASHTO T48
Specific Gravity	1.03	AASHTO T228
Penetration at 25°C, dmm	64.7	AASHTO T316
Mass Loss, %	0.07	ASTM E595 (ASTM 2015)
Softening point, °C	51.7	AASHTO T53
Ductility at 25°C, cm	143	AASHTO T51

4.4 Experimental Procedure

4.4.1 Rutting test (Asphalt Pavement Rutting Analyzer Test)

For each mix, two samples were made, resulting in a total of 14 samples (3x OPC; 3x CF; 1x control with no filler). During the rutting test, two samples of each HMA composition were tested at the same time. The sample dimensions were 180 mm by 500 mm by 50 mm. The rutting test consists of a pneumatic tire inflated to 600 kPa passing over the sample with a load of 500 N. The tests were conducted at room temperature of 60 °C to simulate a hot climate. The weighted tire was passed over the sample a total of 30,000 times and the samples were measured for rutting deformation at various stages throughout the test, at 1,000, 3,000, 10,000 and 30,000 cycles (Guha & Assaf 2020a). The deformation created by the tire was measured as a function of the percentage of the slab's original thickness. The measurements were taken across the width of the tire track at 15 different points; these measurements determined the average depth of the rutting and defined the deformation. Once the depth measurement is recorded, it was compared with the standards and specifications of the Minister des Transports, Québec (MTQ) (MTQ 2016).

4.4.2 The Indirect Tensile Stiffness Modulus Test

ITSM test was conducted to measure the stiffness modulus of the HMA samples, following EN 12697-26 standard (Italiana, 2005). The tests were conducted at -5°C, 10 °C, and 25 °C to investigate the modulus's temperature sensitivity. As in the rutting test, two samples were used to test each mix variety. The samples were 100 mm wide and 63.5 mm high. For the six hours before the test, the samples were in the testing chamber at the chosen temperature. The following equation was used to calculate the stiffness modulus:

$$S_m = \frac{F\times(\mu+0.27)}{h\times Z} \tag{4.1}$$

where,

Sm refers to the stiffness modulus, MPa; F refers to peak load, N; m refers to the Poisson ratio (0.25, 0.30, 0.40 at -5°C,15°C, 25°C respectively); Z refers to the displacement in the horizontal plane in mm; h refers to the specimen height in mm.

4.5 Results and Discussion

4.5.1 Rutting Test Results

The test studied two samples in seven mixes, for a total of 14 samples. All samples were determined at the rutting test of 1,000, 3,000, 10,000, and 30,000 passes. The process for determining the average of difference in the rutting is measured after each cycle of passes. Each sample's total compressive load can be calculated as the applied force of 80 KN standard axle load, cycle repetitions of up to 30,000, and distance covered 500 mm (length of samples).

Table 4 shows that asphalt mixtures with a greater percentage of OPC compared to mixes containing less OPC have lower rut depths. Conversely, asphalt fiber mixes with lower percentages of CF have a lower rut depth than mixes with a higher amount of CF. After repetitions of up to 30,000, the 2% and 4% OCP mixes showed the highest amount of rutting, while the 6% OCP mix showed the least. In addition, the rutting test highlighted the effect of the cement percentages (2%, 4% and 6%) in the rutting test. On the other hand, the different percentages of CF (0.25%, 0.5%, and 0.75%) all have better performance than the best OPC result. The lab results showed that the best resistance to rutting was with samples containing a very small percentage of fiber. Both mixes (OPC and Fiber) showed better rutting performance compared to the control mix.

It is well recognized that the rutting analyzer measures the material's resistance to shear stresses, permanent deformation, and, thus, rutting. The high rutting analyzer values indicate a high stiffness mix with resistance to creep deformation. Fig. 2 (below) illustrates the rutting analyzer results for all mixtures. The results show that the CF has the highest rutting analyzer value, and, the less CF added, the higher the rutting analyzer can be observed. Conversely, the OPC has less influence on the rutting analyzer value. However, the combination of CF and OPC as fillers can significantly increase the rutting analyzer value of the mixtures.

Table 4.4 Rutting Test Results

Cycle Number	**Filler Content**							**LC 4202 ESG10**
	0.25% Fiber	**0.5% Fiber**	**0.75% Fiber**	**0% Control**	**2% Cement**	**4% Cement**	**6% Cement**	
1,000	3.32	3.52	4.03	5.75	5.12	4.92	4.00	≥ 10
3,000	4.5	4.64	5.01	8.42	7.49	6.95	5.41	≥ 15
1,0000	5.47	5.71	6.39	12.76	11.42	10.35	7.55	-
3,0000	7.1	7.36	7.48	20.63	15.49	13.26	9.88	-

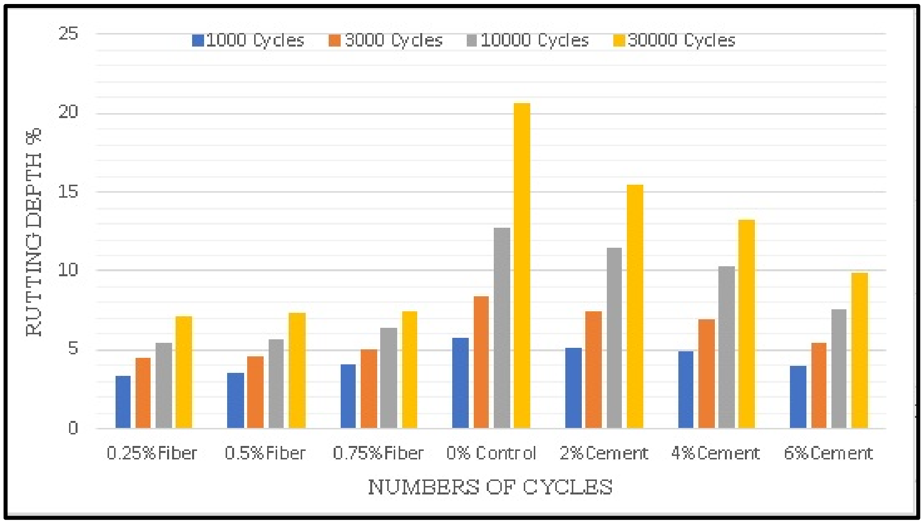

Figure 4. 2 Rutting Test Results

In accordance with the Quebec Department of Transportation Standards (MTQ 2016), the average of rutting depth was tested with the rutting analyzer and calculated for all samples. The standards require that a sample does not have more than 10% rutting over 1,000–3,000 cycles, from its actual height, as shown in Fig. 3. The data demonstrates that there is less rutting with an increase in the percentage of OPC, and that asphalt samples with greater OPC percentages have lower rutting depths.

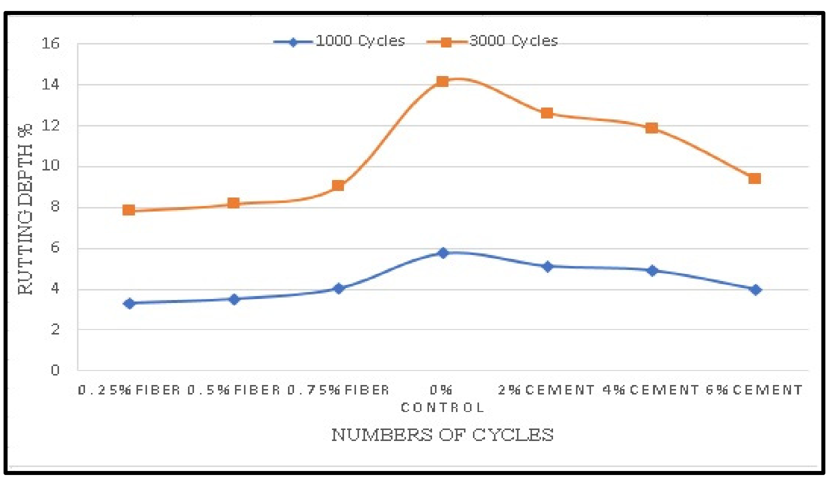

Figure 4. 3 The Average rutting depth for each mix

4.5.2 Results of ITSM Test Modulus

ITSM tests were carried out in accordance with the standard (EN 12697-26) (Italiana, 2005) for all samples and the control mix at -5°C, 15 °C and 25 °C to investigate stiffness modulus. At each temperature, all samples' stiffness moduli were higher than that of the control mix. With an increase in temperature, the stiffness modulus of each mix decreases, excluding the control mix. The comparative analysis cannot be made directly using the stiffness modulus since the stiffness modulus has different values at different temperatures.

The modulus ratio has been widely used to evaluate the modification effect of modifiers in the area of composite material. Thus, we evaluate the stiffness modulus ratio of the mixes using different fillers with different ratios to the control mix. Then the ratios were measured at each temperature for this test.

Fig. 4 shows the cement mixes on the left side, the CF mixes on the right side, and the control mix with no filler in the middle. The most significant percentage of cement is at the far left, and it gets progressively smaller as it gets closer to the center, where there is no filler. To the right of the center, there is the smallest proportion of CF filler that progressively gets bigger as it approaches the outside. This was done to show that the higher the percentage of cement, the greater the stiffness modulus, as its results were effectively linear. In contrast, the effect of adding CF was non-linear, where 0.25% and 0.5% provide results that are superior to those produced by a 0.75% mix. The stiffness moduli of OPC mixes are lower compared to CF mixes, especially at the highest temperatures. Furthermore, the stiffness modulus increased when the temperature decreased for both combinations, and the lab results indicated that adding CF or OPC to the mix improved its final quality when compared to the control mix. However, an excessive amount of filler reduces the viscous behaviour of asphalt mastic and results in decreasing the SM value. In this study, a suitable amount of CF and OPC was found to be in the range of 0.75–6%.

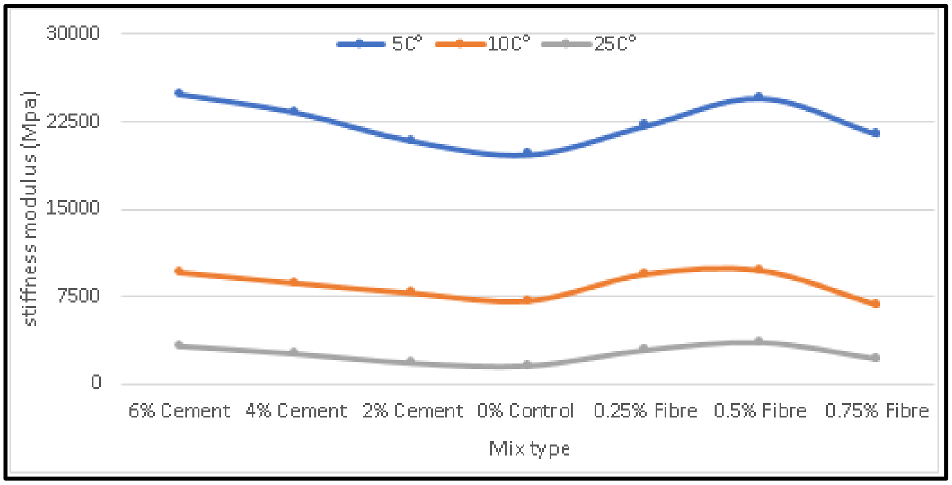

Figure 4. 4 Average ITSM tests for each type of cement design mix

4.6 Conclusion and Limitations

Fillers are usually added to asphalt-concrete mixtures as a stiffening and void-filling material. The present study evaluated a total of 28 specimens with various CF and OPC contents, and a 5% asphalt content. The influence of such an additive material can be described as follows:

- Both OPC and CF are superior to the control mix.

- In all mix samples with OPC, rutting is reduced. It is the most reduced in the sample with 6% OPC, as determined by the rutting test. This was the highest percentage of OPC tested in this study. Therefore, a mix of 6% OPC can be recommended for hot regions where the most common type of pavement distress is rutting.

- Nonetheless, all mix samples with CF performed better than any of the mixes with OPC, as determined by the rutting text. As opposed to the mixes with OPC, mixes with fiber performed better with lower percentages. Which is to say that both the 0.25% and the 0.5% CF mixes were superior to the 0.75% CF mix, and all were superior to either the OPC or the control samples. Therefore, an HMA with CF can be recommended for HMA construction in hot regions instead of OCP mixes.

This study also has some limitations, which are as follows. To keep the project costs low, it used a mix of natural and crushed aggregates from 0 to 10 mm. Also, the study only used B60/70 bitumen because it is, at present, the most common bitumen formulation used in Libyan roadworks. Further research should also consider HMA additives, such as fiber, polymer, fly ash, or other recycled materials. Lastly, longitudinal testing is recommended to better understand how it might withstand daily axle loads over the course of many years.

CHAPITRE 5

USING CEMENT AS FILLER TO ENHANCE ASPHALT MIXES PERFORMANCE IN HOT REGIONS

Aioub H. Guha [(a)] & Gabriel J. Assaf [(b)]

[(a)], [(b)] Construction Engineering Department Ecole de Technologies Superieure,
1100 Notre-Dame West, Montreal, Quebec H3C 1K3, Canada.

Paper submitted to the Journal of Transportation Geotechnics, October 2021

ABSTRACT

This paper investigates the addition of different percentages of ordinary Portland cement as a filler in conventional asphalt concrete (AC) for a range of heavy traffic. The examined properties include the resilient modulus and the resistance to rutting. Findings indicate that the resistance to rutting and the rigidity of the AC are both substantially increased as the cement content is increased. Moreover, to meet the heavy traffic spectrum requirements, increasing the embedded cement content in the asphalt concrete improves pavement structural capacity. Finally, based on the rigidity expected for different cement levels, design curves are provided for pavement design in hot climates using low quality aggregate materials.

Keywords: Portland cement, filler, Hot Mix Asphalt, rutting, B60/70.

5.1 Introduction

Pavement rutting is often observed in countries where good construction material is not always available to build pavements that can withstand heavy traffic. Rutting is even more severe when the in-service is high. This is because Marshall formulated conventional Hot Mix Asphalt (HMA) mix designs still employ conventional filler materials. They also do not use the temperature equivalent modulus of the HMA to withstand the expected traffic loads resulting in substantial rutting and shoving (Almadwi and Assaf 2017).

The temperatures of pavement surfaces in the Sahara and other hot geographical areas can rise up to 70°C (Salem et al. 2014). Unfortunately, the HMA mix design for these roads relies on traditional materials like bitumen penetration grade asphalt binders (e.g., B60/70). The inappropriate bitumen for this hot environment results in considerable shoving and rutting. Moreover, Libya's present road construction testing uses the conventional "Marshall Method" (MM) since 1939 (Zumrawi & Sheikh Edrees 2016). This test is unsuitable for roads in hot countries, such as Libya. Nonetheless, it is presently almost exclusively used for HMA mix designs in high climates.

The "Superpave Mix Design Method" (SPM) was developed as part of the Strategic Highway Research Program (SHRP) undertaken in 1987-1993 (Swami et al. 2004). One benefit of SPM is that it uses various pavement additives, such as cement, polymers, or fibers, to improve asphalt-concrete mix performance (Guha & Assaf 2020b). This paper investigates the recourse to OPC as a substitute to fillers with B60/70 bitumen to increase asphalt mixture stability against rutting and rigidity to reduce the thickness. This new mix therefore offsets the B60/70 bitumen's soft performance.

5.2 Background

Asphalt pavements rapidly deteriorate, resulting in much shorter lifespans than originally projected. It is well documented that asphalt pavements fail to perform as required in hot countries, by demonstrating permanent deformation (e.g., rutting and shoving). The primary causes of deformation are heavy traffic and high temperatures (Guha & Assaf 2020a). Pavement constructed using MM regulations with the B60/70 bitumen demonstrate high occurrences of deformation that require higher maintenance costs. The substantial deformation of road surfaces in desert regions is due to: a) the use of widely available rounded Saharan sand and b) poor bitumen deformation resistance in hot temperatures (Almadwi & Assaf 2018). Therefore, the challenge, particularly in hot developing countries, is to both use better quality materials and minimize the project's total cost.

HMA develops rutting when the vertical compressive strain exerted by the axle loads is higher than the allowable strain obtained from the fatigue curve for that HMA at the prevailing temperatures. Rutting is therefore conditioned by the bitumen viscosity at the established service temperature, but also the angularity of the aggregates, and the asphalt mix's design per se. Various studies explore how to increase HMA stability with OPC as an alternative filler. These challenges have been widely investigated by (Willway et al. 2008)). Zhao and Pang (1998) found that composites of OPC-asphalt emulsion maintain the asphalt binders' flexibility and the OPC's strength. Using recycled, wet aggregates in the asphalt mix, OPC has been shown to both prevent binder stripping and enhance the bitumen coating (James & Reid, 1969). Schmidt and Graf (1974) have shown that lime and OPC improve the resistance of HMAs to wet and dry conditions. (Head, 1974) also reported that OPC additives not only improve the stability of cold-mix asphalt, but also its resilience. Likewise (Uemura & Nakamori 1993) found that adding a mere one percent more of OPC enhances MM stability from 250% to 300%.

Furthermore (Al-khateeb & Al-Akha, 2011) show that mixing cement with asphalt binders enhances both their speed of rotation and viscosity (up to 135ºC). They also report that a cement-to-asphalt ratio of 0.15 is needed for a stable rise of the rotational viscosity. These changes improve the HMA's successful performance and overall stiffness at hot temperatures.

Additionally, (Brown & Needham, 2000) report that parameters such as curing time, void content, additives (e.g., OPC), and binder grades affect the mechanical properties of OPC in asphalt emulsions. They also report that adding OPC changes the emulsion droplet characteristics, in which its electronic charge converts from negative to positive. Other qualities this addition influences are temperature, pressure, emulsifier level, and bitumen type.

Conversely (Pouliot et al., 2003) analyzed the hydration process of mortars, microstructures, and their mechanical properties with a binder made of a small portion of asphalt emulsion (SS-1 and CSS-1) and a cement slurry. Their findings indicate that an asphalt emulsion added to the mix in small amounts had a slight yet significant influence on the OPC's hydration process. Furthermore, mortars that use cationic emulsions (CSS-1) have an elevated elastic modulus than those using anionic emulsions (SS-1), and, therefore, have increased strength.

In a study on the practical use of polymeric admixtures in pavement emulsions (Song et al. 2006) found significant pavement quality improvements by raising the polymer-cement ratios. These improvements affect waterproofness, chloride-ion penetration, and carbonation resistance. Increasing polymer-cement ratios was also found to reduce the mix's compressive strength and its propensity to cling to the mortar substrate.

Wang and Sha (2010) demonstrate that the interactions from the aggregate and the OPC-asphalt emulsion differ from the interactions of mixes with either the bitumen or OPC and the aggregate. This study also uses an apparatus that measures micro hardness (MH-5) to estimate the impacts of OPC varieties, aggregate lithology, and fineness of differences in pavement rigidity due to binder and aggregate interactions. Finally, the study shows that additional OPC and fine mineral filler improves pavement rigidity. However, when the mineral filler was too fine, this advantage was lost.

Oruc (2013) investigated various asphalt additives' influence on creep-strain in heavily used roads, such as highways. The authors added various percentages of salvaged factory waste asphalt as a mineral filler in their HMA mixtures. Moreover, they used the MM to prepare a series of cold-mix asphalt emulsion mixtures. The literature shows that asphalt works as a subordinate binder for emulsion mixtures. Both creep-resistance and pavement deformation were enhanced in mixtures with more OPC.

Another work by (Amhadi & Assaf, 2019) studied how by mixtures of manufactured aggregates, OPC, and natural sand were impacted by base course layer stabilization in low-volume roads. Traditionally, a mixture of cement and sand are used for base-course stabilization, as both of OPC's physical and chemical properties enhance the characteristics of natural sand. Previous studies demonstrate that when base materials are of low-grade, mixtures using 30% (by weight) crushed sand (i.e., manufactured) and 70% natural sand is successfully stabilized. Stabilization also depends on the amount of added OPC (e.g., 3%, 5%, and 7%). Ultimately, the economic advantages of this approach are clear since the transportation of manufactured sand results in higher costs compared to those combining OPC with local materials.

The penetration grade of the chosen aggregate's bitumen is determined by the final asphalt mixture's quality. This mixture quality includes characteristics such as flexibility, stability, durability, as well as moisture and fatigue resistance. Bitumen excess causes wheel pathway bleeding and a reduced pavement lifecycle operation. Therefore, the bitumen's properties directly affect those of the HMA. Standard B60/70 penetration grade bitumen is customarily chosen for pavement works at high temperature locations (Almadwi & Assaf, 2018). To evaluate bitumen hardness, there is a standard test requiring a specific needle gauge that, during a period of five seconds, repeatedly penetrates a sample vertically at 25°C. During the day, pavement surface temperatures in Libya often reach 70°C. This temperature is well above 49-54°C, which is bitumen B60/70s softening point. (Amhadi & Assaf, 2019) tested two approaches to this problem, which consist of a polymer-modified pavement and a harder grade of bitumen mix (e.g., PG70-10).

The current study's primary purpose is to examine whether substituting with an OPC filler can enhance asphalt-concrete mixtures' rigidity when made with low-quality aggregates and B60/70 bitumen. OPC filler substitute was selected since it enables the application of inferior aggregates and binders, maintaining the HMA's good rigidity levels and rutting resistance.

This mixture improves the stability of the HMA and its resilience against shear failure at elevated temperatures. The superpave mix design methods used in the current study are new to various hot, arid, and developing countries. However, research demonstrates that these new designs demonstrate improved durability results compared to the MM (i.e., the most prevalent mix-design method used at present). The four mixtures' performances are assessed using the tensile modulus and wheel track tests. Specifically, to determine the OPC's effect on the pavement mixes' performance in high temperature climates, four diverse amounts of OPC (including 0%, 2%, 4%, and 6%) are used as alternative fillers in four different mixtures. The resulting pavement's structural capacity is also shown to significantly improve as the cement content embedded in the asphalt concrete increases.

5.3 Experimental Procedure and Material

5.3.1 Materials

In this study, asphalt mixtures with a nominal maximum aggregate size of 10 mm, called "ESG10," which is normally used as for surface and binder layers, according to the *Ministère des Transports de Québec* (MTQ 2016). Also, B60/70 bitumen is one of the components in the mixture, with OPC used as filler. The main variable in the four mixtures is the percentage content of the filler. To guarantee a low-cost result, 20% of the mix consists of sand. Also, 74% consists of two types of finely grained, manufactured granite aggregate of between 0 to 5 mm and 5 to 10 mm. The remaining 6% of the mixture is B60/70 bitumen.

5.3.1.1 Aggregate

As presented in Figure 1, sieving was used to separate the aggregate particles by the two required size ranges. Then, the proposed asphalt mixture was combined with the approved aggregates gradation. Next, we tested and summarized the aggregate's fundamental properties. Figure 1 shows that the used aggregate gradation is from between 0 mm to 10 mm.

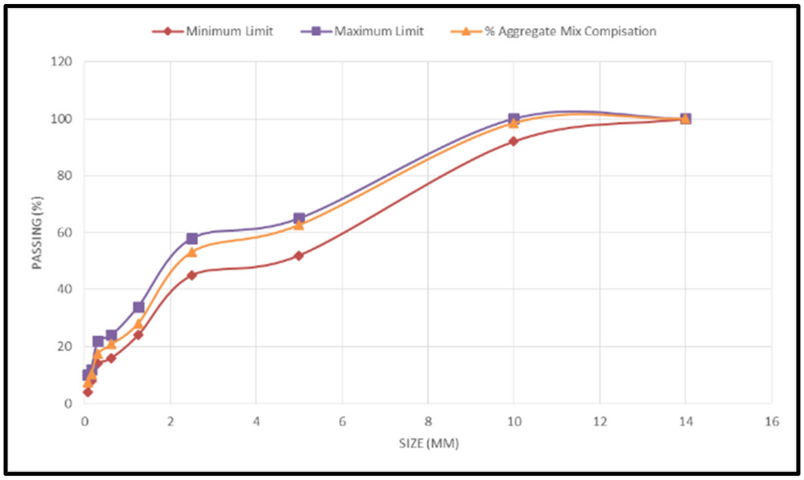

Figure 5. 1 Aggregate gradation curves of the mix

5.3.1.2 Portland Cement

The filler used in the present study is OPC, which is a common construction material locally made and consumed in Libya. Table 1 presents the properties of the OPC additive material.

Table 5. 1 Chemical composition of OPC

Compound	%
Loss on Ignition (LOI)	7.91
SiO2	20.6
CaO	62.8
MgO	2.0
Al2O3	4.3
Fe2O3	3.15
Na2O	0.81
K2O	0.29
SO3	2.65
Materials not solvent	1.02

5.3.1.3 Bitumen

Most road projects in developing countries are constructed using a penetration grade bitumen, consisting of B60/70. The B60/70 is recommended to be mixed at 156°C and compacted at 143°C. Table 2 shows the properties of the binder used here.

Table 5. 2 Chemical composition of bitumen B60/70

Bitumen composition	**Limitation**	**Lab results of B60/70**
Specific Gravity	T228	1.03
Flash point, °C	T48	302
Mass Loss, %	T240	0.07
Penetration at 25°C, dmm	T316	64.7
Ductility at 25°C, cm	T51	143
Softening point, °C	T53	51.7

5.4 Experimental Procedure

5.4.1 Wheel Tracking Tester (WTT)

The WTT is a laboratory for analyzing bituminous mixtures' rutting resistance under various pressure conditions and temperatures. In accordance with the EN 12697-22 (MTQ 2016) standard, this process simulates the many conditions pavement experiences. To induce permanent deformation, bituminous mix specimens are exposed to various passes of a tire that is mounted on a carriage, moving back and forth (see Figure 2). When testing two specimens under the same conditions (i.e., temperature and pressure) they can be placed in the same WTT at once, using two different supports.

For the wheel tracking test, a tire is repeatedly passed over a pavement sample's center twice per second. To achieve sample loading, a tire pressure of 600 kPa and a load of 500-N is applied to the sample. Each slab's dimensions are 500 × 180 × 50-100 mm. A steady temperature of 60°C is applied to all samples throughout the tests to simulate a high temperature climate. The samples were compressed and assessed using the WTT (Figure 2) and are consistent with the (MTQ 2016). Once we completed the mix design experiments and their analyses, we created two pavement slabs for each mix design (i.e. each cement percentage has two samples – 0%, 2%, 4%, and 6%).

To define deformation and find the average rut depth, 15 measurements were taken for each sample - 120 total for the four mixes. The depth was established by loading samples at all repetitions and checking them against the same specifications and standards. We made the first sample measurement after 1,000 cycles at an ambient room temperature of 60°C. The following measurements were made after the next 3,000, 10,000, and 30,000 cycles.

Figure 5. 2 WTT specimen position

5.4.2 The Indirect Tensile Stiffness Modulus (ITSM) Test

Following EN 12697-26 standards, the ITSM test was performed to calculate the HMA samples' stiffness modulus. Specifically, each sample was tested at -5°C, 10°C, and 25°C to investigate the temperature sensitivity of the modulus. Similar to the rutting test, each mix variety was tested using two samples. Each sample was 100 mm wide and 63.5 mm in height. Moreover, for six hours prior to the test, the samples were stored in the ITSM at the particular temperature under investigation. Figure 2 illustrates the test procedures. The equation below is for calculating the stiffness modulus:

$$S_m = (F\times(\mu+0.27))/(h\times Z) \tag{5.1}$$

where, S_m stands for the stiffness modulus, MPa; N; μ refers to the Poisson ratio (i.e., 0.25, 0.30, and 0.40 at -5°C, 10°C, and 25°C, respectively); F is the peak load; h refers to the specimen height in mm; and Z refers to the deformation in the horizontal plane in mm.

5.4.3 WinJulea Software

The WinJulea is pavement thickness design software developed by US Army Corps of Engineers (USACE). This software calculates the stresses, strains and deflections anywhere on or under the pavement for any applied load or set of loads. The input values include pavement materials design parameters, coordinates of the applied load/s and coordinates of points where the operator requires the stresses, strains and/or deflections.

5.5 Results and Discussion

5.5.1 Results of The Rutting Tests

A total of 16 samples were used to evaluate the four mixes, with each mix percentage having four slabs. All samples' rutting depths were established at 1,000, 3,000, 10,000 and 30,000 passes. Table 4 shows that, compared to samples with a lower cement content, rut depths are lesser for the mixes that had higher cement percentages. After the test, the average of different samples was used by the loading system to determine the rutting. Once 30,000 repetitions were achieved, the sample with 0% cement (i.e., the control mix) showed the greatest rutting, while the 6% cement mix (i.e., the highest percentage tested) had the least rutting. Moreover, the rutting test very clearly highlighted the OPC ratio's influence on the rutting performance.

Finally, regarding the various OPC filler percentages (i.e., 0%, 2%, 4%, and 6%), the rut depth was lessened with an equivalent asphalt filler reduction.

Table 5. 3 Rut depth deformation for each sample

Asphalt	**B 60/70**				**LC 4202, ESG10**
Content (%)	**0%Cement**	**2%Cement**	**4%Cement**	**6%Cement**	
1,000 Cycles	5.75	5.12	4.92	4.00	≥ 10
3,000 Cycles	8.42	7.49	6.95	5.41	≥ 15
10,000 Cycles	12.76	11.42	10.35	7.55	-
30,000 Cycles	20.63	15.49	13.26	9.88	-

Each samples' average rut depth values were determined in accordance with the MTQ 4202, ESG10 standard. As demonstrated in Figure 5, the standard requires that each sample shows under 10% rutting from its original height after 1,000-3,000 tire passes. These findings show that adding cement to the mixture (especially at increasingly higher percentages) results in progressively less rutting.

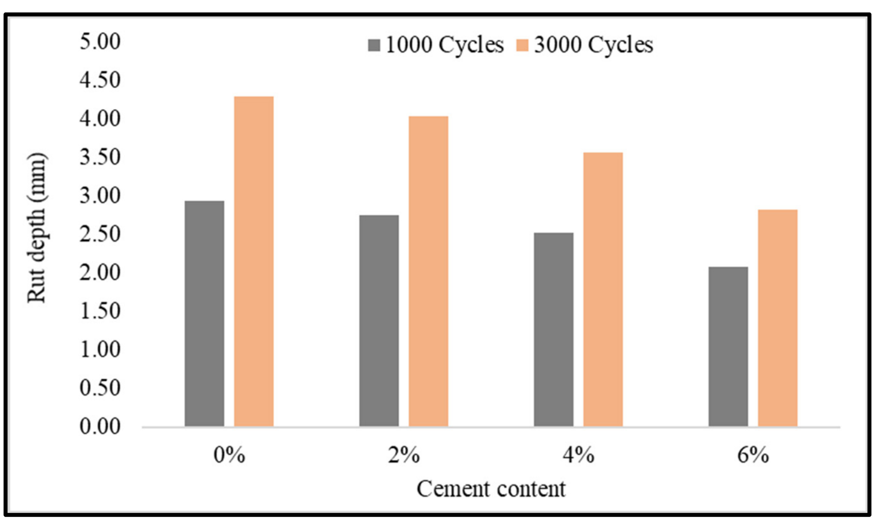

Figure 5. 3 Rutting tests performed at 60°C, rutting depth values for each mix

5.5.2 Results of the ITSM Tests

ITSM tests were carried out to investigate resilient modulus on 12 samples for the four mixes, with all three mix percentages (i.e., -5°C, 15°C, and 25°C) having three samples each. At each temperature, all samples' resilient modulus was superior to the control, and increased with each rise in OPC percentage. As the temperature was increased, each mix's resilient modulus decreased. This was done to show the linear relationship between the cement percentages and the resilient modulus (i.e., with each cement percentage increase is a comparative increase in resilient modulus). Furthermore, each sample's resilient modulus increased as the temperature was reduced, and the lab results showed that the addition of OPC improved the mix's final quality. However, as Figure 5 demonstrates, because of the modulus's different values at various temperatures, the resilient modulus is unable to run comparative analyses on the mixtures.

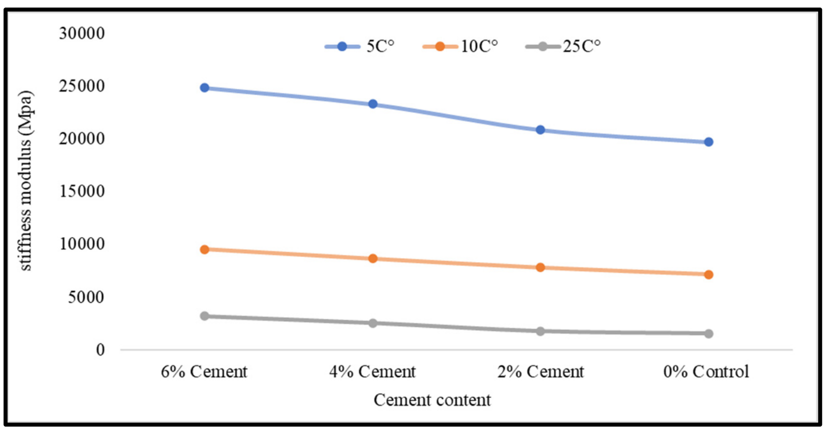

Figure 5. 4 Average ITSM test results for all cement mixtures

5.5.3 Increase of Pavement File

In order to assess the impact of OPC as a filler in asphalt mixes, on the pavement lifetime before rupture, a throughout mechanistic analysis is presented in **Appendix 2**. Eight (8) scenarios are compared: the top layers of the analyzed structures are respectively composed of 75 mm and 100 mm of asphalt concrete with different percentages of OPC as filler (0%, 2%, 4% and 6%). The modulus for each asphalt concrete mix is presented in Figure 5 and rounded up in table 5.4 below:

Table 5. 4 Elastic modulus for each asphalt concrete mix

Asphalt concrete with	**Modulus (25C°)**
0% cement	1,500 MPa
2% cement	2,000 MPa
4% cement	2,500 MPa
6% cement	3,000 MPa

This asphalt concrete layer covers a 300 mm granular base composed of 50% of natural sand and 50% of manufactured sands, deploying CBR of 52 (Amhadi & Assaf, 2019), i.e., an elastic modulus of 520 MPa. The subbase is composed of natural desert sand, deploying CBR of 12 (Fattah, Joni & Ahmed, 2016), i.e., an elastic modulus of 120 MPa. The structural design of the pavement needs to verify four (4) modes of failure:

- Failure in tension at the bottom of the asphalt concrete;
- Failure in compression at the top of the asphalt concrete;
- Failure in compression at the top of the granular base;
- Failure in compression at the top of the subbase.

For the two (2) alternatives proposed *(75 mm and 100 mm of asphalt concrete)*, graphs showing the number of allowable repetitions of an 8-ton axle load for all modes of failure versus the percentage of OPC added (0%, 2%, 4% and 6%) are proposed in Figures 5 and 6 below.

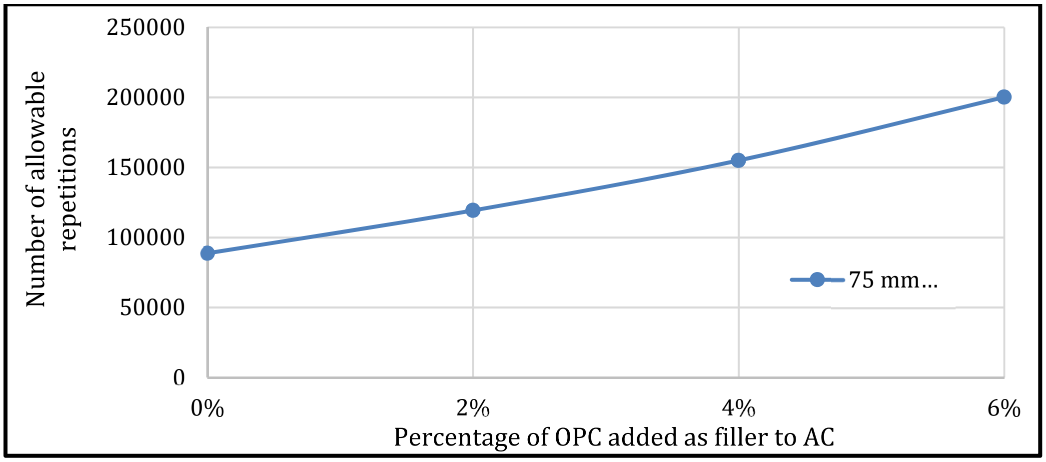

Figure 5. 5 Number of allowable repetitions of an 8-ton axle load for all modes of failure versus the percentage of OPC added as filler to AC (75 mm)

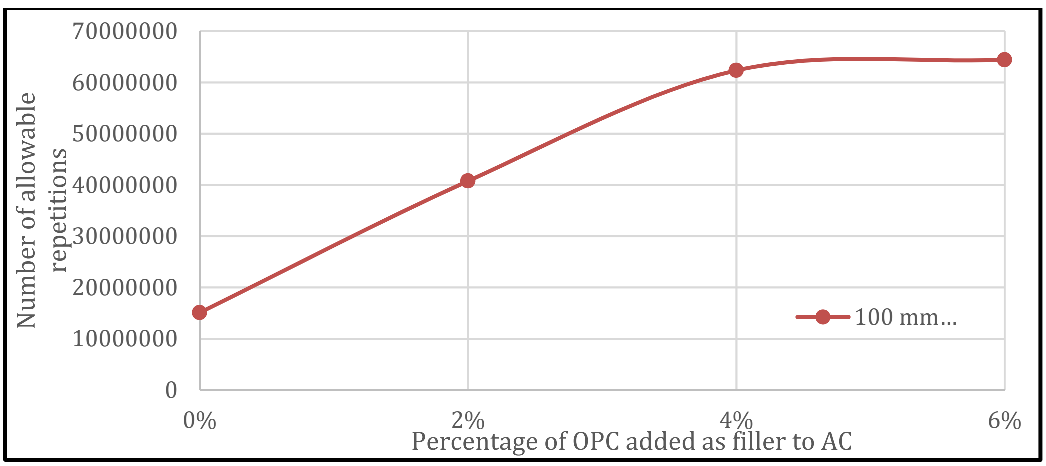

Figure 5. 6 Number of allowable repetitions of an 8-ton axle load for all modes of failure versus the percentage of OPC added as filler to AC (100 mm)

As shown in figures above, for an asphalt top layer of 75 mm, between 0% and 6% OPC adding as a filler to the asphalt mix, the number of allowable repetitions is more than doubled; for an asphalt top layer of 100 mm, between 0% and 6% OPC, the pavement lifetime is 4 times longer. The number of allowable repetitions of an 8-ton axle load, and therefore the lifetime of a pavement structure, is substantially increased as the cement content is increased.

5.5.4 Cost Analysis

The functional unit of the cost analysis is the total cost, expressed in millions of US dollars, with a 1 km road extending the life of the pavement by 10 years. Life cycle cost analysis focuses on those parts of the costs associated with the construction of pavements that have an impact and are paid by stakeholders, i.e., construction firms, road agencies, etc. The stages involved are cash flows and life cycle costs. the entire process of laying the asphalt concrete pavement, as well as the total cost of production, which includes the raw materials involved in the asphalt mixture, additives and various types of graded aggregates required to build 1 km of road per unit length.

5.5.4.1 Calculate Asphalt Quantity

Asphalt is a composite material mixture of aggregate, binder (bitumen) and sand. Aggregate used for asphalt mix could be crushed rock, sand, gravel, or slags. Whereas bitumen actually the liquid binder that holds asphalt together. The term bitumen is often mistakenly used to describe asphalt. Asphalt is widely used for construction and maintaining all types of roads be it for highways, inner-city and inter-city roads, local roads, car parks, or paving driveways pavements.

To calculate the quantity of asphalt and its cost for road construction. The calculation is very easy, you only need some data. For example, here the quantity needs for 1 kilometer with Width of 6m:

Quantity of asphalt calculation:

The volume of asphalt = L x W x H

= 1000 x 6 x .10 = 600 m^3

Therefore, quantity of asphalt = volume of asphalt x Density of asphalt

= 600 x 2330 = 1398000 kg = 1398 Tons

Cost of asphalt:

Suppose the cost of 1 ton asphalt without additive materials is 122.139 USD dollar.

Cost of asphalt = 1398 x 122.139 = 170750.84 $

5.5.4.2 Materials Cost

The purpose of the evaluation is to evaluate a cost-effective material alternative with minimal environmental impact. The study focuses on two main types of mix, the first mix is the control mix without any additive and the second mix with the additive materials for paving, namely OPC and CF. The aggregate for both mixes are the same. Table 1 shows the quantity and the cost for control mix to build 1 km asphalt concrete pavement.

Table 5. 5 Cost and quantity breakdown for control mix to build 1 km of asphalt materials

Aggregate size	Mass (ton)	Material %	Material mass	Quantity (Ton)	Cost $
5-10 mm	1398	65	0.945	858.72	100184.0
0-5 mm	1398	27	0.945	356.69	29724.17
Natural sand	1398	8	0.945	105.68	2642.0
Bitumen	1398	5.5	0.055	76.89	38200.67
Total				1398	170750.84

The second alternative consists of asphalt pavement with Winjulea software, as shown in table 2. The additional materials considered consist of OPC (6%) and the required aggregates.

Suppose the cost of 1 ton asphalt with additive materials 6% 0f OPC is 116.044 USD dollar.

Cost of asphalt = 1398 x 116.044 = 162229.80 $

Table 5. 6 Cost breakdown of road pavement materials using Winjulea Software

Aggregate size	Mass (ton)	Material %	Material mass	Quantity (Ton)	Cost $
5-10 mm	1398	48	0.945	634.1	73978.33
0-5 mm	1398	36	0.945	475.6	39474.8
Natural sand	1398	10	0.945	132.1	2650.0
OPC	1398	6	0.945	79.26	7926.0
Bitumen	1398	5.5	0.055	76.89	38200.67
Total				1398	162229.80

5.5.4.3 Costs of Traffic Signs

The approximate cost of installing the figures and signs. They are based on the offer prices of construction projects in Libya. These costs will vary depending on location, type, quantity, etc. On irregularly shaped signs such as numbered highway route signs, stop and give way signs, or no-travel pennants, the area of the sign to pay is usually based at the largest width multiplied by the largest height. All costs are for complete on-site assembly of the sign, including all panels, reflective sheets and legend, labor, fabrication, films, shipping, equipment, and pole painting/finishing. Note that inflation, changes in labor costs, and fluctuations in commodity markets and metal prices can quickly render some of these figures obsolete. Use with caution. Sign panels: warning, marker, Regulatory, and for the small guide signs on flat sheet panels the cost is $25 to $35 per square foot. Larger guide signs on extruded panels or frames the cost is $30 to $40 per square foot.

5.6 CONCLUSION

The present study investigates the use of OPC in HMA at various percentages (i.e., 0%, 2%, 4%, and 6%) to determine its range of road surface performance under typical environmental conditions. In particular, laboratory tests were conducted on various HMA mixtures with a range of OPC percentages from zero to six. Ultimately, percentages were identified based on the mix's total weight and the test results are as follows:

1. As OPC is increased, rutting is reduced. The 6% OPC mixtures demonstrate the best performance of all the samples and are recommended in this study for hot regions.

2. Adding OPC to HMA enhances pavement stability and reduces flow, resulting in decrease rutting. Thus, OPC improves the final mix's overall strength.

3. As the temperature applied to each mix was increased, their resilient modulus decreased. By contrast, each sample's resilient modulus increased as the temperature was reduced.

Therefore, the laboratory results indicate that the addition of OPC improves pavement's final quality.

4. These findings are based on figure analyses that demonstrate how adding 6% OPC to HMA is recommended in hot and arid countries since it is a low-cost method of strengthening asphalt in such areas.

CONCLUSION

The present study's objective is to increase the pavement stability and resistance to permanent deformation and to determine the range of properties for pavement performance. Laboratory tests were performed on different HMA with different percentages of OPC and CF incorporated into the HMA. Percentages were determined by total weight and then used to determine the feasibility of incorporating OPC and/or CF as an additive in HMA. The influence of such an additive can be discussed as follows:

- Rutting is reduced with an increase in OPC, as determined by the rutting test. 6% mixtures of OPC show superior performance and are recommended for hot regions where the most common type of pavement distress is rutting.

- OPC as an additive to HMA creates better stability and decreases flow, leading to less rutting and improving the overall strength of the final mix.

- The 6% cement mixes have a lower air-void percentage and result in less moisture damage when compared with mix percentages of 4% and 2%.

- These conclusions are based on the laboratory data analysis, all showing that 6% OPC content is recommended for use in modifying the HMA in hot and arid countries like Libya. It is a low-cost way to improve pavement in these regions.

- As the temperature applied to each mix was increased, their resilient modulus decreased. By contrast, each sample's resilient modulus increased as the temperature was reduced. Therefore, the laboratory results indicate that the addition of OPC improves pavement's final quality.

- These findings are based on figure analyses that demonstrate how adding 6% OPC to HMA is recommended in hot and arid countries since it is a low-cost method of strengthening asphalt in such areas.

- Both OPC and CF are superior to the control mix. In all mix samples with OPC, rutting is reduced. It is the most reduced in the sample with 6% OPC, as determined by the rutting test. This was the highest percentage of OPC tested in this study. Therefore, a mix of 6% OPC can be recommended for hot regions where the most common type of pavement distress is rutting.

- Nonetheless, all mix samples with CF performed better than any of the mixes with OPC, as determined by the rutting text. As opposed to the mixes with OPC, mixes with fiber performed better with lower percentages. This is to say that both the 0.25% and the 0.5% CF mixes were superior to the 0.75% CF mix, and all were superior to either the OPC or the control samples. Therefore, an HMA with CF can be recommended for HMA construction in hot regions instead of OCP mixes.

This study also has some limitations, which are as follows. To keep the project costs low, it used a mix of natural and crushed aggregates from 0 to 10 mm. Furthermore, the study only used B60/70 bitumen because it is, at present, the most common bitumen formulation used in Libyan roadworks. Further research should also consider HMA additives, such as fiber, polymer, fly ash, or other recycled materials. Lastly, longitudinal testing is recommended to better understand how it might withstand daily axle loads over the course of many years.

RECOMMENDATIONS

This study presents recommendations for using asphalt mixes in hot regions. These asphalt mixtures require the use of an asphalt binder to reduce the negative impacts of pavement temperature shifts and higher traffic loads. Asphalt binders are largely unaffected by significant temperature changes in hot regions, such as the Middle East. Thus, asphalt binders are highly recommended for hot region pavement mixes.

Road engineers must consider climate factors, such as solar radiation and air temperature. Also, the maximum and minimum temperatures of the region's asphalt pavement should inform the use of asphalt binders. Otherwise, by continuing to use conventional B60/70 mixes, failures, such as premature rutting and disintegration, will appear.

In the Sahara region, desert jurisdictions should be divided into climate zones based on the maximum and minimum pavement temperatures. These zones will help engineers select the most appropriate asphalt binder for each area.

Modifying the traditional MM by using additives, such as polymer (BSR), RAP, brick powder, rubber, and performance grade binders (PG), is strongly recommended. However, the use of mixtures with PG, or any other additives, has not been investigated but might change the pavement's performance and characteristics. In addition, a highly detailed gyratory compactor evaluation is needed for designing asphalt mixtures in hot regions, such as Libya and the Middle East.

It is recommended that future studies include a life cycle cost analysis to help choose the optimum HMA structure and material;

The durability and performance of asphalt pavement subjected to repeated daily hot wind currents has not been studied yet. There have not been any rutting criteria to take into account daily repeated high temperature winds.

The SPM is a helpful field management tool whose effectiveness is comparable to the MM in various respects. Findings indicate that modifying the existing asphalt mix improves the asphalt binder characteristics. Moreover, the SPM compaction method enhances the hot mix asphalt's mechanical and physical properties in hot regions.

APPENDIX I

REPRESENTING COLLECTED ROAD CONDITION DATA WITH CHERNOFF FACES FOR EVALUATION OF PAVEMENT CONDITIONS

Aioub H. Guha [(a)] & Gabriel J. Assaf [(b)]

[(a)], [(b)] Construction Engineering Department Ecole de Technologies Superieure,
1100 Notre-Dame West, Montreal, Quebec H3C 1K3, Canada.

Conference Paper Published in Testing and Characterization of Asphalt Materials and Pavement Structures. The 5th GeoChina International Conference 2018. HangZhou, China. Sustainable Civil Infrastructures. Springer.

Abstract: Maintenance engineers have a problem because of the large quantity of data they must consider when evaluating kilometres of roads and because road roughness data measured with IRI (or possibly PCI) cannot be considered in isolation from other data such as Construction and Workmanship; Mix and Structural Design; Traffic; Climate (during and after construction). Incorporating these five data points into a single conventional graph would require a graph in five dimensions and such a graph would lose much of the benefits that a graph is meant to give (i.e., speed of data comprehension and readability). The Chernoff Face Method (CFM) is an iconic visualization technique used to code multivariate data to simplify two-dimensional line drawings of faces so as to create a representation of the data that is more intuitively comprehensible to humans. The theory behind CFM is that humans have a special sensitivity to details in a facial representation that they do not have with data representations such as conventional graphic displays (e.g., line and bar graphs). The objective is to find an optimum balance between the volume of the data represented and the comprehensibility of the data. In particular, humans can discern eye size and eyebrows slant in faces with finer distinctions than they would be able to intuitively understand when reading another graph. This promises to be a means of displaying fine-grained data for analysis by mapping data points to possible display variables such as eye size, face shape, eyebrows slant angle (inward, outward, neutral). In order to map the IRI, construction, design, traffic and climate data to the CFM, a Multi-Criteria Analysis (MCA) model was used to determine the optimal number for the scale for each data category. The total number of Chernoff Faces for this problem was found to be

243, so that all five categories of data could be represented. Using CFM in conjunction with this data allows better evaluation of pavement distress.

Keywords: Chernoff face, International roughness index, traffic levels Climate zone, Structural design, material & construction, and Multi-criteria analysis.

1. Introduction

Planners and maintenance engineers are often confronted by the problem of how to understand and analyze large quantities of data. In the domain of roadwork, the data is relatively simple, pertaining to qualities such as road surface roughness, traffic levels, climatic zones, structural design and materials and construction. While these five basic qualities are relatively uncomplicated, if they are defined, for example, every 200 m over many kilometres of roads, the data describing these small variations become overwhelming. The problem is worsened if, for each of those data points, the engineer must either assign or read a number that represents the actual real-world condition. Keeping this all-in active human memory is an almost impossible task.

1.1. Benefits and Limits of Measuring Factors in Pavement Distress

Among the various things affecting pavement quality (and therefore ride quality) pavement distress is considered to be the most important. This distress plays a cumulative role in long-term and incremental degradation caused by traffic and the environment, but this distress can be accurately measured with the International Roughness Index (IRI) (Von Quintus El *et al.,* 2001). Presently, to simplify this data, it is often indicated in terms of the short, word descriptions of the IRI where road surfaces are graded and referred to in general terms such as “smooth”, “rough”, and “very rough” (as in Table 1, row 1) in order to help planners, remember the basic quality of a road. Pavement evaluation methods, such as the IRI and the Pavement Condition Index, PCI, the standard alternative to IRI, are already very sophisticated in terms of data collection but the data these methods collect are hard to communicate to engineers and planners.

Table- A I-1 The levels of quality for each pavement condition factor
Taken from Visintine et al. (2015)

	Factors Types	Status	Description
1	Pavement Roughness IRI	Good (= "smooth")	IRI < 8 m/km
		Fair (= "rough")	8 ≤ IRI ≤ 4 m/km
		Poor (= "very rough")	IRI > 4 m/km
2	Materials and Quality	Good	Material meets specifications
		Fair	Material does not always meet specifications
		Poor	Material often does not meet specifications
3	Construction and Workmanship	Good	All work meets specifications
		Fair	Work does not always meet specifications
		Poor	Most work does not meet specifications
4	Mix and structural design	Good	Meets specifications
		Fair	Mix and/or structural design recommendations does not met structural considered
		Poor	No mix and/or structural design recommendations
5	Traffic Level	Low volume	Fewer than 5000 vehicles per lane per day
		Medium volume	From 5000 to 20,000 vehicles per lane per day
		High volume	Over 20,000 vehicles per lane per day
6	Climate zone during and after construction	Good	No weather problems during or right after construction
		Fair	Some weather problems during or right after construction
		Poor	Significant weather problems during or right after construction

This project uses IRI because it is one of the most common ranking systems for pavement surface smoothness and therefore ride quality (Tighe *et al.,* 2003). Note that the present proposal is not for a new means of measuring pavement distress but simply a method to communicate pavement condition findings that have already been recorded with IRI (or possibly PCI) alongside contributing factors influencing the results collected by the IRI to engineers in a more intuitive way.

Beyond this consideration, the IRI (or PCI) data on their own is not entirely sufficient to communicate everything that an engineer needs in planning maintenance; it would be much more useful to have the IRI data displayed alongside corresponding contributory data (e.g., climate data). This is because the distress of traffic and the environmental factors depends greatly on several factors. Following Adlinge and Gupta (2009) the factors under consideration in the present research are: Pavement Roughness (IRI); Construction and Workmanship; Mix and Structural Design; Traffic; Climate (during and after construction). A better understanding of how these factors interact would help predict the change in the road rating and the changes in the performance of the pavement (Haider and Chatti 2009). For example, with empirical data collected in Virginia, New Jersey, and Maryland, Zhou and Wang (2009) created a predictive model for IRI. The results of this model were then compared with similar models helping them to identify qualities that indicated pavement distress.

These were evaluated in terms of standard criteria for the progression of roughness in pavement over time. Not all pavement distresses have an equal effect on future performance and they therefore affected the reliability of these predictive models (Wang et al. 2007). Smith and Tighe (2004) used the Long-Term Pavement Performance (LTPP) index to research what affected the development of pavement roughness and reported that regional environmental factors and asphalt design had the greatest influence on pavement quality. Several research papers have summarized factors contributing to ride quality, but they are limited because there are many obstacles to empirical data representation (Haider and Chatti 2009). This seemingly simple detail is important in the study of pavement deterioration, particularly when trying to correlate such things as environmental effects with pavement quality changes over time. As such, systems like IRI and PCI are not, on their own, sufficient to communicate all the details that may be important in judging road quality and planning maintenance.

1.2. Problems With Graphs and Data Representation

In order to detect patterns, clusters of effects and even outlying data points in a dataset, researchers have often used graphical representations. These help people see trends that are not obvious without such graphical representations or “graphs”. In such graphs, a balance must be found between data volume and practical means of displaying the data. Nonetheless, indicating more details, in terms of numerical values, as conveyed in a standard graph (bar, line graph, etc.), is hard to remember and is generally considered to be unworkable. Furthermore, a standard graph starts to become hard to read beyond two dimensions (x, y), starting with a graph including three dimensions (x, y, z) and it becomes time consuming to read when there are more dimensions than this, losing many of the advantages of having a graph in the first place. Nonetheless, when engineers are examining many kilometres of roads and must make decisions as to the priority of what to repair sooner and what to repair later, they need more than just two data points; for example, understanding the structural design of a segment of the road can help in those repair decisions. Again, this problem is multiplied by the amount of data represented, i.e. kilometres of roads described every 200 m.

1.3. The Chernoff Face Method (CFM)

One innovative idea was published by Herman Chernoff, a statistician, as “The Use of Faces to Represent to Points in K-Dimensional Space Graphically,” in 1973 in the Journal of the American Statistical Association (Chernoff 1973). His idea was to exploit the human brain’s greater sensitivity to human faces in order to represent complex multivariate data and to assimilate it with others such data at the same time. As described in his 1973 paper, he encoded such multivariate data in the features of simplified human faces; the faces generated by this technique are now known as Chernoff faces and here as the Chernoff Face Method (CFM). In Fig. 2, several of these variables are assigned to a facial trait; from this, a face is generated for each case. In practical terms, Chernoff faces are two-dimensional images, often line drawings, each containing very specific features. Each detail of these facial features can be correlated to features in a dataset. Chernoff faces have been applied to visualization problems in areas such as intelligence analysis, information retrieval and data mining (Chernoff 1973) and using Chernoff faces may allow engineers to represent large datasets in a way that is intuitively accessible for people.

In order to take advantage of the human brain's natural capacities for recognition of various facial features, the options in the Chernoff faces have to be limited to stay within a range of realistic or semi-realistic expressions or characteristics. Therefore, the quantity of features that are adjusted is restricted to that which would make any face contrast with another. Nonetheless, some characteristics are more noticeable to us than others. The human capacity to notice small changes in these features can be ordered as follows: face size; face shape; nose length; mouth location; degree of curves of the smile, location; eye characteristics such as angles, shape, separation, width; location of pupils; width, angles, location of eyebrows. By means of these variables, an engineer can display and store many of these data in a single facial representation, i.e., as opposed displaying a data point as a point on a line graph, the engineer displays a Chernoff face with, for example, five data points within it. Nonetheless, this data could be greater than five with enhancements such as hair, beards, and colour, they were able to display up to twenty dimensions in a single face. Therefore, CFM promises to be a means of displaying fine-grained data for analysis by collecting data points such as: Pavement Roughness (IRI Materials and Quality); Construction and Workmanship; Mix and Structural Design; Traffic; Climate (during and after construction) (Adlinge and Gupta 2009). These will be mapped to display variables such as shape (everything), colour (face, eyes), size (all except the face), spacing (eyes), slant angle (eyebrows, e.g., inward, outward, neutral). See Fig. 1. Mapping data to CFM promises to assist engineers in their recognition and recall of prominent features and patterns of data; these simple but powerful visualization tools can help projects to better understand variations in road pavement quality along the course of a road (Fig. 2).

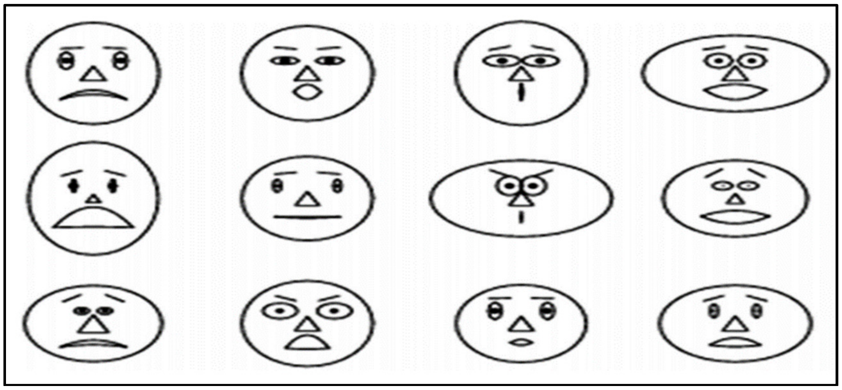

Figure AI- 1 Examples Chernoff faces
Taken from Zhou (2004)

As any conventional graph, using CFM helps recognize clusters and single instances of changes in the quality roads as well as the variables that affect such changes. For the simulations, five facial features were used to characterize the greatest variations in the factors proposed by Adlinge and Gupta (2009) (i.e. traffic loads, environment, pavement thickness, material). These were represented by facial characteristics including nose width and length; mouth curvature; eyebrow length and angle. In order to speed processing, the facial variables that were not needed for the study were set as default values; these included width and shape of eyes and face (Zhou 2004).

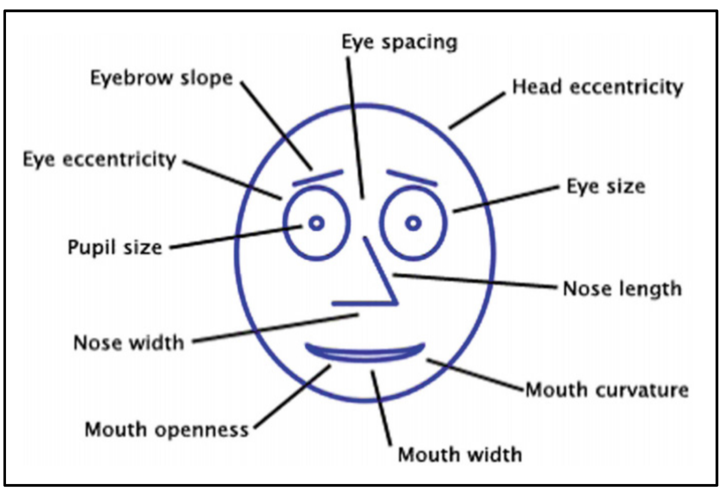

Figure AI- 2 Facial variations
Taken from Zhou (2004)

1.4. Incorporating CFM with Multivariate Data

At this point the benefits of using CFM in conjunction with IRI seem apparent. If the project only considers incorporating the IRI into the CFM, it could simply improve on the standard IRI designations of smooth, rough, and very rough. Initially this was the approach and, for the purposes of integrating the IRI into a broader scale, this study did the following equivalences: Good (= "smooth") IRI < 8 m/km; Fair (= "rough") 8 IRI 4 m/km; Poor (= "very rough") IRI > 4 m/km. In order to evaluate the overall quality of the pavement, this study determined a scale based on common representations of pavement conditions. For practical purposes, this study initially chose a ten-point scale, following the scale discussed in the PASER Asphalt Roads Manual (Walker *et al.,* 2002) where 10 is excellent and 1 is failed; see Table 2. Each step of the PASER scale, as shown in Table 2 (adopted from the PASER manual), gives detailed criteria relating to the road's condition and whether or not it needs repair. 10 indicates a new construction; 9 is a "like new recent overly; 8 is a recent seal coat or new cold mix that requires little or no maintenance; 7 shows first signs of aging; 6 shows signs of aging and the road life could be extended with the seal coat; 5 indicates surface aging but with sound structural conditions; 4 has significant aging and would benefit from 2 inches or more of structural overlay; 3 needs patching and repair before a major overlay; 2 indicates severe deterioration and a need for reconstruction with extensive base repair; 1 indicates a failed pavement with a need for total reconstruction (from the PASER evaluation in Table 2). As such, the PASER scale in Table 2 is a practical needs-based evaluation scale. Details of the points proposed by Adlinge and Gupta (2009) follow.

Table- A I-2 Pavement rating condition based on the PASER scale
Taken from Walker (2002)

Surface Rating	Visible Distress	Photo Surface Distress	General condition
10 Excellent	None.	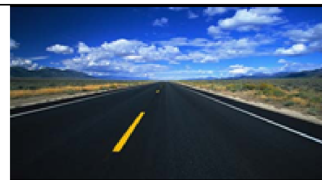	New construction.
9 Excellent	None.	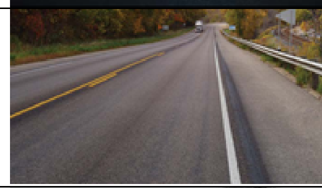	Recent overlay. Like new.
8 Very Good	All cracks sealed or tight (open less than 1⁄4”).		Recent sealcoat or new cold mix. Little or no maintenance required.
7 Good	Very slight or no raveling, surface shows some traffic wear.		First signs of aging. Maintain with routine crack filling.
6 Good	Sight to moderate flushing or polishing. Occasional patching in good condition.		Shows signs of aging. Sound structural condition. Could extend life with sealcoat.

Table- A I-2 Pavement rating condition based on the PASER scale Taken from Walker (2002) (**Continued**)			
Surface Rating	**Visible Distress**	**Photo Surface Distress**	**General condition**
5 Fair	Moderate to severe raveling (loss of fine and coarse aggregate). Extensive to severe flushing or polishing. Some patching or edge wedging in good condition.		Surface aging. Sound structural condition. Needs sealcoat or thin non-structural overlay (less than 2")
4 Fair	Severe surface raveling. Multiple longitudinal and transverse cracking with slight raveling. Longitudinal cracking in wheel path.		Significant aging and first signs of need for strengthening. Would benefit from a structural overlay (2" or more).
3 Poor	Closely spaced longitudinal and transverse cracks often showing raveling and crack erosion. Patches in fair to poor condition. Moderate rutting or distortion (1" or 2" deep).		Needs patching and repair prior to major overlay. Milling and removal of deterioration extends the life of overlay.
2 Very Poor	Alligator cracking (over 25% of surface). Severe distortions (over 2" deep) Extensive patching in poor condition. Potholes.		Severe deterioration. Needs reconstruction with extensive base repair. Pulverization of old pavement is effective.

1.4.1. Structural Design

Al-Suleiman and Shiyab (2003) used roughness data to build a model that estimated the length of the service life of existing roads in Dubai. They created two regression simulations that proved to be statistically significant and that successfully estimated how much service life remained in a slower high traffic lane and an express traffic lane. Hall et al., (2003) studied how control sections compared with test sections of the road with regards to long-term roughness, cracking and rutting. With Canadian LTPP data (Raymond et al. 2003) analyzed the progress of pavement roughness in the first eight years of the lifespan of a new road construction. Their findings indicated that overlay thickness, location, and preexisting cracking all played sizeable roles in the progression of pavement roughness. Prior to resurfacing, factors such as overlay thickness, pavement roughness and how much the surface had been prepared all played a statistically significant effect (95% significance) on the degree of roughness of a newly resurfaced pavement (Raymond et al. 2003). Perera and Kohn (2006) replicated an earlier study tracking roughness on resurfaced pavements showing that the IRI of the pavements depended on the IRI prior to overlay of a new layer, as well as the thickness of the new overlay. Their conclusions did not find that type of asphalt pavement or milling before a new overlay was important to the later progression of pavement roughness, i.e. while a thicker overlay resulted in a surface with a lower IRI (smoother) thickness did not affect IRIs for sections laid over unbound bases (Rahim *et al.,* 2009).

Within the realm of structural design, moisture is the single greatest cause of deterioration of an asphalt road, at all levels of construction. Which is to say, it degrades the surface asphalt level but also the subgrade. Water penetrates the pavement in three general ways: by way of holes and cracks in the top layers; laterally, through the subgrade itself; with capillary action from the water table below the road. Moisture causes particles to be lubricated, which itself causes the interlocking between the particles to deteriorate and for particle displacement. This causes pavement failure (Adlinge and Gupta 2013).

Whether or not moisture has entered the subgrade, ultimately, it is these soils of the subgrade, under the pavement, that support the axle loads. When the subgrade is not sufficient to support these axle loads, the road again becomes too prone to movement and this greater movement eventually results in pavement failure. In cases where there are variations in the subgrade composition that are not or cannot be sufficiently compacted or otherwise compensated for during the pavement design or construction, it can be expected that the pavement will perform poorly or for a shorter time (Adlinge and Gupta 2013).

1.4.2. Climate Zone

Haider and Chatti (2009) found that another important factor affecting IRI was environmental factors. In climates that did not freeze, the greater the variation and degree of moisture in the subgrade, the greater and the faster the increase in pavement roughness. In freezing sites, they found a parallel, where freezing and moisture combined to influence the progression of roughness indices. As might be expected, sites that experienced high degrees of both moisture and freezing indicated the highest reported roughness levels.

Controlling for subgrade types, thinner overlays in areas with high levels of moisture and freezing had higher roughness progression than thicker ones. Nonetheless, roughness progression was the highest in sites with thin overlays, fine subgrade, situated in low-freeze but wet areas (Tighe *et al.,* 2000). Although the condition of a pavement before overlay has an important effect on the as-built roughness of a road (Pais *et al.,* 2013) there is, as yet, no study of how overlays on concrete or asphalt roads progress in terms of roughness.

1.4.3. Traffic Levels

The greatest influence on pavement lifespan and performance is traffic. Specifically, the effects of traffic that play the greatest role in the deterioration of pavement are factors such as the configuration, loading magnitude, and load repetitions by vehicles, particularly heavy trucks (Pais *et al.,* 2013). Every axle load contributes to this deterioration and the standard single-axle load is defined as 80 KN (E80). This defines the deterioration of the road per axle per pass. As such, an asphalt pavement is planned for a given quantity of standard axle loads (i.e., E80s) before it falls below the service level for which it was designed (Adlinge and Gupta 2013).

1.4.4. Quality of Construction

Pavement is directly affected by material quality, moisture levels (during and after construction), degree of compaction, and correct final layer thickness. Due to the critical nature of these factors, skilled design, construction, and quality control inspection crews are very important for road construction. Table 1 shows the levels of quality for each factor for pavement (Visintine et al. 2015).

2. Results

The initial project idea was that the PASER-inspired ten-point scale should be sufficient to determine the factors influencing pavement quality mentioned above. These data were then graded according to whether they are good, fair, or poor except in the case of traffic, where they were graded as: low volume, medium volume, high volume. These data were then going to be mapped to the CFM to provide a better understanding of the existing pavement quality so engineers could make better predictions about what is happening below the pavement surface. An initial Table 1, was created to show the qualities of the IRI as they had been ranked with Traffic Level, Climate Zone, Structural Design, and Material & Construction on a ten-point scale derived from the PASER Manual scale, where 1 = Failed and 10 = Excellent.
Nonetheless, because the project has as an objective the representation of multivariate data, it soon became clear that the dataset would be much too large and therefore unworkable. If many of the variables (e.g. IRI, structural design) were assigned a ten-point scale, the output would give us an outcome of 105 faces. This is clearly not a satisfactory result.

2.1. Multi-criteria Analysis Model

With the project objective of displaying both the IRI data and the data representing these last four areas (structural design, climate zone, traffic levels and quality of construction) a reduced scale for each of these had to be determined. These new scales were chosen based on output from a Multi-Criteria Analysis model (MCA). MCA is a way to make an informed choice when there are many small data points that might otherwise be too complex to navigate and hard to get an actionable outcome. Therefore, the MCA is set up so that many small choices are made between two variables and this is repeated until a final outcome is determined.
Using MCA, the final scale is comprised of 243 faces. Following the logic that a viewer can easily discern between three states of a feature, there are only three states to each feature. For example, with the mouth, a poor road surface is mapped to a frowning mouth; an adequate

road surface is mapped to a neutral mouth (shown with a flat line); an excellent road surface is mapped to a smiling mouth.

The mappings, e.g. of IRI to Mouth, and Traffic Level to Nose, are somewhat arbitrary; because IRI is the determining scale that gives us an overall idea of the quality of the road surface, it is mapped to the mouth, on the assumption that a mouth gives the most obvious impression of an emotional state, i.e. it would make little intuitive sense to have a bad road surface and a happy expression on the mouth, as it is shown in Fig. 3.

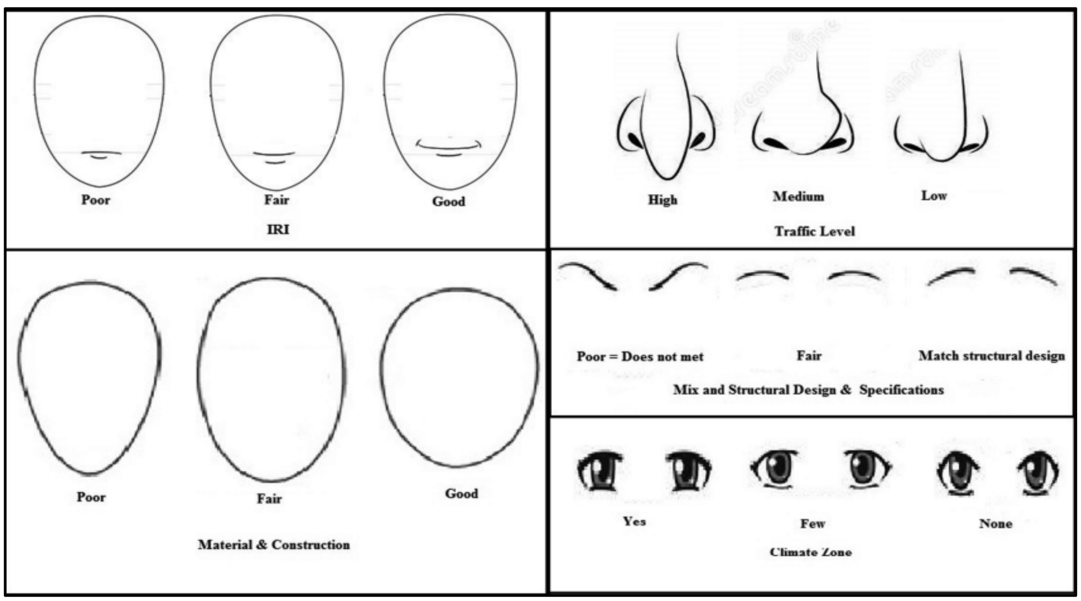

Figure AI- 3 Example of shapes to each feature according to the factors in Table 3

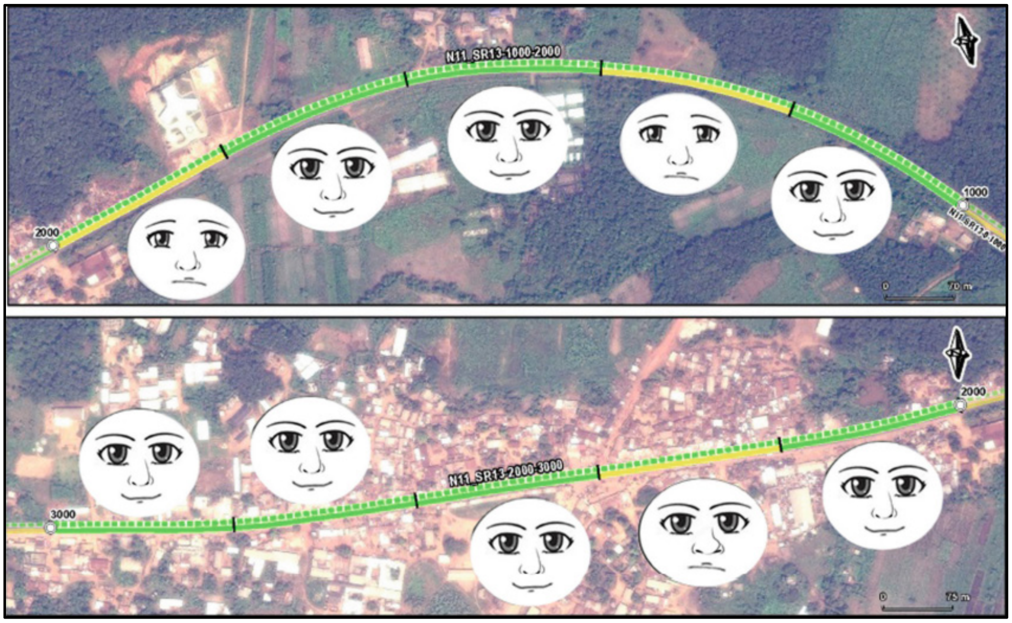

Figure AI- 4 Examples of Chernoff faces showing the factors affecting the surface pavement condition

Figure 4 shows a GIS-generated map with the Chernoff Faces superimposed on it, that indicate the road quality alongside the other data points from Table 3. The image in Figs. 3 and 4 is an example of the standard output of the CFM and could be easily distributed to planners and maintenance engineers making decisions as to what repairs to schedule.

3. Discussion

Evaluating the condition of pavement surfaces is complicated in many ways. In this paper, there were ten initial levels in the scale to reflect the condition of the pavement surface, represented in Table 2. This table shows the initial choices for this project with all the levels and the pavement rating based on the ten-point scale discussed in the "PASER Asphalt Roads Manual" (Walker *et al.,* 2002). For example, with a rating of 9– 10, no maintenance is needed; with a rating of 8, little or no maintenance is needed; with ratings 6–7, routine maintenance is needed; with a rating of 5, preservative treatments are needed; with a rating of 3–4, structural improvements and levelling are needed; with a rating from 1 to 2, reconstruction is needed. These two systems, the PASER scale and the CFM, have been represented in a new scale, called here the CFPSC, the Chernoff Faces Surface Pavement Condition scale, illustrated in

Table 3. The five categories, seen as column designations, represent the data variables with Chernoff faces. These can then be correlated to the pavement rating conditions, seen as rows, and then correlated with the found levels of pavement deterioration.

Table- A I-3 Pavement rating condition ten-point scale

<table>
<tr><th colspan="2" rowspan="2">Segment</th><th colspan="2">IRI m/km</th><th colspan="2">Traffic Level</th><th colspan="2">Climate Zone</th><th colspan="2">Structural design</th><th colspan="2">Material & Construction</th></tr>
<tr><td colspan="2">Mouth</td><td colspan="2">Nose</td><td colspan="2">Eye</td><td colspan="2">Eyebrow</td><td colspan="2">Face</td></tr>
<tr><td rowspan="3">Good</td><td rowspan="3">5</td><td>10</td><td rowspan="3">5</td><td>10</td><td rowspan="3">5</td><td>10</td><td rowspan="3">5</td><td>10</td><td rowspan="3">5</td><td>10</td><td rowspan="3">5</td></tr>
<tr><td>9</td><td>9</td><td>9</td><td>9</td><td>9</td></tr>
<tr><td>8</td><td>8</td><td>8</td><td>8</td><td>8</td></tr>
<tr><td rowspan="3">Fair</td><td rowspan="3">3</td><td>7</td><td rowspan="3">3</td><td>7</td><td rowspan="3">3</td><td>7</td><td rowspan="3">3</td><td>7</td><td rowspan="3">3</td><td>7</td><td rowspan="3">3</td></tr>
<tr><td>6</td><td>6</td><td>6</td><td>6</td><td>6</td></tr>
<tr><td>5</td><td>5</td><td>5</td><td>5</td><td>5</td></tr>
<tr><td rowspan="4">Poor</td><td rowspan="4">1</td><td>4</td><td rowspan="4">1</td><td>4</td><td rowspan="4">1</td><td>4</td><td rowspan="4">1</td><td>4</td><td rowspan="4">1</td><td>4</td><td rowspan="4">1</td></tr>
<tr><td>3</td><td>3</td><td>3</td><td>3</td><td>3</td></tr>
<tr><td>2</td><td>2</td><td>2</td><td>2</td><td>2</td></tr>
<tr><td>1</td><td>1</td><td>1</td><td>1</td><td>1</td></tr>
</table>

As explained in the Results, if the PASER scale were directly implemented into a Chernoff Face Method, there would be as many as 105 face icons. These are clearly too many options for the practical effects that are needed for a successful implementation of the Chernoff Face Method. Therefore, the 10-point scale seen in Table 2 was reduced to three levels for each of the five categories as shown in Table 3, using a Multi-Criteria Analysis model (MCA).

This new scale takes the numerical and the word values from Table 2 and gives new designations in Table 3; these new designations are much simpler but still capture the information required. The Table 2 values of 10, 9, 8 indicate that the pavement condition is “excellent” or “very good”; these are simplified in Table 3 and coded as “green/5/good” (where the number corresponds to the value needed for the MCA). The same equivalences are made from Table 2 where grades 7, 6, 5 are indicated in Table 3 as “yellow/3/fair”. In the final equivalence from Tables 2 to 3, Table 2 grades 4, 3, 2, 1 is indicated in Table 3 as “red/1/poor”. (This conversion process relates to the present project only and would not be entered into for the end user, because it is unnecessary and possibly confusing).

The final Table 3 ratings are determined according to the need for maintenance or repair. Where roads coded “green/5/good” are in good condition and need little to no maintenance. Roads coded “yellow/3/fair” show some surface aging and may benefit from some non-structural maintenance. Roads coded “red/1/poor” require more work, ranging from structural overlay to total reconstruction. These, in turn, indicate the ride quality of the pavement surface.

Figure 3 clearly shows the features of Chernoff faces related to the pavement surface. As indicated above, the variations in faces have been determined, in part, using a Multi-Criteria Analysis model (MCA), using excel. The MCA determined that 243 faces are sufficient to show all the conditions discussed in Table 3. Figure 4 was generated with the Geographic Information System software (GIS), although other software could also be used. To prepare to output an image, such as in Fig. 4, the 243 faces need to be input into the GIS; in Fig. 4, the road was divided into 200 m segments; according to the condition of the road, the GIS maps the correct Chernoff face to each stretch of road.

4. Summary and Conclusions and Further Research

Pavement rating is an important part of an agency’s approach to evaluating road performance. This paper determines how the Chernoff faces help engineers to evaluate the performance of pavement according to many factors, such as pavement condition, construction quality, quality of materials, traffic, and climate. The results clearly show that the deviations from good conditions can have a dramatic effect on the acceptable service life of the pavement, where pavement roughness as determined by the IRI. This new technique will avoid the problem of conflating general pavement quality of a large area of pavement with the quality of a small area contained within the greater pavement surface area.

The challenge for the project now is to determine the best output values for the various shapes and details of the faces so that they represent data points that can be easily read in the field. For example, if the CFPSC (The Chernoff Faces Surface Pavement Condition Scale) relies too much on colour, it may prove difficult to read with a black and white printout; likewise, if it relies too much on size, the data may prove to be harder to judge quickly on a low quality computer screen or printout. Therefore, these variations are being tested and considered with care.

It is clear that the Chernoff Faces Surface Pavement Condition scale (CFPSC), once fine-tuned, is superior to crude descriptions such as good, fair, or poor condition.

APPENDIX II

STRUCTURAL ANALYSIS WITH WINJULEA

In order to assess the impact of cement as a filler in asphalt mixes, on the lifetime of a pavement before rupture, a throughout mechanistic analysis is presented below.

Eight (8) scenarios are considered: the top layer of the analyzed structures is respectively composed of 75 mm and 100 mm of asphalt concrete with different percentages of OPC as filler (0%, 2%, 4% and 6%).

Table- A II-1 Mechanistic analysis

Asphalt concrete with	**Modulus (25C°)**
0% cement	1,500 MPa
2% cement	2,000 MPa
4% cement	2,500 MPa
6% cement	3,000 MPa

This asphalt concrete layer covers a 300 mm granular base composed of 50% of natural sand and 50% of manufactured sands, deploying a CBR of 52, i.e a modulus of 520 MPa.

The subbase is composed natural desert sand deploying a CBR of 12 (Fattah et al. 2016), i.e a modulus of 120 MPa.

The structural design of the pavement needs to verify four (4) modes of failure:

a. Failure in tension at the bottom of the asphalt concrete;

b. Failure in compression at the top of the asphalt concrete;

c. Failure in compression at the top of the granular base;

d. Failure in compression at the top of the subbase.

For the two (2) alternatives proposed (75 mm and 100 mm of asphalt concrete), graphs showing the number of allowable repetitions of an 8-ton axle load for all modes of failure versus the percentage of OPC added (0%, 2%, 4% and 6%) are plotted.

Failure in tension

The Asphalt Institute (1982) suggested that the relationship between fatigue failure of the pavement and tensile strain is represented by the number of load repetitions as follows:

$$N_f = 0.0796(\varepsilon_t)^{-3.291}(E)^{-0.854} \qquad (8.0)$$

Where;
N_f = Number of load applications to failure
ε_t = Horizontal tensile strain at the bottom of asphalt bound layer
E = Elastic Modulus of asphalt concrete

Figure AII- 1 Asphalt Institute Equation to determine structural fatigue life based on tensile strain Taken from Ekwulo and Eme (2009)

Failure in compression

The relationship between fatigue failure of the pavement and compressive strain is represented by the number of load repetitions as follows:

$$N_f = 1.365\,x10^{-9}(\varepsilon_c)^{-4.477} \qquad (11.0)$$

Where;
N_f = Number of load applications to failure
ε_c = Vertical Compressive strain at the bottom of asphalt bound layer

Figure AII- 2 Asphalt Institute Equation to determine structural fatigue life based on compressive strain Taken from Ekwulo and Eme (2009)

Table- A II-2 Results Number of allowable repetitions (Nf) in compression for 75 mm of AC

		(AC) Compressive Strain	**(BASE) Compressive Strain**	**(SUBBASE) Compressive Strain**	**Nf**
Scenario 1	0% cement	0,000093007	0,00082167	0,00041864	88722
Scenario 2	2% cement	0,000088735	0,00076907	0,00040502	119306
Scenario 3	4% cement	0,000089932	0,00072541	0,0003949	154988
Scenario 4	6% cement	0,000087173	0,00068511	0,00038684	200186

Table- A II-3 Number of allowable repetitions (Nf) in compression for 100 mm of AC

		(AC) Compressive Strain	(BASE) Compressive Strain	(SUBBASE) Compressive Strain	Nf
Scenario 5	0% cement	0,000095492	0,00026086	0,00012029	15096501
Scenario 6	2% cement	0,000093172	0,00019905	0,00011624	50661607
Scenario 7	4% cement	0,000094812	0,00016271	0,00011309	124919741
Scenario 8	6% cement	0,000091828	0,00013881	0,00011046	254398728

Table- A II-4 Number of allowable repetitions (Nf) in tension for 75 mm of AC

		Modulus E of AC (MPa)	Tensile strain	Nf
Scenario 1	0% cement	1,500	0,00019037	3858930
Scenario 2	2% cement	2,000	0,00016329	5001243
Scenario 3	4% cement	2,500	0,000159	4511998
Scenario 4	6% cement	3,000	0,00015657	4062189

Table- A II-5 Number of allowable repetitions (Nf) in tension for 100 mm of AC

		Modulus E of AC (MPa)	Tensile strain	Nf
Scenario 5	0% cement	1,500	0,00011562	19915177
Scenario 6	2% cement	2,000	0,000086314	40764734
Scenario 7	4% cement	2,500	0,000071598	62328691
Scenario 8	6% cement	3,000	0,000067611	64410834

Screenshots of WinJulea workspace for each scenario and each mode of failure

Scenario 1: 75 mm of AC + 0% cement

Failure in tension at the bottom of the asphalt concrete

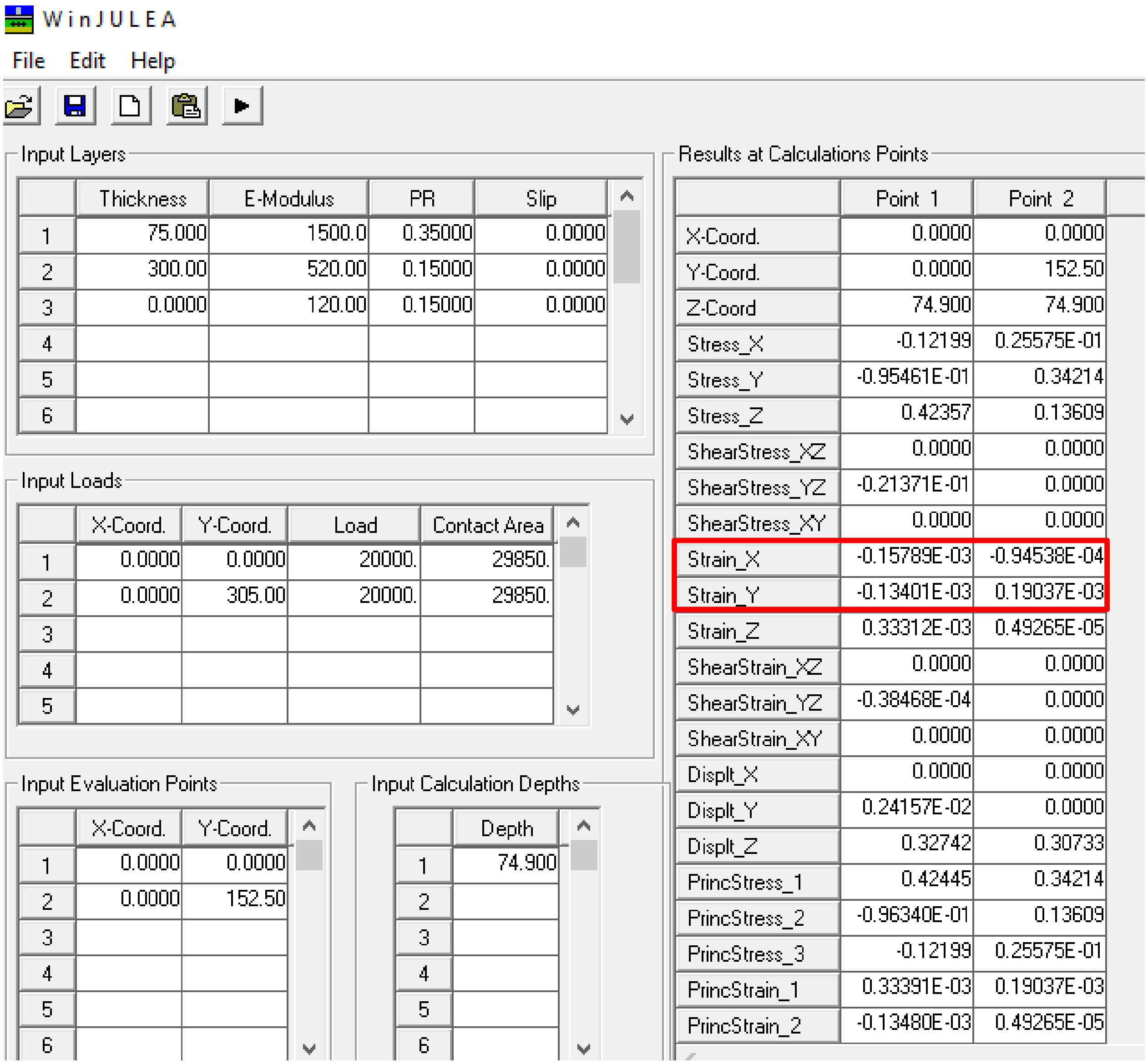

Input Layers

	Thickness	E-Modulus	PR	Slip
1	75.000	1500.0	0.35000	0.0000
2	300.00	520.00	0.15000	0.0000
3	0.0000	120.00	0.15000	0.0000
4				
5				
6				

Input Loads

	X-Coord.	Y-Coord.	Load	Contact Area
1	0.0000	0.0000	20000.	29850.
2	0.0000	305.00	20000.	29850.
3				
4				
5				

Input Evaluation Points

	X-Coord.	Y-Coord.
1	0.0000	0.0000
2	0.0000	152.50
3		
4		
5		
6		

Input Calculation Depths

	Depth
1	74.900
2	
3	
4	
5	
6	

Results at Calculations Points

	Point 1	Point 2
X-Coord.	0.0000	0.0000
Y-Coord.	0.0000	152.50
Z-Coord	74.900	74.900
Stress_X	-0.12199	0.25575E-01
Stress_Y	-0.95461E-01	0.34214
Stress_Z	0.42357	0.13609
ShearStress_XZ	0.0000	0.0000
ShearStress_YZ	-0.21371E-01	0.0000
ShearStress_XY	0.0000	0.0000
Strain_X	-0.15789E-03	-0.94538E-04
Strain_Y	-0.13401E-03	0.19037E-03
Strain_Z	0.33312E-03	0.49265E-05
ShearStrain_XZ	0.0000	0.0000
ShearStrain_YZ	-0.38468E-04	0.0000
ShearStrain_XY	0.0000	0.0000
Displt_X	0.0000	0.0000
Displt_Y	0.24157E-02	0.0000
Displt_Z	0.32742	0.30733
PrincStress_1	0.42445	0.34214
PrincStress_2	-0.96340E-01	0.13609
PrincStress_3	-0.12199	0.25575E-01
PrincStrain_1	0.33391E-03	0.19037E-03
PrincStrain_2	-0.13480E-03	0.49265E-05

Failure in compression at the top of the asphalt concrete

WinJULEA

File Edit Help

Input Layers

	Thickness	E-Modulus	PR	Slip
1	75.000	1500.0	0.35000	0.0000
2	300.00	520.00	0.15000	0.0000
3	0.0000	120.00	0.15000	0.0000
4				
5				
6				

Input Loads

	X-Coord.	Y-Coord.	Load	Contact Area
1	0.0000	0.0000	20000.	29850.
2	0.0000	305.00	20000.	29850.
3				
4				
5				

Input Evaluation Points

	X-Coord.	Y-Coord.
1	0.0000	0.0000
2	0.0000	152.50
3		
4		
5		
6		

Input Calculation Depths

	Depth
1	0.10000
2	
3	
4	
5	
6	

Results at Calculations Points

	Point 1	Point 2
X-Coord.	0.0000	0.0000
Y-Coord.	0.0000	152.50
Z-Coord	0.10000	0.10000
Stress_X	1.0126	0.38043
Stress_Y	0.94051	0.18168E-01
Stress_Z	0.67002	0.0000
ShearStress_XZ	0.0000	0.0000
ShearStress_YZ	0.0000	0.0000
ShearStress_XY	0.0000	0.0000
Strain_X	0.29931E-03	0.24938E-03
Strain_Y	0.23439E-03	-0.76656E-04
Strain_Z	-0.90582E-05	-0.93007E-04
ShearStrain_XZ	0.0000	0.0000
ShearStrain_YZ	0.0000	0.0000
ShearStrain_XY	0.0000	0.0000
Displt_X	0.0000	0.0000
Displt_Y	0.14712E-01	0.0000
Displt_Z	0.34276	0.30207
PrincStress_1	1.0126	0.38043
PrincStress_2	0.94051	0.18168E-01
PrincStress_3	0.67002	0.55511E-16
PrincStrain_1	0.29931E-03	0.24938E-03
PrincStrain_2	0.23439E-03	-0.76656E-04

Failure in compression at the top of the granular base

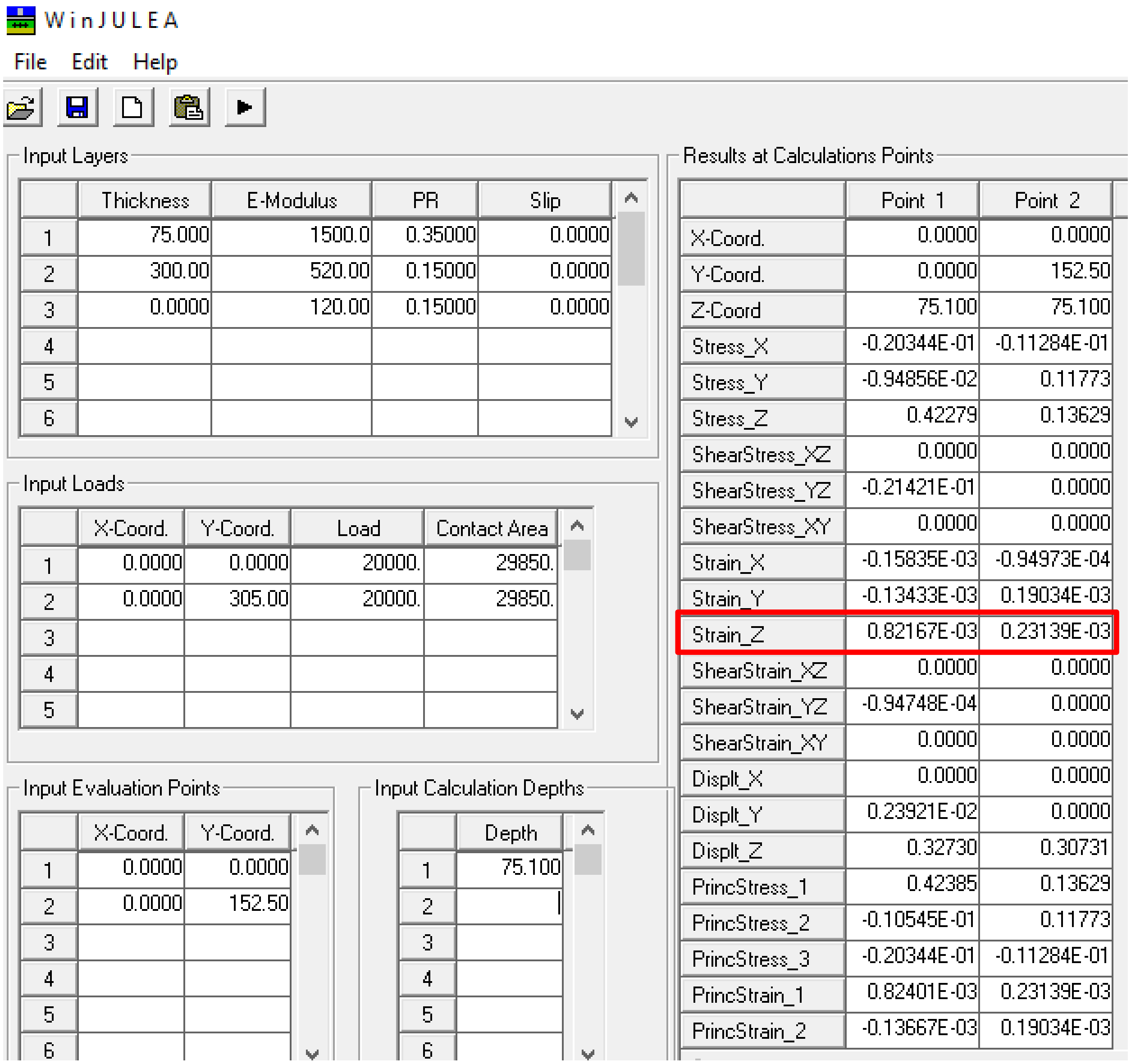

WinJULEA

File Edit Help

Input Layers

	Thickness	E-Modulus	PR	Slip
1	75.000	1500.0	0.35000	0.0000
2	300.00	520.00	0.15000	0.0000
3	0.0000	120.00	0.15000	0.0000
4				
5				
6				

Input Loads

	X-Coord.	Y-Coord.	Load	Contact Area
1	0.0000	0.0000	20000.	29850.
2	0.0000	305.00	20000.	29850.
3				
4				
5				

Input Evaluation Points

	X-Coord.	Y-Coord.
1	0.0000	0.0000
2	0.0000	152.50
3		
4		
5		
6		

Input Calculation Depths

	Depth
1	75.100
2	
3	
4	
5	
6	

Results at Calculations Points

	Point 1	Point 2
X-Coord.	0.0000	0.0000
Y-Coord.	0.0000	152.50
Z-Coord	75.100	75.100
Stress_X	-0.20344E-01	-0.11284E-01
Stress_Y	-0.94856E-02	0.11773
Stress_Z	0.42279	0.13629
ShearStress_XZ	0.0000	0.0000
ShearStress_YZ	-0.21421E-01	0.0000
ShearStress_XY	0.0000	0.0000
Strain_X	-0.15835E-03	-0.94973E-04
Strain_Y	-0.13433E-03	0.19034E-03
Strain_Z	0.82167E-03	0.23139E-03
ShearStrain_XZ	0.0000	0.0000
ShearStrain_YZ	-0.94748E-04	0.0000
ShearStrain_XY	0.0000	0.0000
Displt_X	0.0000	0.0000
Displt_Y	0.23921E-02	0.0000
Displt_Z	0.32730	0.30731
PrincStress_1	0.42385	0.13629
PrincStress_2	-0.10545E-01	0.11773
PrincStress_3	-0.20344E-01	-0.11284E-01
PrincStrain_1	0.82401E-03	0.23139E-03
PrincStrain_2	-0.13667E-03	0.19034E-03

Failure in compression at the top of the subbase

WinJULEA

File Edit Help

Input Layers

	Thickness	E-Modulus	PR	Slip
1	75.000	1500.0	0.35000	0.0000
2	300.00	520.00	0.15000	0.0000
3	0.0000	120.00	0.15000	0.0000
4				
5				
6				

Input Loads

	X-Coord.	Y-Coord.	Load	Contact Area
1	0.0000	0.0000	20000.	29850.
2	0.0000	305.00	20000.	29850.
3				
4				
5				

Input Evaluation Points

	X-Coord.	Y-Coord.
1	0.0000	0.0000
2	0.0000	152.50
3		
4		
5		
6		

Input Calculation Depths

	Depth
1	375.10
2	
3	
4	
5	
6	

Results at Calculations Points

	Point 1	Point 2
X-Coord.	0.0000	0.0000
Y-Coord.	0.0000	152.50
Z-Coord	375.10	375.10
Stress_X	-0.10492E-01	-0.11432E-01
Stress_Y	-0.56934E-02	-0.66837E-02
Stress_Z	0.43755E-01	0.47520E-01
ShearStress_XZ	0.0000	0.0000
ShearStress_YZ	-0.88562E-02	0.0000
ShearStress_XY	0.0000	0.0000
Strain_X	-0.13501E-03	-0.14631E-03
Strain_Y	-0.89024E-04	-0.10081E-03
Strain_Z	0.38486E-03	0.41864E-03
ShearStrain_XZ	0.0000	0.0000
ShearStrain_YZ	-0.16974E-03	0.0000
ShearStrain_XY	0.0000	0.0000
Displt_X	0.0000	0.0000
Displt_Y	-0.14868E-01	0.0000
Displt_Z	0.23474	0.24437
PrincStress_1	0.45294E-01	0.47520E-01
PrincStress_2	-0.72317E-02	-0.66837E-02
PrincStress_3	-0.10492E-01	-0.11432E-01
PrincStrain_1	0.39960E-03	0.41864E-03
PrincStrain_2	-0.10377E-03	-0.10081E-03

Scenario 2: 75 mm of AC + 2% cement

Failure in tension at the bottom of the asphalt concrete

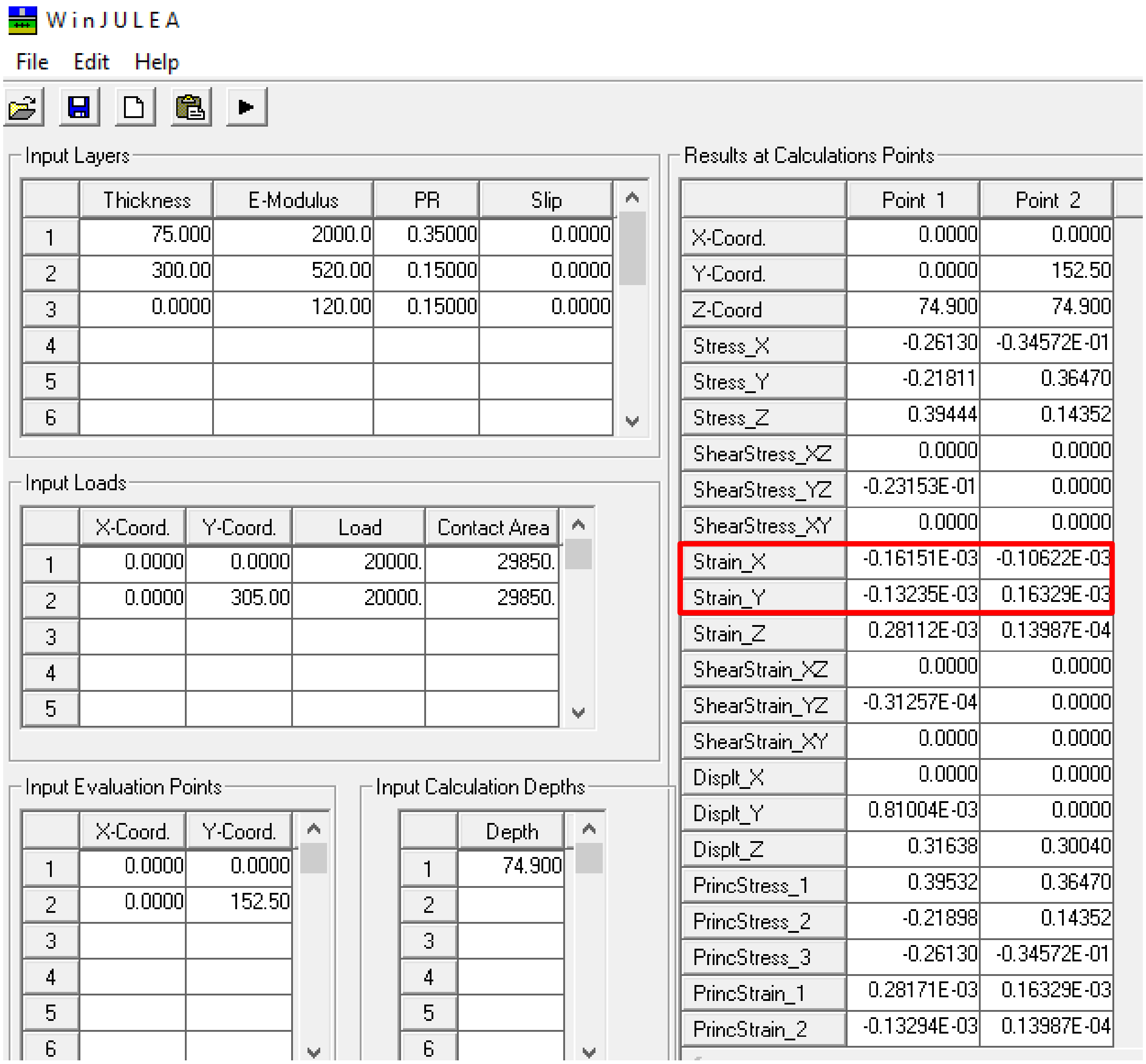

WinJULEA

File Edit Help

Input Layers

	Thickness	E-Modulus	PR	Slip
1	75.000	2000.0	0.35000	0.0000
2	300.00	520.00	0.15000	0.0000
3	0.0000	120.00	0.15000	0.0000
4				
5				
6				

Input Loads

	X-Coord.	Y-Coord.	Load	Contact Area
1	0.0000	0.0000	20000.	29850.
2	0.0000	305.00	20000.	29850.
3				
4				
5				

Input Evaluation Points

	X-Coord.	Y-Coord.
1	0.0000	0.0000
2	0.0000	152.50
3		
4		
5		
6		

Input Calculation Depths

	Depth
1	74.900
2	
3	
4	
5	
6	

Results at Calculations Points

	Point 1	Point 2
X-Coord.	0.0000	0.0000
Y-Coord.	0.0000	152.50
Z-Coord	74.900	74.900
Stress_X	-0.26130	-0.34572E-01
Stress_Y	-0.21811	0.36470
Stress_Z	0.39444	0.14352
ShearStress_XZ	0.0000	0.0000
ShearStress_YZ	-0.23153E-01	0.0000
ShearStress_XY	0.0000	0.0000
Strain_X	-0.16151E-03	-0.10622E-03
Strain_Y	-0.13235E-03	0.16329E-03
Strain_Z	0.28112E-03	0.13987E-04
ShearStrain_XZ	0.0000	0.0000
ShearStrain_YZ	-0.31257E-04	0.0000
ShearStrain_XY	0.0000	0.0000
Displt_X	0.0000	0.0000
Displt_Y	0.81004E-03	0.0000
Displt_Z	0.31638	0.30040
PrincStress_1	0.39532	0.36470
PrincStress_2	-0.21898	0.14352
PrincStress_3	-0.26130	-0.34572E-01
PrincStrain_1	0.28171E-03	0.16329E-03
PrincStrain_2	-0.13294E-03	0.13987E-04

Failure in compression at the top of the asphalt concrete

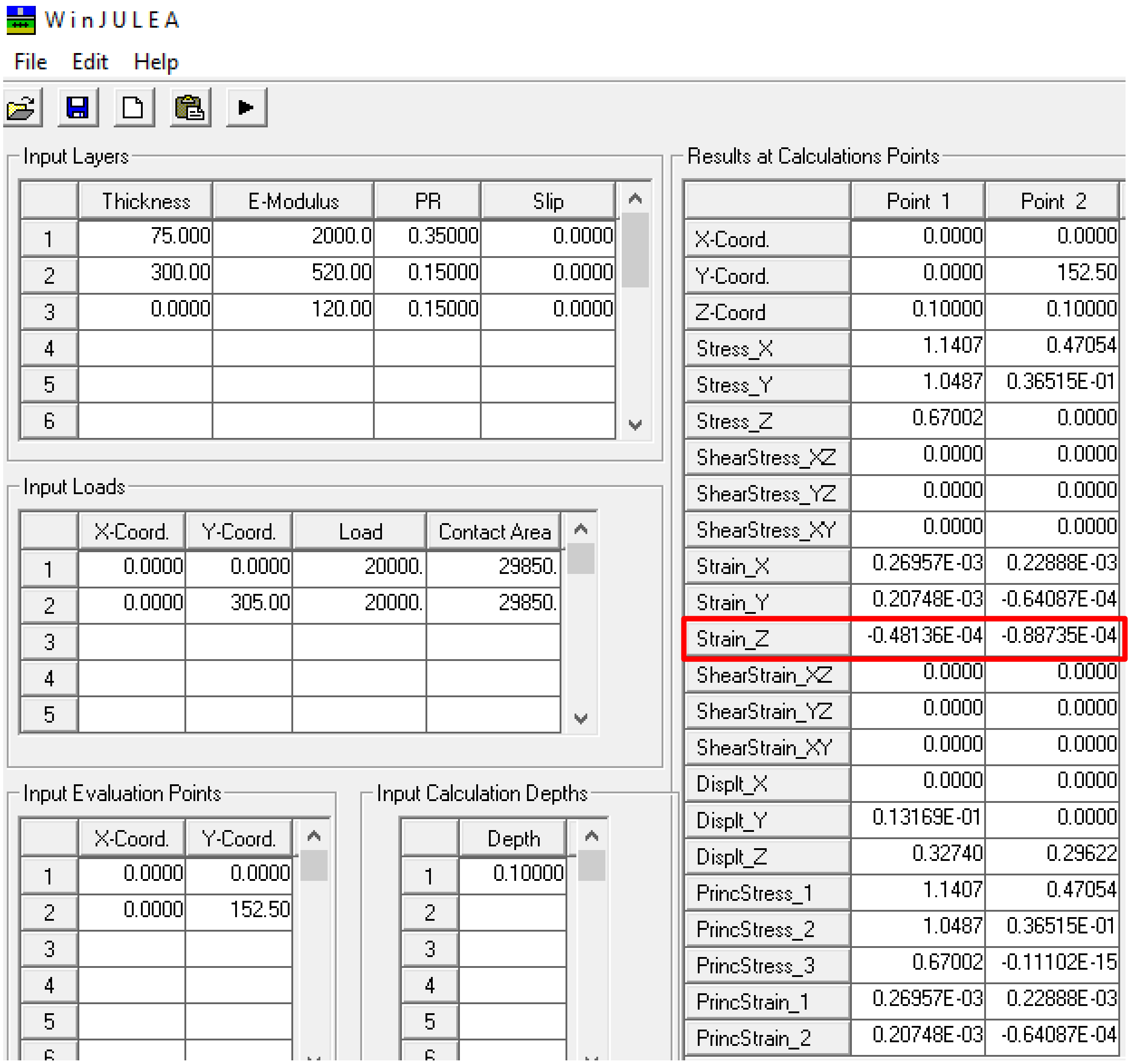

WinJULEA

File Edit Help

Input Layers

	Thickness	E-Modulus	PR	Slip
1	75.000	2000.0	0.35000	0.0000
2	300.00	520.00	0.15000	0.0000
3	0.0000	120.00	0.15000	0.0000
4				
5				
6				

Input Loads

	X-Coord.	Y-Coord.	Load	Contact Area
1	0.0000	0.0000	20000.	29850.
2	0.0000	305.00	20000.	29850.
3				
4				
5				

Input Evaluation Points

	X-Coord.	Y-Coord.
1	0.0000	0.0000
2	0.0000	152.50
3		
4		
5		
6		

Input Calculation Depths

	Depth
1	0.10000
2	
3	
4	
5	
6	

Results at Calculations Points

	Point 1	Point 2
X-Coord.	0.0000	0.0000
Y-Coord.	0.0000	152.50
Z-Coord	0.10000	0.10000
Stress_X	1.1407	0.47054
Stress_Y	1.0487	0.36515E-01
Stress_Z	0.67002	0.0000
ShearStress_XZ	0.0000	0.0000
ShearStress_YZ	0.0000	0.0000
ShearStress_XY	0.0000	0.0000
Strain_X	0.26957E-03	0.22888E-03
Strain_Y	0.20748E-03	-0.64087E-04
Strain_Z	-0.48136E-04	-0.88735E-04
ShearStrain_XZ	0.0000	0.0000
ShearStrain_YZ	0.0000	0.0000
ShearStrain_XY	0.0000	0.0000
Displt_X	0.0000	0.0000
Displt_Y	0.13169E-01	0.0000
Displt_Z	0.32740	0.29622
PrincStress_1	1.1407	0.47054
PrincStress_2	1.0487	0.36515E-01
PrincStress_3	0.67002	-0.11102E-15
PrincStrain_1	0.26957E-03	0.22888E-03
PrincStrain_2	0.20748E-03	-0.64087E-04

Failure in compression at the top of the granular base

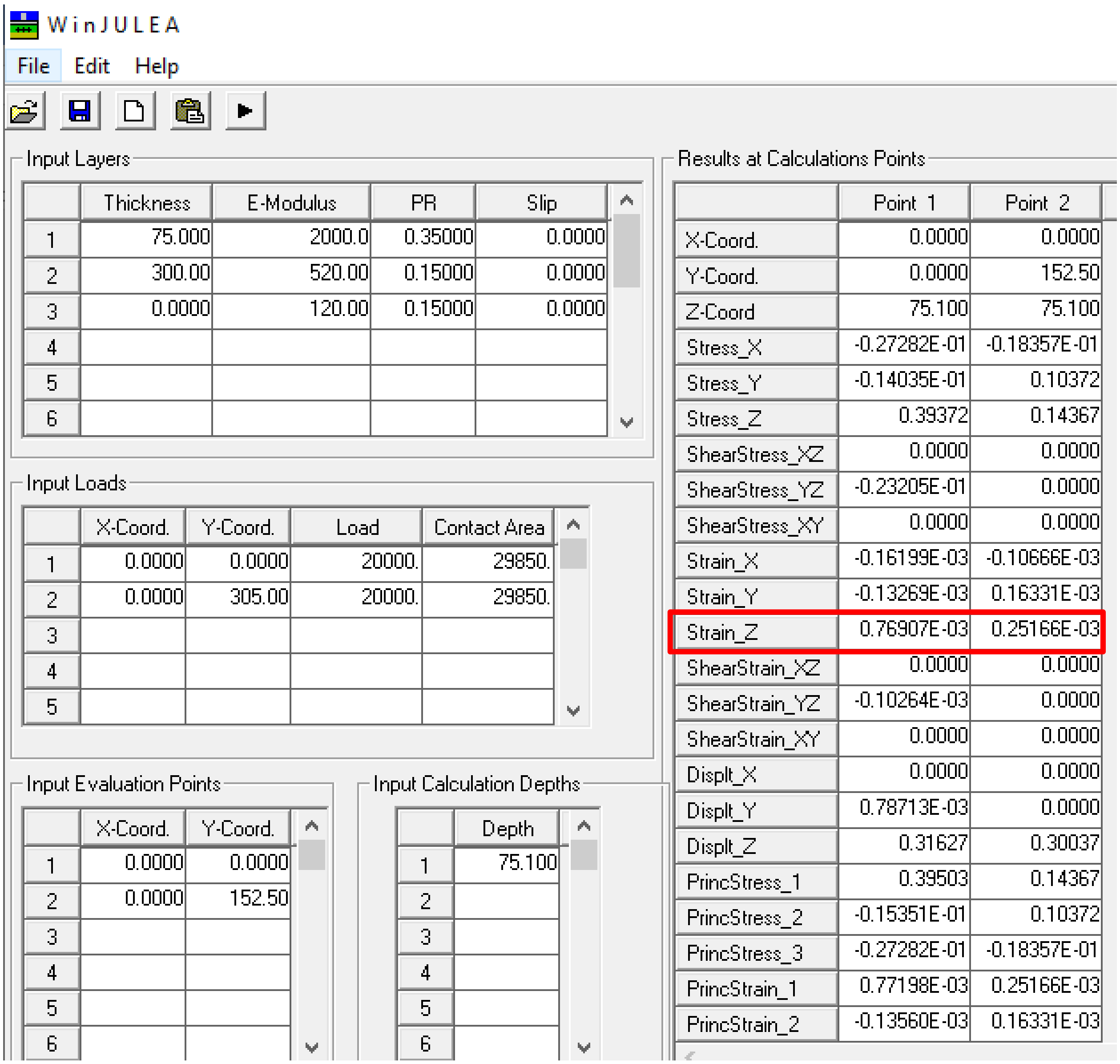

Input Layers

	Thickness	E-Modulus	PR	Slip
1	75.000	2000.0	0.35000	0.0000
2	300.00	520.00	0.15000	0.0000
3	0.0000	120.00	0.15000	0.0000
4				
5				
6				

Input Loads

	X-Coord.	Y-Coord.	Load	Contact Area
1	0.0000	0.0000	20000.	29850.
2	0.0000	305.00	20000.	29850.
3				
4				
5				

Input Evaluation Points

	X-Coord.	Y-Coord.
1	0.0000	0.0000
2	0.0000	152.50
3		
4		
5		
6		

Input Calculation Depths

	Depth
1	75.100
2	
3	
4	
5	
6	

Results at Calculations Points

	Point 1	Point 2
X-Coord.	0.0000	0.0000
Y-Coord.	0.0000	152.50
Z-Coord	75.100	75.100
Stress_X	-0.27282E-01	-0.18357E-01
Stress_Y	-0.14035E-01	0.10372
Stress_Z	0.39372	0.14367
ShearStress_XZ	0.0000	0.0000
ShearStress_YZ	-0.23205E-01	0.0000
ShearStress_XY	0.0000	0.0000
Strain_X	-0.16199E-03	-0.10666E-03
Strain_Y	-0.13269E-03	0.16331E-03
Strain_Z	0.76907E-03	0.25166E-03
ShearStrain_XZ	0.0000	0.0000
ShearStrain_YZ	-0.10264E-03	0.0000
ShearStrain_XY	0.0000	0.0000
Displt_X	0.0000	0.0000
Displt_Y	0.78713E-03	0.0000
Displt_Z	0.31627	0.30037
PrincStress_1	0.39503	0.14367
PrincStress_2	-0.15351E-01	0.10372
PrincStress_3	-0.27282E-01	-0.18357E-01
PrincStrain_1	0.77198E-03	0.25166E-03
PrincStrain_2	-0.13560E-03	0.16331E-03

Failure in compression at the top of the subbase

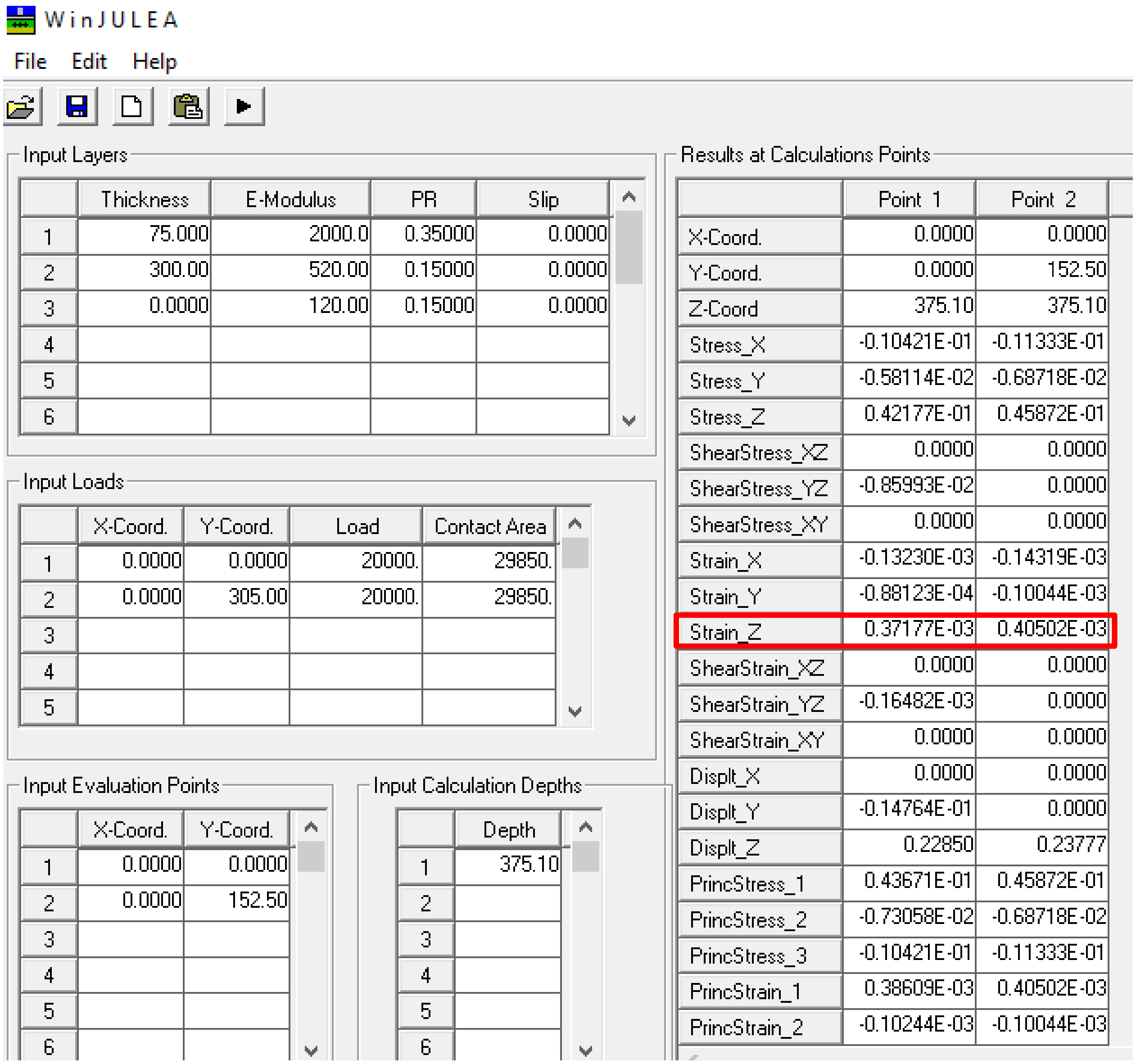

Input Layers

	Thickness	E-Modulus	PR	Slip
1	75.000	2000.0	0.35000	0.0000
2	300.00	520.00	0.15000	0.0000
3	0.0000	120.00	0.15000	0.0000
4				
5				
6				

Input Loads

	X-Coord.	Y-Coord.	Load	Contact Area
1	0.0000	0.0000	20000.	29850.
2	0.0000	305.00	20000.	29850.
3				
4				
5				

Input Evaluation Points

	X-Coord.	Y-Coord.
1	0.0000	0.0000
2	0.0000	152.50
3		
4		
5		
6		

Input Calculation Depths

	Depth
1	375.10
2	
3	
4	
5	
6	

Results at Calculations Points

	Point 1	Point 2
X-Coord.	0.0000	0.0000
Y-Coord.	0.0000	152.50
Z-Coord	375.10	375.10
Stress_X	-0.10421E-01	-0.11333E-01
Stress_Y	-0.58114E-02	-0.68718E-02
Stress_Z	0.42177E-01	0.45872E-01
ShearStress_XZ	0.0000	0.0000
ShearStress_YZ	-0.85993E-02	0.0000
ShearStress_XY	0.0000	0.0000
Strain_X	-0.13230E-03	-0.14319E-03
Strain_Y	-0.88123E-04	-0.10044E-03
Strain_Z	0.37177E-03	0.40502E-03
ShearStrain_XZ	0.0000	0.0000
ShearStrain_YZ	-0.16482E-03	0.0000
ShearStrain_XY	0.0000	0.0000
Displt_X	0.0000	0.0000
Displt_Y	-0.14764E-01	0.0000
Displt_Z	0.22850	0.23777
PrincStress_1	0.43671E-01	0.45872E-01
PrincStress_2	-0.73058E-02	-0.68718E-02
PrincStress_3	-0.10421E-01	-0.11333E-01
PrincStrain_1	0.38609E-03	0.40502E-03
PrincStrain_2	-0.10244E-03	-0.10044E-03

Scenario 3: 75 mm of AC + 4% cement

Failure in tension at the bottom of the asphalt concrete

WinJULEA

File Edit Help

Input Layers

	Thickness	E-Modulus	PR	Slip
1	75.000	2500.0	0.35000	0.0000
2	300.00	520.00	0.15000	0.0000
3	0.0000	120.00	0.15000	0.0000
4				
5				
6				

Input Loads

	X-Coord.	Y-Coord.	Load	Contact Area
1	0.0000	0.0000	20000.	29850.
2	0.0000	305.00	20000.	29850.
3				
4				
5				

Input Evaluation Points

	X-Coord.	Y-Coord.
1	0.0000	0.0000
2	0.0000	152.50
3		
4		
5		
6		

Input Calculation Depths

	Depth
1	74.900
2	
3	
4	
5	
6	

Results at Calculations Points

	Point 1	Point 2
X-Coord.	0.0000	0.0000
Y-Coord.	0.0000	152.50
Z-Coord	74.900	74.900
Stress_X	-0.38054	-0.98069E-01
Stress_Y	-0.32062	0.37202
Stress_Z	0.36906	0.14846
ShearStress_XZ	0.0000	0.0000
ShearStress_YZ	-0.24439E-01	0.0000
ShearStress_XY	0.0000	0.0000
Strain_X	-0.15900E-03	-0.11209E-03
Strain_Y	-0.12664E-03	0.14175E-03
Strain_Z	0.24579E-03	0.21031E-04
ShearStrain_XZ	0.0000	0.0000
ShearStrain_YZ	-0.26394E-04	0.0000
ShearStrain_XY	0.0000	0.0000
Displt_X	0.0000	0.0000
Displt_Y	-0.29319E-03	0.0000
Displt_Z	0.30788	0.29510
PrincStress_1	0.36993	0.37202
PrincStress_2	-0.32148	0.14846
PrincStress_3	-0.38054	-0.98069E-01
PrincStrain_1	0.24626E-03	0.14175E-03
PrincStrain_2	-0.12711E-03	0.21031E-04

Failure in compression at the top of the asphalt concrete

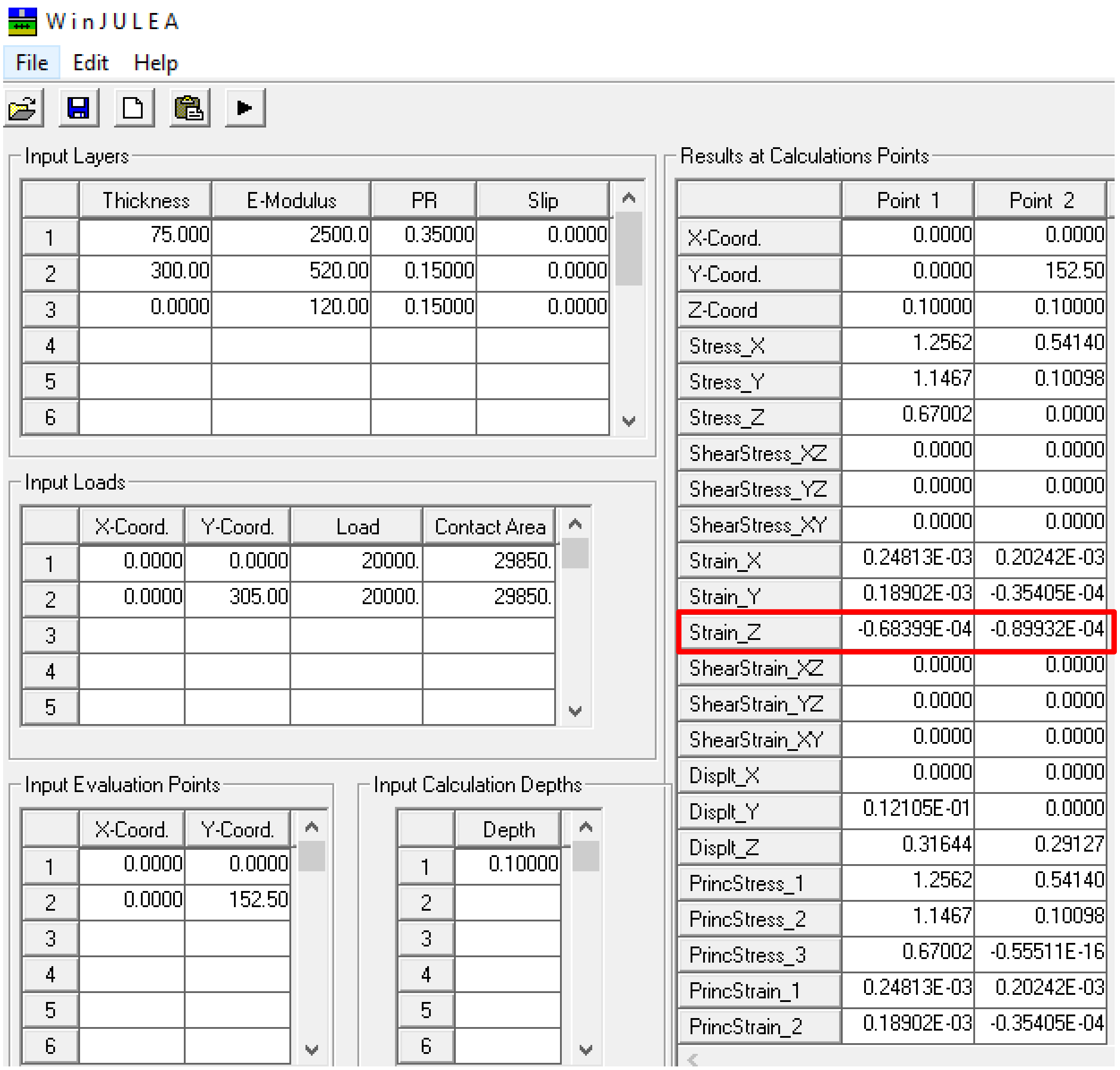

WinJULEA

File Edit Help

Input Layers

	Thickness	E-Modulus	PR	Slip
1	75.000	2500.0	0.35000	0.0000
2	300.00	520.00	0.15000	0.0000
3	0.0000	120.00	0.15000	0.0000
4				
5				
6				

Input Loads

	X-Coord.	Y-Coord.	Load	Contact Area
1	0.0000	0.0000	20000.	29850.
2	0.0000	305.00	20000.	29850.
3				
4				
5				

Input Evaluation Points

	X-Coord.	Y-Coord.
1	0.0000	0.0000
2	0.0000	152.50
3		
4		
5		
6		

Input Calculation Depths

	Depth
1	0.10000
2	
3	
4	
5	
6	

Results at Calculations Points

	Point 1	Point 2
X-Coord.	0.0000	0.0000
Y-Coord.	0.0000	152.50
Z-Coord	0.10000	0.10000
Stress_X	1.2562	0.54140
Stress_Y	1.1467	0.10098
Stress_Z	0.67002	0.0000
ShearStress_XZ	0.0000	0.0000
ShearStress_YZ	0.0000	0.0000
ShearStress_XY	0.0000	0.0000
Strain_X	0.24813E-03	0.20242E-03
Strain_Y	0.18902E-03	-0.35405E-04
Strain_Z	-0.68399E-04	-0.89932E-04
ShearStrain_XZ	0.0000	0.0000
ShearStrain_YZ	0.0000	0.0000
ShearStrain_XY	0.0000	0.0000
Displt_X	0.0000	0.0000
Displt_Y	0.12105E-01	0.0000
Displt_Z	0.31644	0.29127
PrincStress_1	1.2562	0.54140
PrincStress_2	1.1467	0.10098
PrincStress_3	0.67002	-0.55511E-16
PrincStrain_1	0.24813E-03	0.20242E-03
PrincStrain_2	0.18902E-03	-0.35405E-04

Failure in compression at the top of the granular base

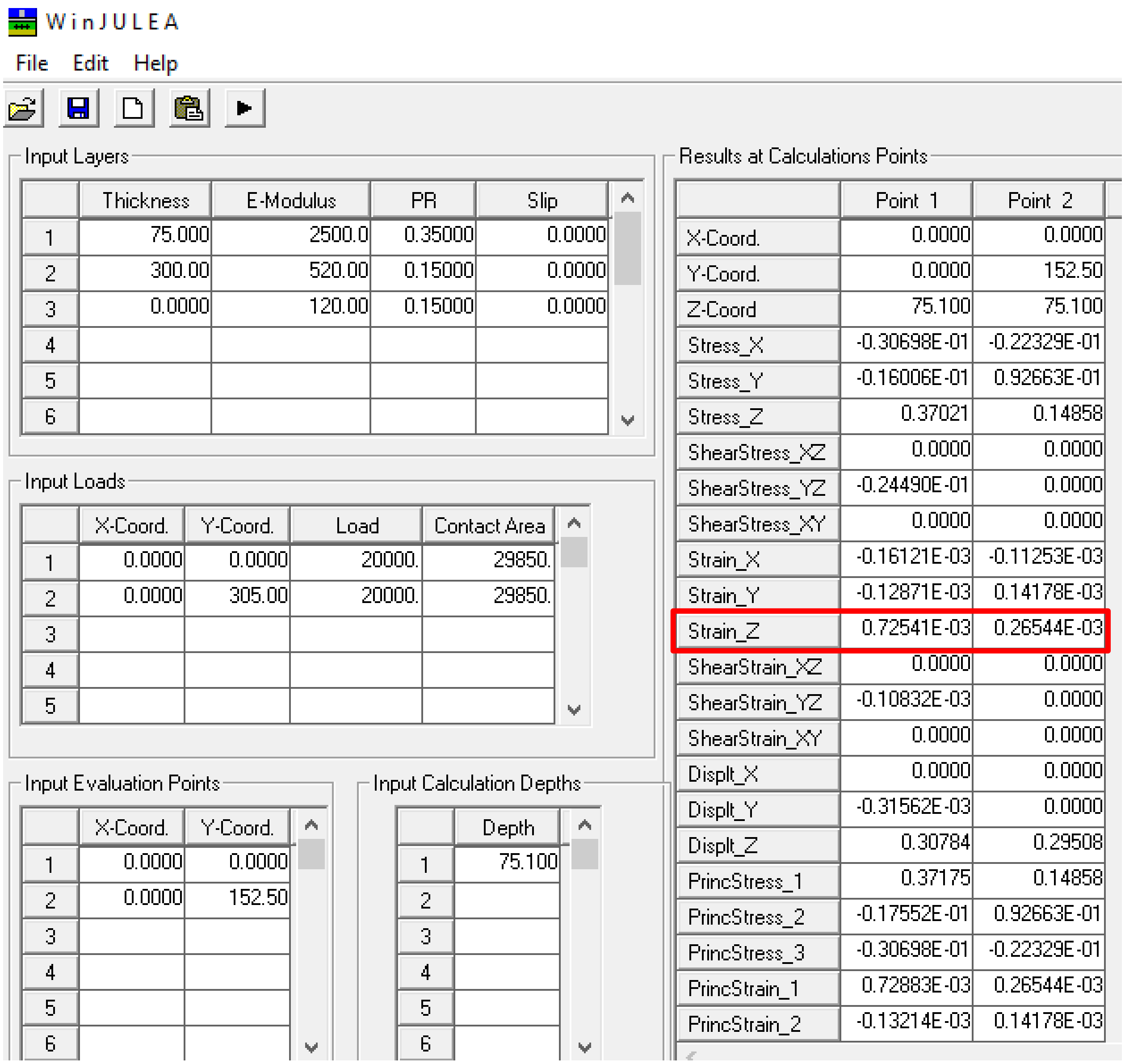

WinJULEA

File Edit Help

Input Layers

	Thickness	E-Modulus	PR	Slip
1	75.000	2500.0	0.35000	0.0000
2	300.00	520.00	0.15000	0.0000
3	0.0000	120.00	0.15000	0.0000
4				
5				
6				

Input Loads

	X-Coord.	Y-Coord.	Load	Contact Area
1	0.0000	0.0000	20000.	29850.
2	0.0000	305.00	20000.	29850.
3				
4				
5				

Input Evaluation Points

	X-Coord.	Y-Coord.
1	0.0000	0.0000
2	0.0000	152.50
3		
4		
5		
6		

Input Calculation Depths

	Depth
1	75.100
2	
3	
4	
5	
6	

Results at Calculations Points

	Point 1	Point 2
X-Coord.	0.0000	0.0000
Y-Coord.	0.0000	152.50
Z-Coord	75.100	75.100
Stress_X	-0.30698E-01	-0.22329E-01
Stress_Y	-0.16006E-01	0.92663E-01
Stress_Z	0.37021	0.14858
ShearStress_XZ	0.0000	0.0000
ShearStress_YZ	-0.24490E-01	0.0000
ShearStress_XY	0.0000	0.0000
Strain_X	-0.16121E-03	-0.11253E-03
Strain_Y	-0.12871E-03	0.14178E-03
Strain_Z	0.72541E-03	0.26544E-03
ShearStrain_XZ	0.0000	0.0000
ShearStrain_YZ	-0.10832E-03	0.0000
ShearStrain_XY	0.0000	0.0000
Displt_X	0.0000	0.0000
Displt_Y	-0.31562E-03	0.0000
Displt_Z	0.30784	0.29508
PrincStress_1	0.37175	0.14858
PrincStress_2	-0.17552E-01	0.92663E-01
PrincStress_3	-0.30698E-01	-0.22329E-01
PrincStrain_1	0.72883E-03	0.26544E-03
PrincStrain_2	-0.13214E-03	0.14178E-03

Failure in compression at the top of the subbase

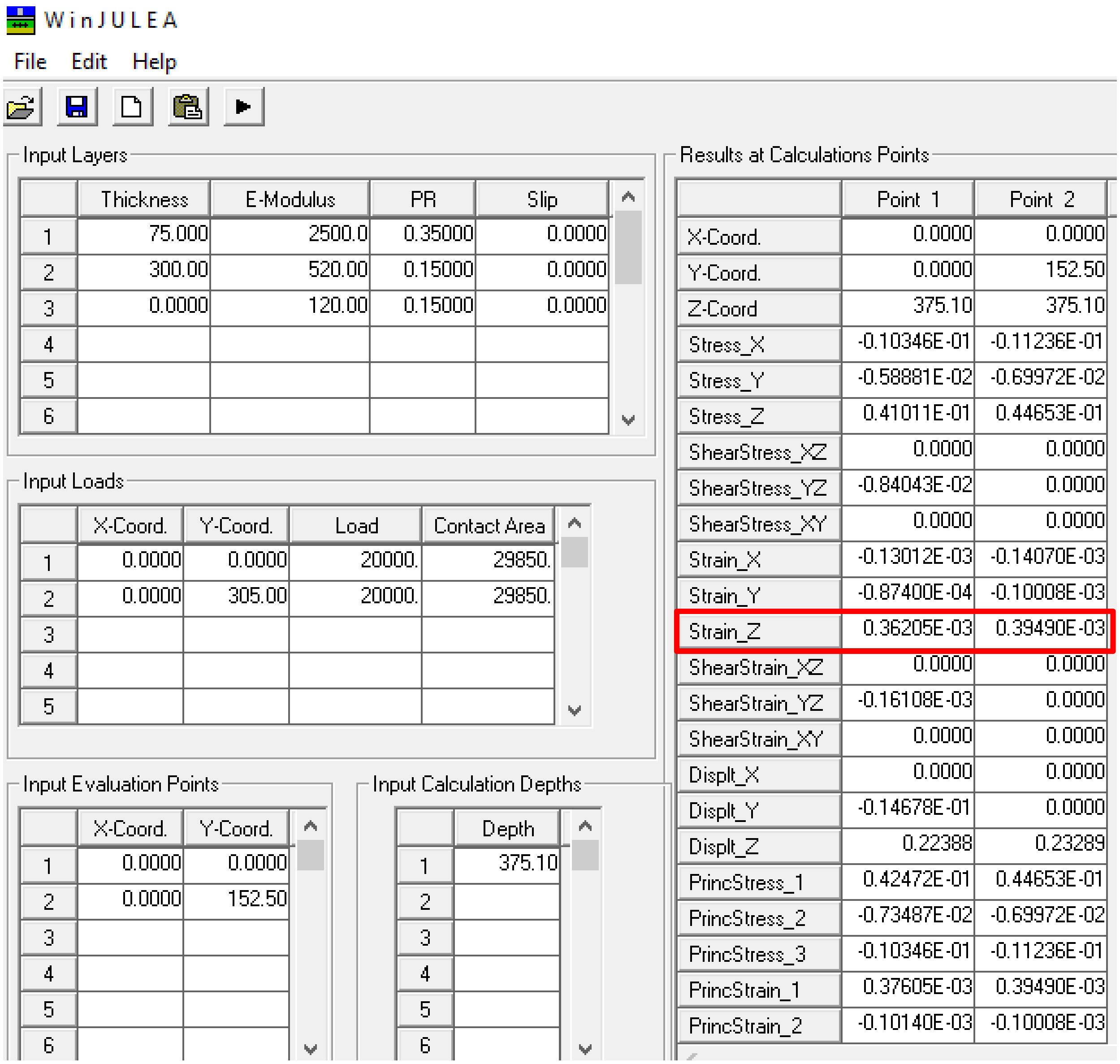
WinJULEA

File Edit Help

Input Layers

	Thickness	E-Modulus	PR	Slip
1	75.000	2500.0	0.35000	0.0000
2	300.00	520.00	0.15000	0.0000
3	0.0000	120.00	0.15000	0.0000
4				
5				
6				

Input Loads

	X-Coord.	Y-Coord.	Load	Contact Area
1	0.0000	0.0000	20000.	29850.
2	0.0000	305.00	20000.	29850.
3				
4				
5				

Input Evaluation Points

	X-Coord.	Y-Coord.
1	0.0000	0.0000
2	0.0000	152.50
3		
4		
5		
6		

Input Calculation Depths

	Depth
1	375.10
2	
3	
4	
5	
6	

Results at Calculations Points

	Point 1	Point 2
X-Coord.	0.0000	0.0000
Y-Coord.	0.0000	152.50
Z-Coord	375.10	375.10
Stress_X	-0.10346E-01	-0.11236E-01
Stress_Y	-0.58881E-02	-0.69972E-02
Stress_Z	0.41011E-01	0.44653E-01
ShearStress_XZ	0.0000	0.0000
ShearStress_YZ	-0.84043E-02	0.0000
ShearStress_XY	0.0000	0.0000
Strain_X	-0.13012E-03	-0.14070E-03
Strain_Y	-0.87400E-04	-0.10008E-03
Strain_Z	0.36205E-03	0.39490E-03
ShearStrain_XZ	0.0000	0.0000
ShearStrain_YZ	-0.16108E-03	0.0000
ShearStrain_XY	0.0000	0.0000
Displt_X	0.0000	0.0000
Displt_Y	-0.14678E-01	0.0000
Displt_Z	0.22388	0.23289
PrincStress_1	0.42472E-01	0.44653E-01
PrincStress_2	-0.73487E-02	-0.69972E-02
PrincStress_3	-0.10346E-01	-0.11236E-01
PrincStrain_1	0.37605E-03	0.39490E-03
PrincStrain_2	-0.10140E-03	-0.10008E-03

Scenario 4: 75 mm of AC + 6% cement

Failure in tension at the bottom of the asphalt concrete

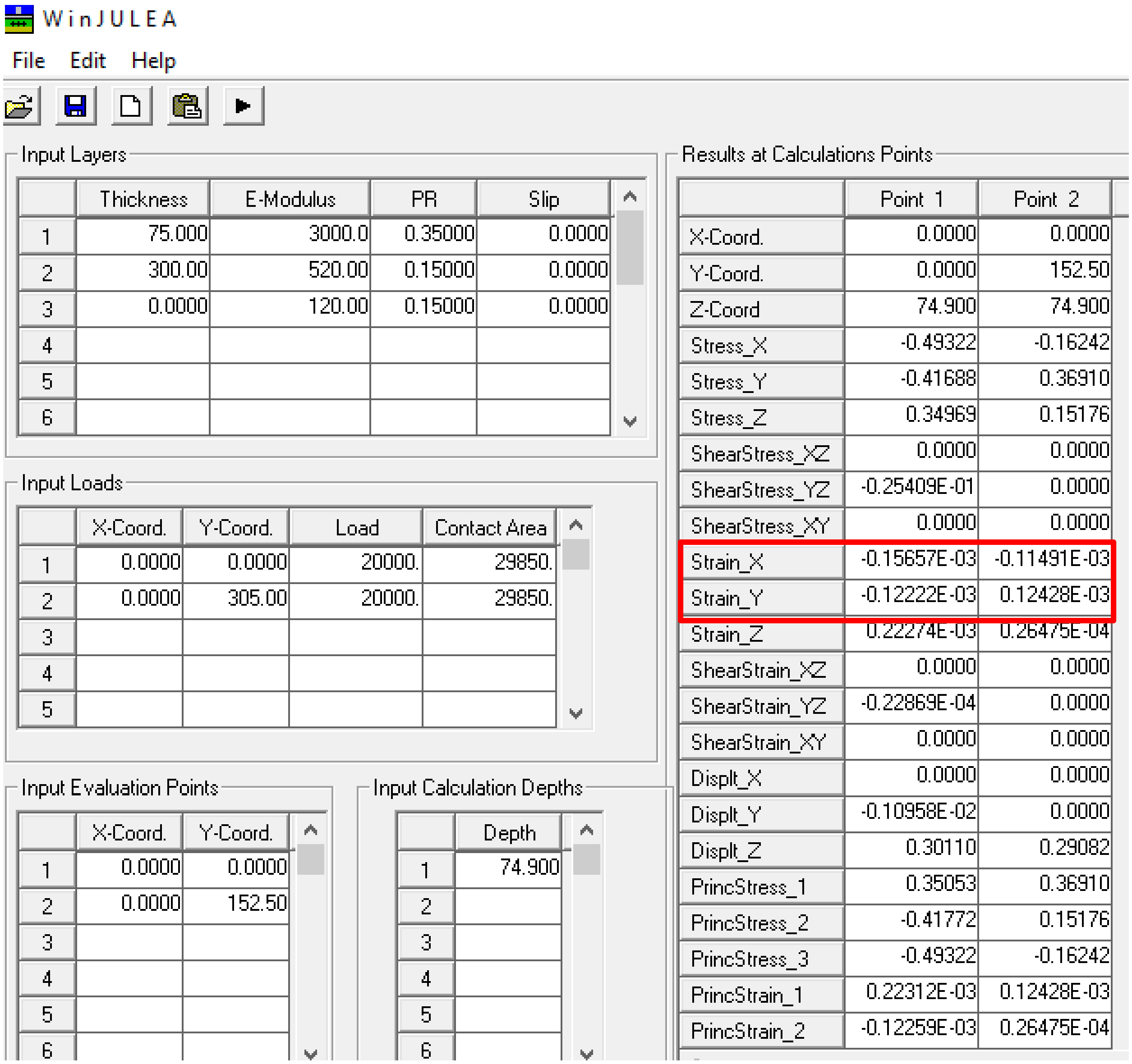

Failure in compression at the top of the asphalt concrete

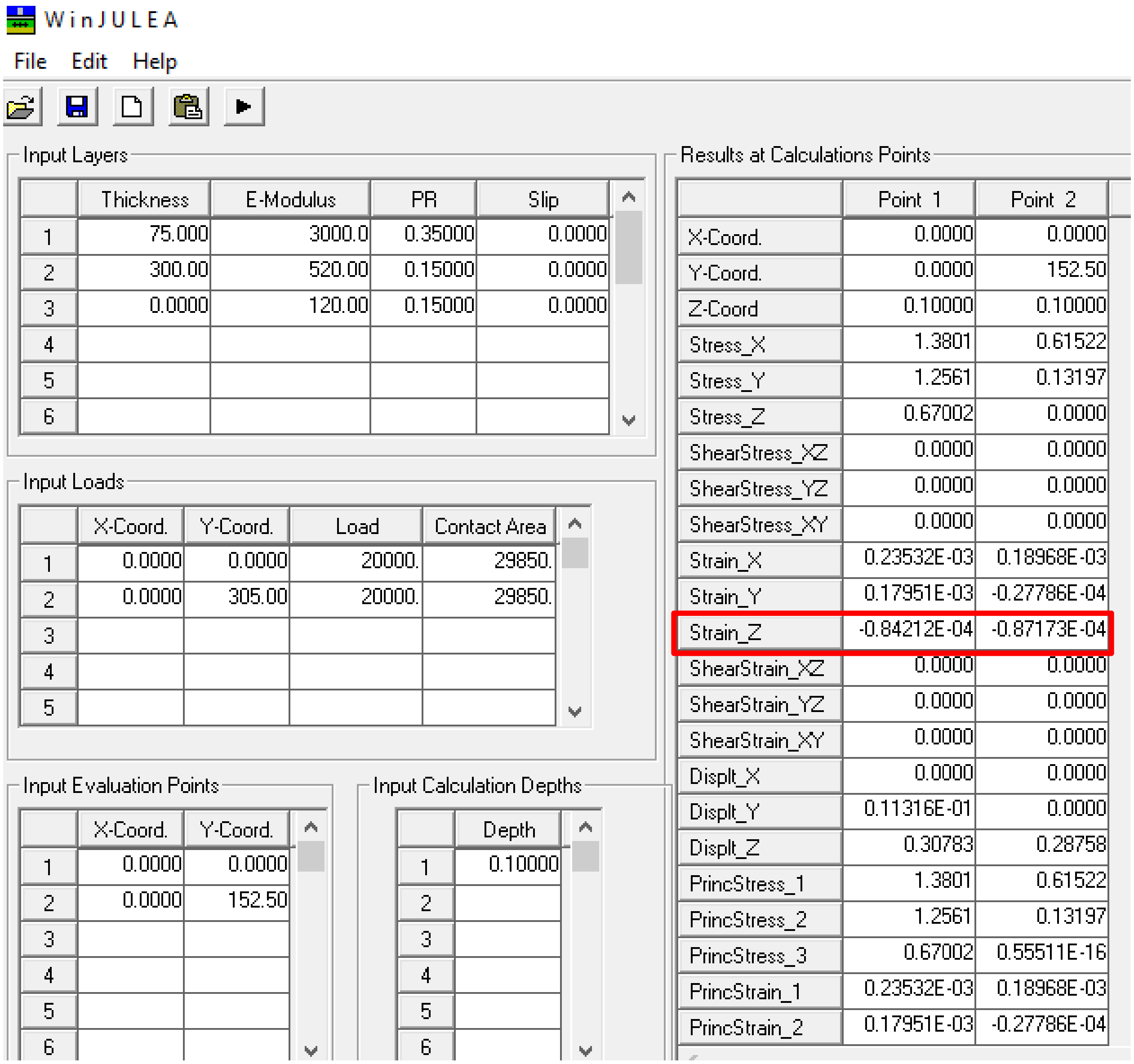

WinJULEA

File Edit Help

Input Layers

	Thickness	E-Modulus	PR	Slip
1	75.000	3000.0	0.35000	0.0000
2	300.00	520.00	0.15000	0.0000
3	0.0000	120.00	0.15000	0.0000
4				
5				
6				

Input Loads

	X-Coord.	Y-Coord.	Load	Contact Area
1	0.0000	0.0000	20000.	29850.
2	0.0000	305.00	20000.	29850.
3				
4				
5				

Input Evaluation Points

	X-Coord.	Y-Coord.
1	0.0000	0.0000
2	0.0000	152.50
3		
4		
5		
6		

Input Calculation Depths

	Depth
1	0.10000
2	
3	
4	
5	
6	

Results at Calculations Points

	Point 1	Point 2
X-Coord.	0.0000	0.0000
Y-Coord.	0.0000	152.50
Z-Coord	0.10000	0.10000
Stress_X	1.3801	0.61522
Stress_Y	1.2561	0.13197
Stress_Z	0.67002	0.0000
ShearStress_XZ	0.0000	0.0000
ShearStress_YZ	0.0000	0.0000
ShearStress_XY	0.0000	0.0000
Strain_X	0.23532E-03	0.18968E-03
Strain_Y	0.17951E-03	-0.27786E-04
Strain_Z	-0.84212E-04	-0.87173E-04
ShearStrain_XZ	0.0000	0.0000
ShearStrain_YZ	0.0000	0.0000
ShearStrain_XY	0.0000	0.0000
Displt_X	0.0000	0.0000
Displt_Y	0.11316E-01	0.0000
Displt_Z	0.30783	0.28758
PrincStress_1	1.3801	0.61522
PrincStress_2	1.2561	0.13197
PrincStress_3	0.67002	0.55511E-16
PrincStrain_1	0.23532E-03	0.18968E-03
PrincStrain_2	0.17951E-03	-0.27786E-04

Failure in compression at the top of the granular base

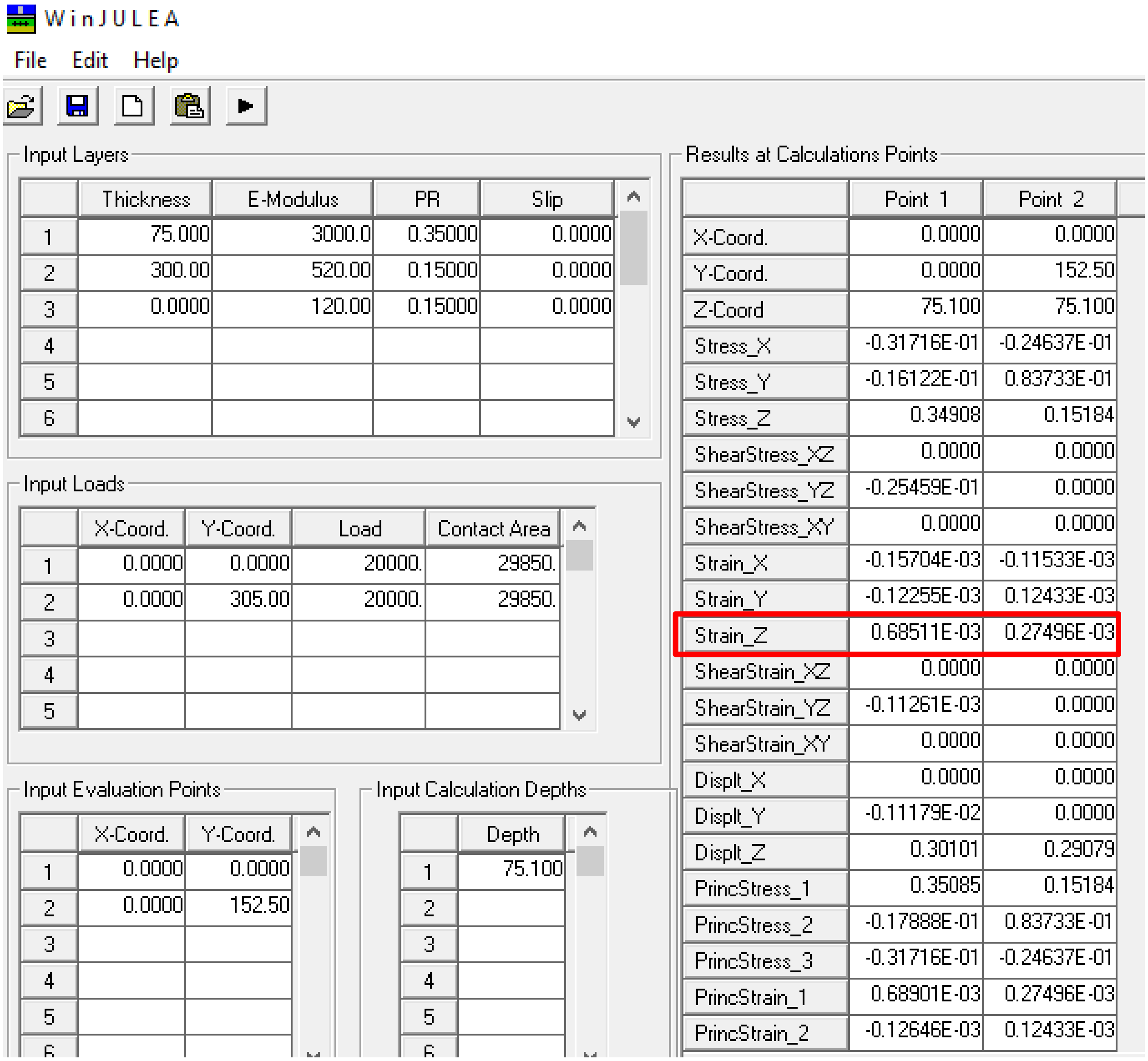
WinJULEA

File Edit Help

Input Layers

	Thickness	E-Modulus	PR	Slip
1	75.000	3000.0	0.35000	0.0000
2	300.00	520.00	0.15000	0.0000
3	0.0000	120.00	0.15000	0.0000
4				
5				
6				

Input Loads

	X-Coord.	Y-Coord.	Load	Contact Area
1	0.0000	0.0000	20000.	29850.
2	0.0000	305.00	20000.	29850.
3				
4				
5				

Input Evaluation Points

	X-Coord.	Y-Coord.
1	0.0000	0.0000
2	0.0000	152.50
3		
4		
5		
6		

Input Calculation Depths

	Depth
1	75.100
2	
3	
4	
5	
6	

Results at Calculations Points

	Point 1	Point 2
X-Coord.	0.0000	0.0000
Y-Coord.	0.0000	152.50
Z-Coord	75.100	75.100
Stress_X	-0.31716E-01	-0.24637E-01
Stress_Y	-0.16122E-01	0.83733E-01
Stress_Z	0.34908	0.15184
ShearStress_XZ	0.0000	0.0000
ShearStress_YZ	-0.25459E-01	0.0000
ShearStress_XY	0.0000	0.0000
Strain_X	-0.15704E-03	-0.11533E-03
Strain_Y	-0.12255E-03	0.12433E-03
Strain_Z	0.68511E-03	0.27496E-03
ShearStrain_XZ	0.0000	0.0000
ShearStrain_YZ	-0.11261E-03	0.0000
ShearStrain_XY	0.0000	0.0000
Displt_X	0.0000	0.0000
Displt_Y	-0.11179E-02	0.0000
Displt_Z	0.30101	0.29079
PrincStress_1	0.35085	0.15184
PrincStress_2	-0.17888E-01	0.83733E-01
PrincStress_3	-0.31716E-01	-0.24637E-01
PrincStrain_1	0.68901E-03	0.27496E-03
PrincStrain_2	-0.12646E-03	0.12433E-03

Failure in compression at the top of the subbase

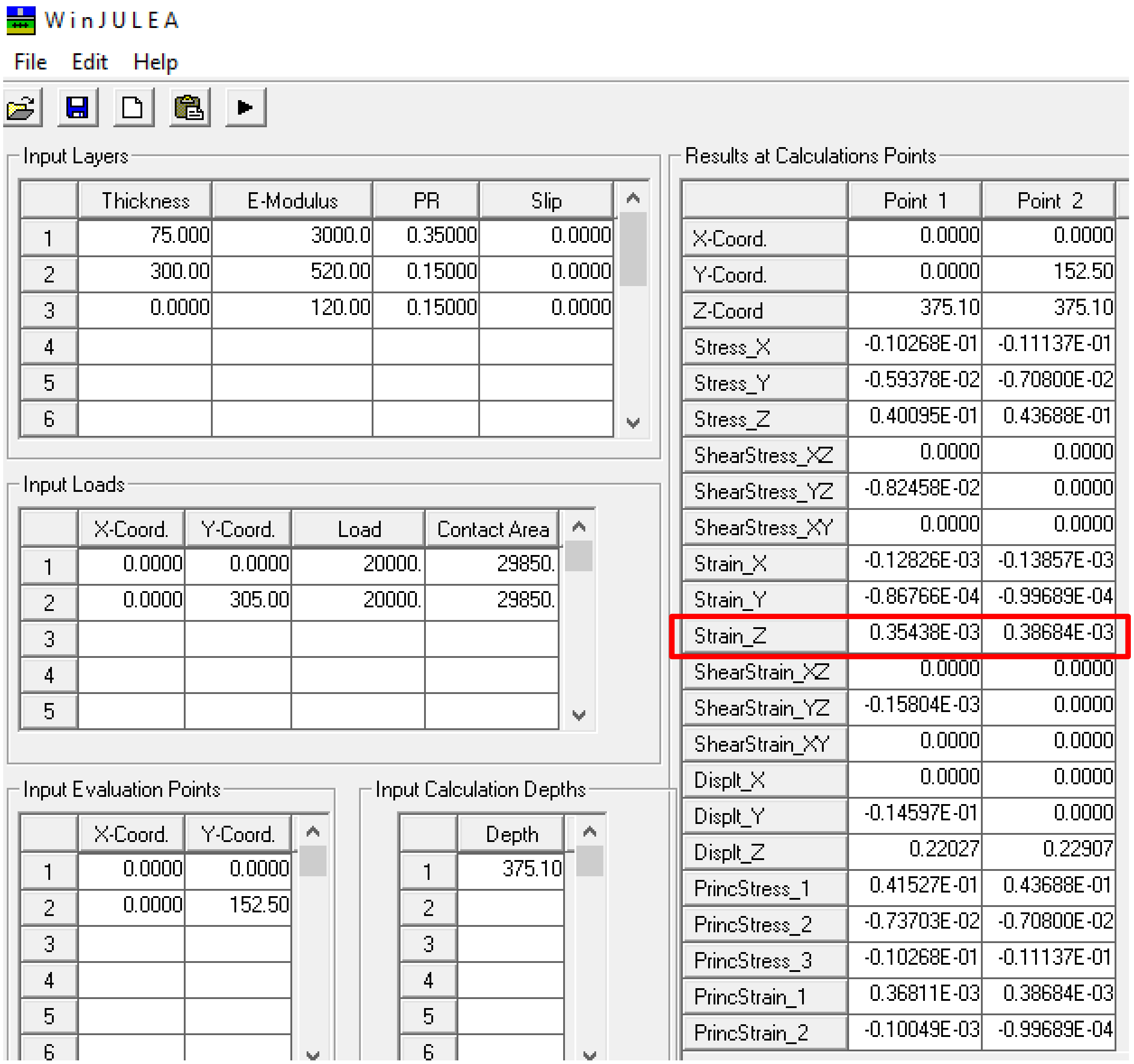

WinJULEA

File Edit Help

Input Layers

	Thickness	E-Modulus	PR	Slip
1	75.000	3000.0	0.35000	0.0000
2	300.00	520.00	0.15000	0.0000
3	0.0000	120.00	0.15000	0.0000
4				
5				
6				

Input Loads

	X-Coord.	Y-Coord.	Load	Contact Area
1	0.0000	0.0000	20000.	29850.
2	0.0000	305.00	20000.	29850.
3				
4				
5				

Input Evaluation Points

	X-Coord.	Y-Coord.
1	0.0000	0.0000
2	0.0000	152.50
3		
4		
5		
6		

Input Calculation Depths

	Depth
1	375.10
2	
3	
4	
5	
6	

Results at Calculations Points

	Point 1	Point 2
X-Coord.	0.0000	0.0000
Y-Coord.	0.0000	152.50
Z-Coord	375.10	375.10
Stress_X	-0.10268E-01	-0.11137E-01
Stress_Y	-0.59378E-02	-0.70800E-02
Stress_Z	0.40095E-01	0.43688E-01
ShearStress_XZ	0.0000	0.0000
ShearStress_YZ	-0.82458E-02	0.0000
ShearStress_XY	0.0000	0.0000
Strain_X	-0.12826E-03	-0.13857E-03
Strain_Y	-0.86766E-04	-0.99689E-04
Strain_Z	0.35438E-03	0.38684E-03
ShearStrain_XZ	0.0000	0.0000
ShearStrain_YZ	-0.15804E-03	0.0000
ShearStrain_XY	0.0000	0.0000
Displt_X	0.0000	0.0000
Displt_Y	-0.14597E-01	0.0000
Displt_Z	0.22027	0.22907
PrincStress_1	0.41527E-01	0.43688E-01
PrincStress_2	-0.73703E-02	-0.70800E-02
PrincStress_3	-0.10268E-01	-0.11137E-01
PrincStrain_1	0.36811E-03	0.38684E-03
PrincStrain_2	-0.10049E-03	-0.99689E-04

Scenario 5: 100 mm of AC + 0% cement

Failure in tension at the bottom of the asphalt concrete

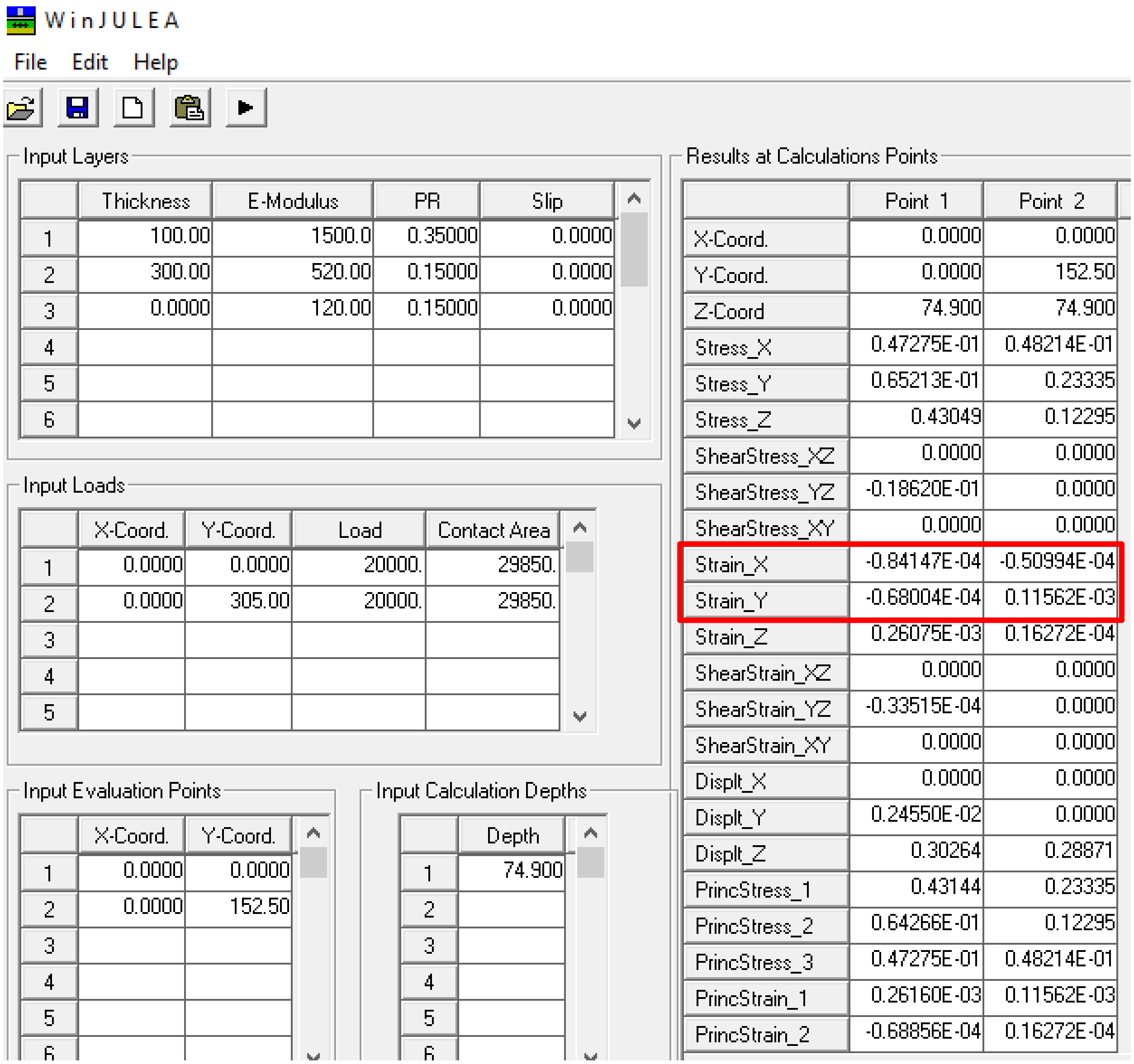

WinJULEA

File Edit Help

Input Layers

	Thickness	E-Modulus	PR	Slip
1	100.00	1500.0	0.35000	0.0000
2	300.00	520.00	0.15000	0.0000
3	0.0000	120.00	0.15000	0.0000
4				
5				
6				

Input Loads

	X-Coord.	Y-Coord.	Load	Contact Area
1	0.0000	0.0000	20000.	29850.
2	0.0000	305.00	20000.	29850.
3				
4				
5				

Input Evaluation Points

	X-Coord.	Y-Coord.
1	0.0000	0.0000
2	0.0000	152.50
3		
4		
5		
6		

Input Calculation Depths

	Depth
1	74.900
2	
3	
4	
5	
6	

Results at Calculations Points

	Point 1	Point 2
X-Coord.	0.0000	0.0000
Y-Coord.	0.0000	152.50
Z-Coord	74.900	74.900
Stress_X	0.47275E-01	0.48214E-01
Stress_Y	0.65213E-01	0.23335
Stress_Z	0.43049	0.12295
ShearStress_XZ	0.0000	0.0000
ShearStress_YZ	-0.18620E-01	0.0000
ShearStress_XY	0.0000	0.0000
Strain_X	-0.84147E-04	-0.50994E-04
Strain_Y	-0.68004E-04	0.11562E-03
Strain_Z	0.26075E-03	0.16272E-04
ShearStrain_XZ	0.0000	0.0000
ShearStrain_YZ	-0.33515E-04	0.0000
ShearStrain_XY	0.0000	0.0000
Displt_X	0.0000	0.0000
Displt_Y	0.24550E-02	0.0000
Displt_Z	0.30264	0.28871
PrincStress_1	0.43144	0.23335
PrincStress_2	0.64266E-01	0.12295
PrincStress_3	0.47275E-01	0.48214E-01
PrincStrain_1	0.26160E-03	0.11562E-03
PrincStrain_2	-0.68856E-04	0.16272E-04

Failure in compression at the top of the asphalt concrete

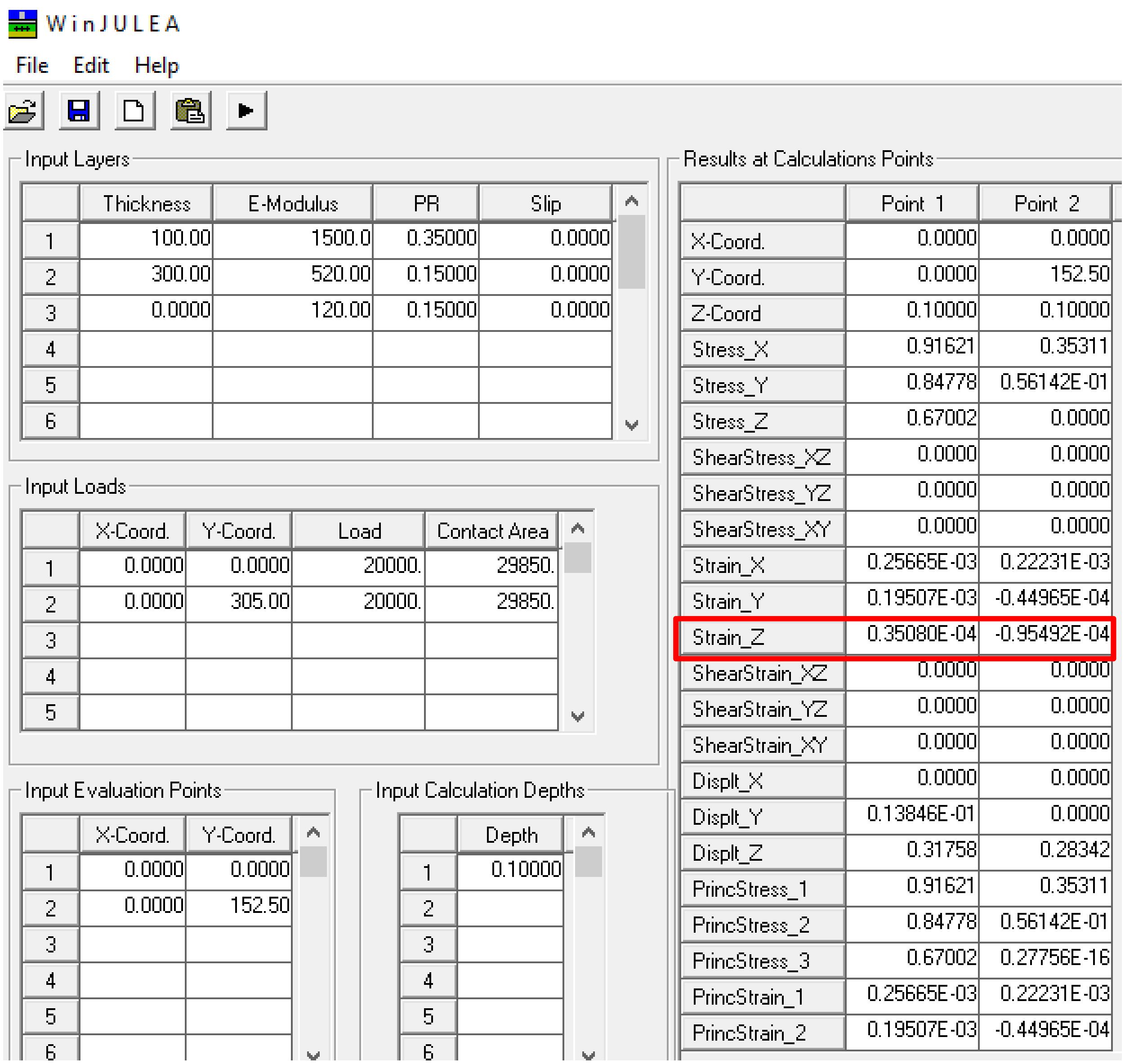

WinJULEA

File Edit Help

Input Layers

	Thickness	E-Modulus	PR	Slip
1	100.00	1500.0	0.35000	0.0000
2	300.00	520.00	0.15000	0.0000
3	0.0000	120.00	0.15000	0.0000
4				
5				
6				

Input Loads

	X-Coord.	Y-Coord.	Load	Contact Area
1	0.0000	0.0000	20000.	29850.
2	0.0000	305.00	20000.	29850.
3				
4				
5				

Input Evaluation Points

	X-Coord.	Y-Coord.
1	0.0000	0.0000
2	0.0000	152.50
3		
4		
5		
6		

Input Calculation Depths

	Depth
1	0.10000
2	
3	
4	
5	
6	

Results at Calculations Points

	Point 1	Point 2
X-Coord.	0.0000	0.0000
Y-Coord.	0.0000	152.50
Z-Coord	0.10000	0.10000
Stress_X	0.91621	0.35311
Stress_Y	0.84778	0.56142E-01
Stress_Z	0.67002	0.0000
ShearStress_XZ	0.0000	0.0000
ShearStress_YZ	0.0000	0.0000
ShearStress_XY	0.0000	0.0000
Strain_X	0.25665E-03	0.22231E-03
Strain_Y	0.19507E-03	-0.44965E-04
Strain_Z	0.35080E-04	-0.95492E-04
ShearStrain_XZ	0.0000	0.0000
ShearStrain_YZ	0.0000	0.0000
ShearStrain_XY	0.0000	0.0000
Displt_X	0.0000	0.0000
Displt_Y	0.13846E-01	0.0000
Displt_Z	0.31758	0.28342
PrincStress_1	0.91621	0.35311
PrincStress_2	0.84778	0.56142E-01
PrincStress_3	0.67002	0.27756E-16
PrincStrain_1	0.25665E-03	0.22231E-03
PrincStrain_2	0.19507E-03	-0.44965E-04

Failure in compression at the top of the granular base

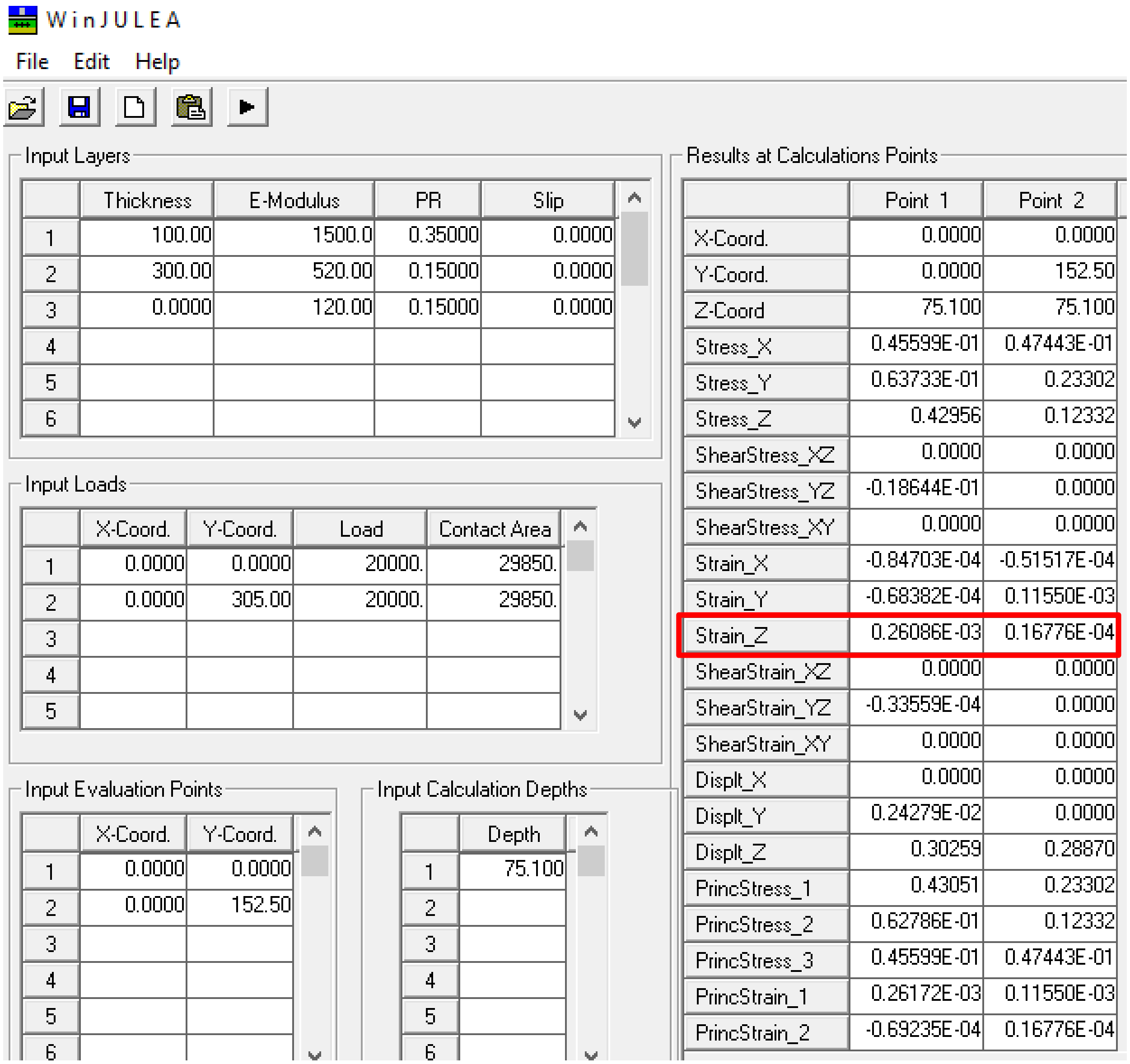
WinJULEA

File Edit Help

Input Layers

	Thickness	E-Modulus	PR	Slip
1	100.00	1500.0	0.35000	0.0000
2	300.00	520.00	0.15000	0.0000
3	0.0000	120.00	0.15000	0.0000
4				
5				
6				

Input Loads

	X-Coord.	Y-Coord.	Load	Contact Area
1	0.0000	0.0000	20000.	29850.
2	0.0000	305.00	20000.	29850.
3				
4				
5				

Input Evaluation Points

	X-Coord.	Y-Coord.
1	0.0000	0.0000
2	0.0000	152.50
3		
4		
5		
6		

Input Calculation Depths

	Depth
1	75.100
2	
3	
4	
5	
6	

Results at Calculations Points

	Point 1	Point 2
X-Coord.	0.0000	0.0000
Y-Coord.	0.0000	152.50
Z-Coord	75.100	75.100
Stress_X	0.45599E-01	0.47443E-01
Stress_Y	0.63733E-01	0.23302
Stress_Z	0.42956	0.12332
ShearStress_XZ	0.0000	0.0000
ShearStress_YZ	-0.18644E-01	0.0000
ShearStress_XY	0.0000	0.0000
Strain_X	-0.84703E-04	-0.51517E-04
Strain_Y	-0.68382E-04	0.11550E-03
Strain_Z	0.26086E-03	0.16776E-04
ShearStrain_XZ	0.0000	0.0000
ShearStrain_YZ	-0.33559E-04	0.0000
ShearStrain_XY	0.0000	0.0000
Displt_X	0.0000	0.0000
Displt_Y	0.24279E-02	0.0000
Displt_Z	0.30259	0.28870
PrincStress_1	0.43051	0.23302
PrincStress_2	0.62786E-01	0.12332
PrincStress_3	0.45599E-01	0.47443E-01
PrincStrain_1	0.26172E-03	0.11550E-03
PrincStrain_2	-0.69235E-04	0.16776E-04

Failure in compression at the top of the subbase

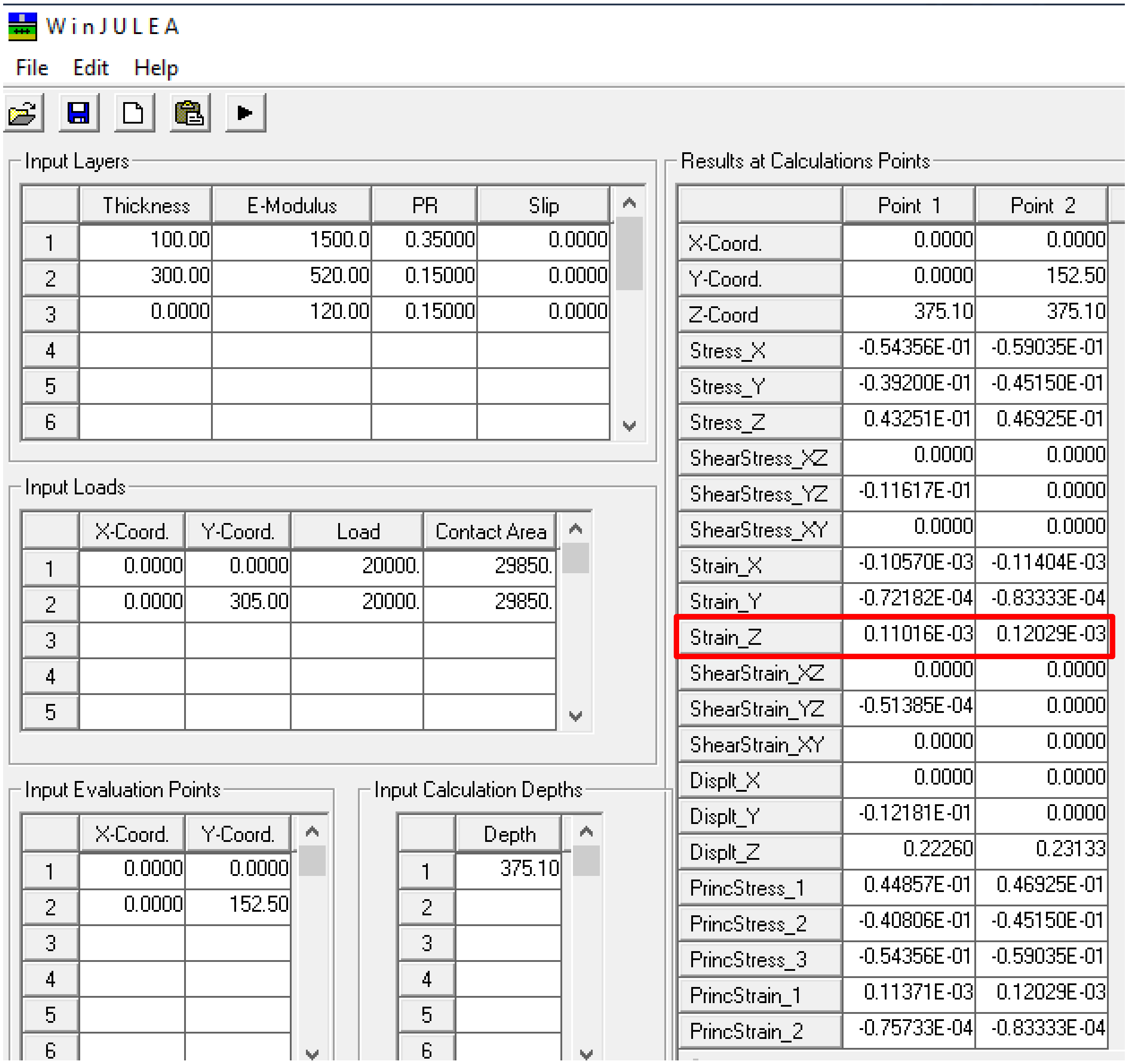

Input Layers

	Thickness	E-Modulus	PR	Slip
1	100.00	1500.0	0.35000	0.0000
2	300.00	520.00	0.15000	0.0000
3	0.0000	120.00	0.15000	0.0000
4				
5				
6				

Input Loads

	X-Coord.	Y-Coord.	Load	Contact Area
1	0.0000	0.0000	20000.	29850.
2	0.0000	305.00	20000.	29850.
3				
4				
5				

Input Evaluation Points

	X-Coord.	Y-Coord.
1	0.0000	0.0000
2	0.0000	152.50
3		
4		
5		
6		

Input Calculation Depths

	Depth
1	375.10
2	
3	
4	
5	
6	

Results at Calculations Points

	Point 1	Point 2
X-Coord.	0.0000	0.0000
Y-Coord.	0.0000	152.50
Z-Coord	375.10	375.10
Stress_X	-0.54356E-01	-0.59035E-01
Stress_Y	-0.39200E-01	-0.45150E-01
Stress_Z	0.43251E-01	0.46925E-01
ShearStress_XZ	0.0000	0.0000
ShearStress_YZ	-0.11617E-01	0.0000
ShearStress_XY	0.0000	0.0000
Strain_X	-0.10570E-03	-0.11404E-03
Strain_Y	-0.72182E-04	-0.83333E-04
Strain_Z	0.11016E-03	0.12029E-03
ShearStrain_XZ	0.0000	0.0000
ShearStrain_YZ	-0.51385E-04	0.0000
ShearStrain_XY	0.0000	0.0000
Displt_X	0.0000	0.0000
Displt_Y	-0.12181E-01	0.0000
Displt_Z	0.22260	0.23133
PrincStress_1	0.44857E-01	0.46925E-01
PrincStress_2	-0.40806E-01	-0.45150E-01
PrincStress_3	-0.54356E-01	-0.59035E-01
PrincStrain_1	0.11371E-03	0.12029E-03
PrincStrain_2	-0.75733E-04	-0.83333E-04

Scenario 6: 100 mm of AC + 2% cement

Failure in tension at the bottom of the asphalt concrete

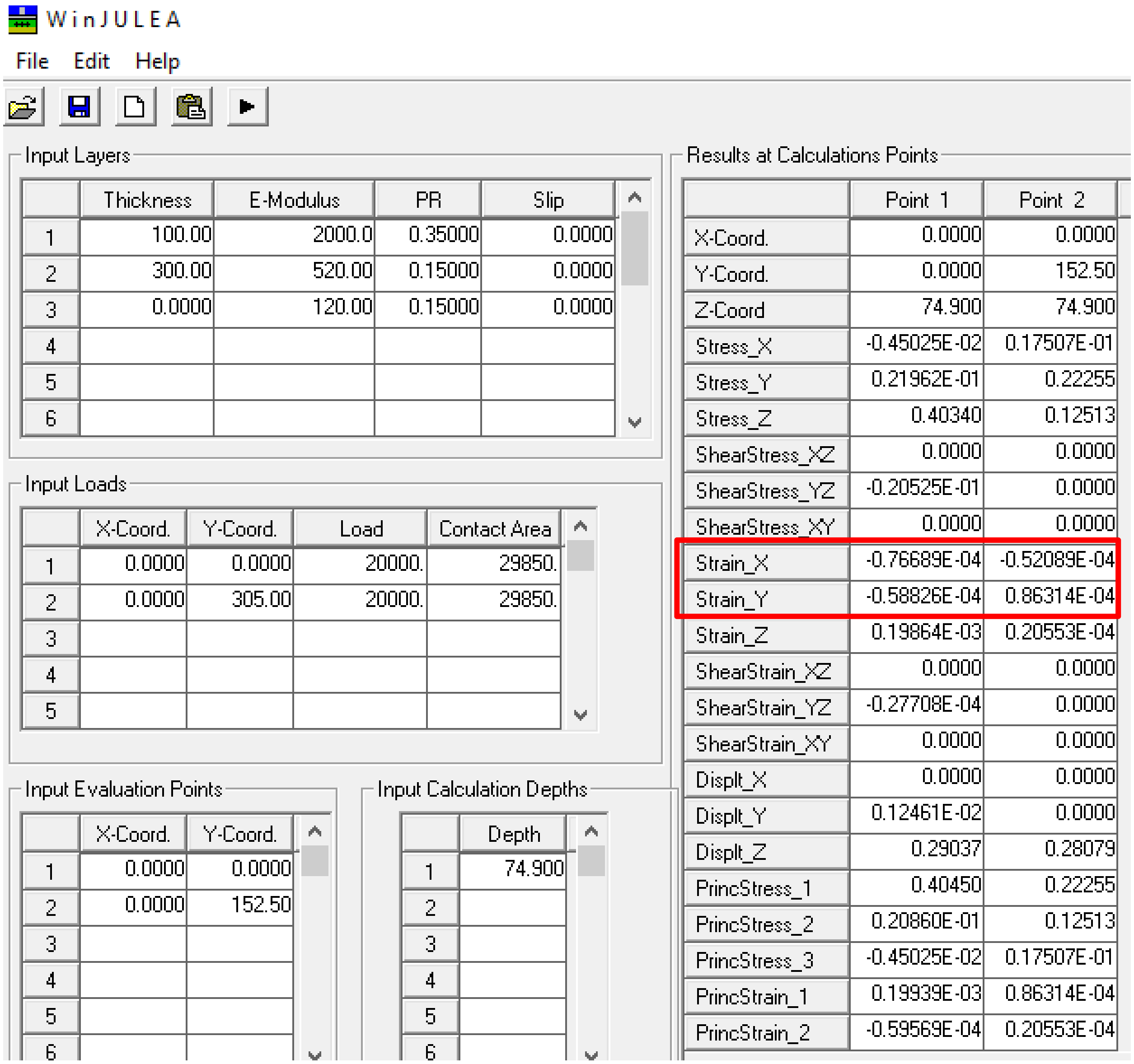

Input Layers

	Thickness	E-Modulus	PR	Slip
1	100.00	2000.0	0.35000	0.0000
2	300.00	520.00	0.15000	0.0000
3	0.0000	120.00	0.15000	0.0000
4				
5				
6				

Input Loads

	X-Coord.	Y-Coord.	Load	Contact Area
1	0.0000	0.0000	20000.	29850.
2	0.0000	305.00	20000.	29850.
3				
4				
5				

Input Evaluation Points

	X-Coord.	Y-Coord.
1	0.0000	0.0000
2	0.0000	152.50
3		
4		
5		
6		

Input Calculation Depths

	Depth
1	74.900
2	
3	
4	
5	
6	

Results at Calculations Points

	Point 1	Point 2
X-Coord.	0.0000	0.0000
Y-Coord.	0.0000	152.50
Z-Coord	74.900	74.900
Stress_X	-0.45025E-02	0.17507E-01
Stress_Y	0.21962E-01	0.22255
Stress_Z	0.40340	0.12513
ShearStress_XZ	0.0000	0.0000
ShearStress_YZ	-0.20525E-01	0.0000
ShearStress_XY	0.0000	0.0000
Strain_X	-0.76689E-04	-0.52089E-04
Strain_Y	-0.58826E-04	0.86314E-04
Strain_Z	0.19864E-03	0.20553E-04
ShearStrain_XZ	0.0000	0.0000
ShearStrain_YZ	-0.27708E-04	0.0000
ShearStrain_XY	0.0000	0.0000
Displt_X	0.0000	0.0000
Displt_Y	0.12461E-02	0.0000
Displt_Z	0.29037	0.28079
PrincStress_1	0.40450	0.22255
PrincStress_2	0.20860E-01	0.12513
PrincStress_3	-0.45025E-02	0.17507E-01
PrincStrain_1	0.19939E-03	0.86314E-04
PrincStrain_2	-0.59569E-04	0.20553E-04

Failure in compression at the top of the asphalt concrete

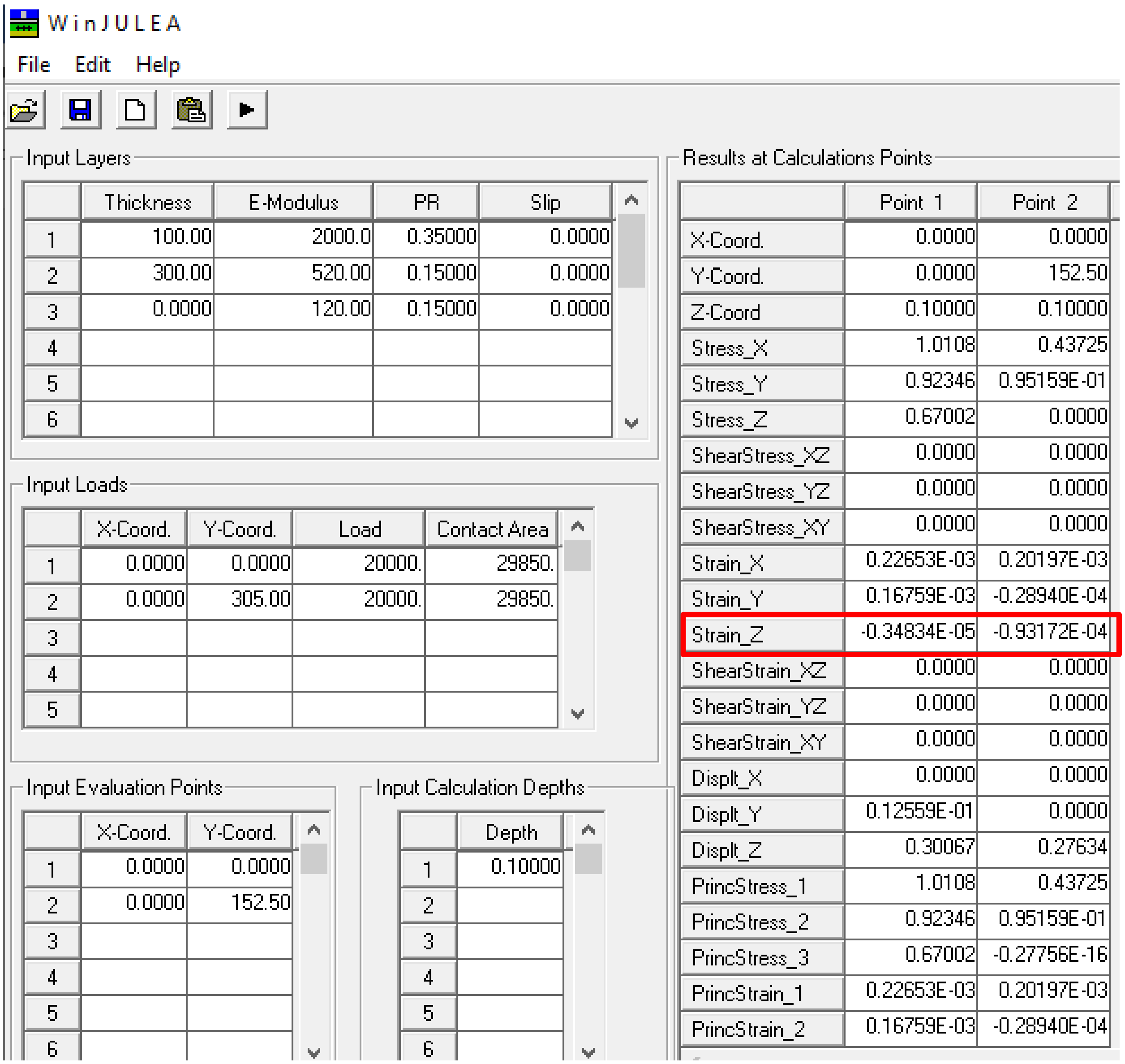

Input Layers

	Thickness	E-Modulus	PR	Slip
1	100.00	2000.0	0.35000	0.0000
2	300.00	520.00	0.15000	0.0000
3	0.0000	120.00	0.15000	0.0000
4				
5				
6				

Input Loads

	X-Coord.	Y-Coord.	Load	Contact Area
1	0.0000	0.0000	20000.	29850.
2	0.0000	305.00	20000.	29850.
3				
4				
5				

Input Evaluation Points

	X-Coord.	Y-Coord.
1	0.0000	0.0000
2	0.0000	152.50
3		
4		
5		
6		

Input Calculation Depths

	Depth
1	0.10000
2	
3	
4	
5	
6	

Results at Calculations Points

	Point 1	Point 2
X-Coord.	0.0000	0.0000
Y-Coord.	0.0000	152.50
Z-Coord	0.10000	0.10000
Stress_X	1.0108	0.43725
Stress_Y	0.92346	0.95159E-01
Stress_Z	0.67002	0.0000
ShearStress_XZ	0.0000	0.0000
ShearStress_YZ	0.0000	0.0000
ShearStress_XY	0.0000	0.0000
Strain_X	0.22653E-03	0.20197E-03
Strain_Y	0.16759E-03	-0.28940E-04
Strain_Z	-0.34834E-05	-0.93172E-04
ShearStrain_XZ	0.0000	0.0000
ShearStrain_YZ	0.0000	0.0000
ShearStrain_XY	0.0000	0.0000
Displt_X	0.0000	0.0000
Displt_Y	0.12559E-01	0.0000
Displt_Z	0.30067	0.27634
PrincStress_1	1.0108	0.43725
PrincStress_2	0.92346	0.95159E-01
PrincStress_3	0.67002	-0.27756E-16
PrincStrain_1	0.22653E-03	0.20197E-03
PrincStrain_2	0.16759E-03	-0.28940E-04

Failure in compression at the top of the granular base

WinJULEA

File Edit Help

Input Layers

	Thickness	E-Modulus	PR	Slip
1	100.00	2000.0	0.35000	0.0000
2	300.00	520.00	0.15000	0.0000
3	0.0000	120.00	0.15000	0.0000
4				
5				
6				

Input Loads

	X-Coord.	Y-Coord.	Load	Contact Area
1	0.0000	0.0000	20000.	29850.
2	0.0000	305.00	20000.	29850.
3				
4				
5				

Input Evaluation Points

	X-Coord.	Y-Coord.
1	0.0000	0.0000
2	0.0000	152.50
3		
4		
5		
6		

Input Calculation Depths

	Depth
1	75.100
2	
3	
4	
5	
6	

Results at Calculations Points

	Point 1	Point 2
X-Coord.	0.0000	0.0000
Y-Coord.	0.0000	152.50
Z-Coord	75.100	75.100
Stress_X	-0.66664E-02	0.16431E-01
Stress_Y	0.19921E-01	0.22211
Stress_Z	0.40273	0.12552
ShearStress_XZ	0.0000	0.0000
ShearStress_YZ	-0.21574E-01	0.0000
ShearStress_XY	0.0000	0.0000
Strain_X	-0.77297E-04	-0.52621E-04
Strain_Y	-0.59351E-04	0.86216E-04
Strain_Z	0.19905E-03	0.21016E-04
ShearStrain_XZ	0.0000	0.0000
ShearStrain_YZ	-0.29125E-04	0.0000
ShearStrain_XY	0.0000	0.0000
Displt_X	0.0000	0.0000
Displt_Y	0.12060E-02	0.0000
Displt_Z	0.29035	0.28079
PrincStress_1	0.40394	0.22211
PrincStress_2	0.18708E-01	0.12552
PrincStress_3	-0.66664E-02	0.16431E-01
PrincStrain_1	0.19986E-03	0.86216E-04
PrincStrain_2	-0.60169E-04	0.21016E-04

Failure in compression at the top of the subbase

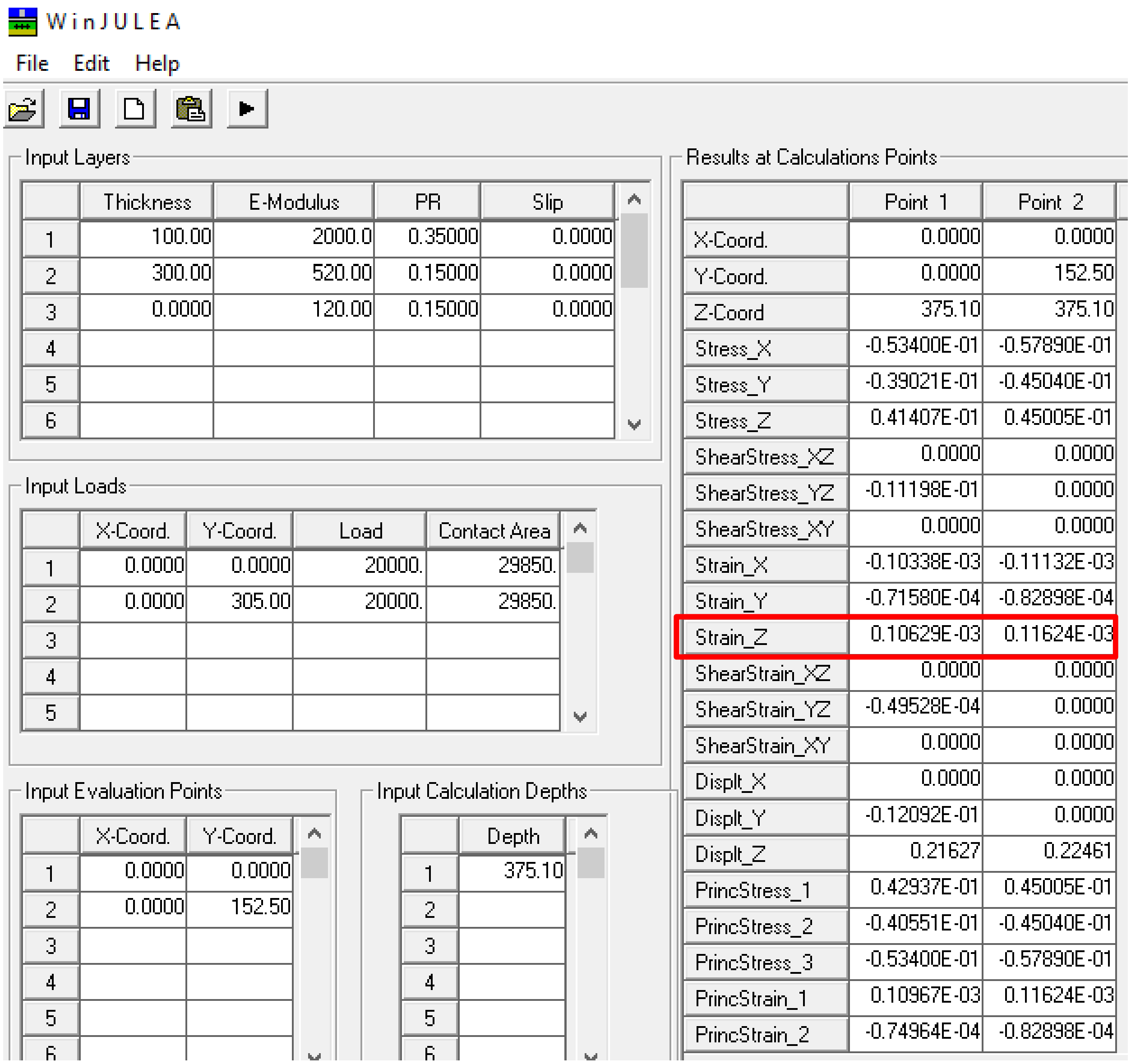

Input Layers

	Thickness	E-Modulus	PR	Slip
1	100.00	2000.0	0.35000	0.0000
2	300.00	520.00	0.15000	0.0000
3	0.0000	120.00	0.15000	0.0000
4				
5				
6				

Input Loads

	X-Coord.	Y-Coord.	Load	Contact Area
1	0.0000	0.0000	20000.	29850.
2	0.0000	305.00	20000.	29850.
3				
4				
5				

Input Evaluation Points

	X-Coord.	Y-Coord.
1	0.0000	0.0000
2	0.0000	152.50
3		
4		
5		
6		

Input Calculation Depths

	Depth
1	375.10
2	
3	
4	
5	
6	

Results at Calculations Points

	Point 1	Point 2
X-Coord.	0.0000	0.0000
Y-Coord.	0.0000	152.50
Z-Coord	375.10	375.10
Stress_X	-0.53400E-01	-0.57890E-01
Stress_Y	-0.39021E-01	-0.45040E-01
Stress_Z	0.41407E-01	0.45005E-01
ShearStress_XZ	0.0000	0.0000
ShearStress_YZ	-0.11198E-01	0.0000
ShearStress_XY	0.0000	0.0000
Strain_X	-0.10338E-03	-0.11132E-03
Strain_Y	-0.71580E-04	-0.82898E-04
Strain_Z	0.10629E-03	0.11624E-03
ShearStrain_XZ	0.0000	0.0000
ShearStrain_YZ	-0.49528E-04	0.0000
ShearStrain_XY	0.0000	0.0000
Displt_X	0.0000	0.0000
Displt_Y	-0.12092E-01	0.0000
Displt_Z	0.21627	0.22461
PrincStress_1	0.42937E-01	0.45005E-01
PrincStress_2	-0.40551E-01	-0.45040E-01
PrincStress_3	-0.53400E-01	-0.57890E-01
PrincStrain_1	0.10967E-03	0.11624E-03
PrincStrain_2	-0.74964E-04	-0.82898E-04

Scenario 7: 100 mm of AC + 4% cement

Failure in tension at the bottom of the asphalt concrete

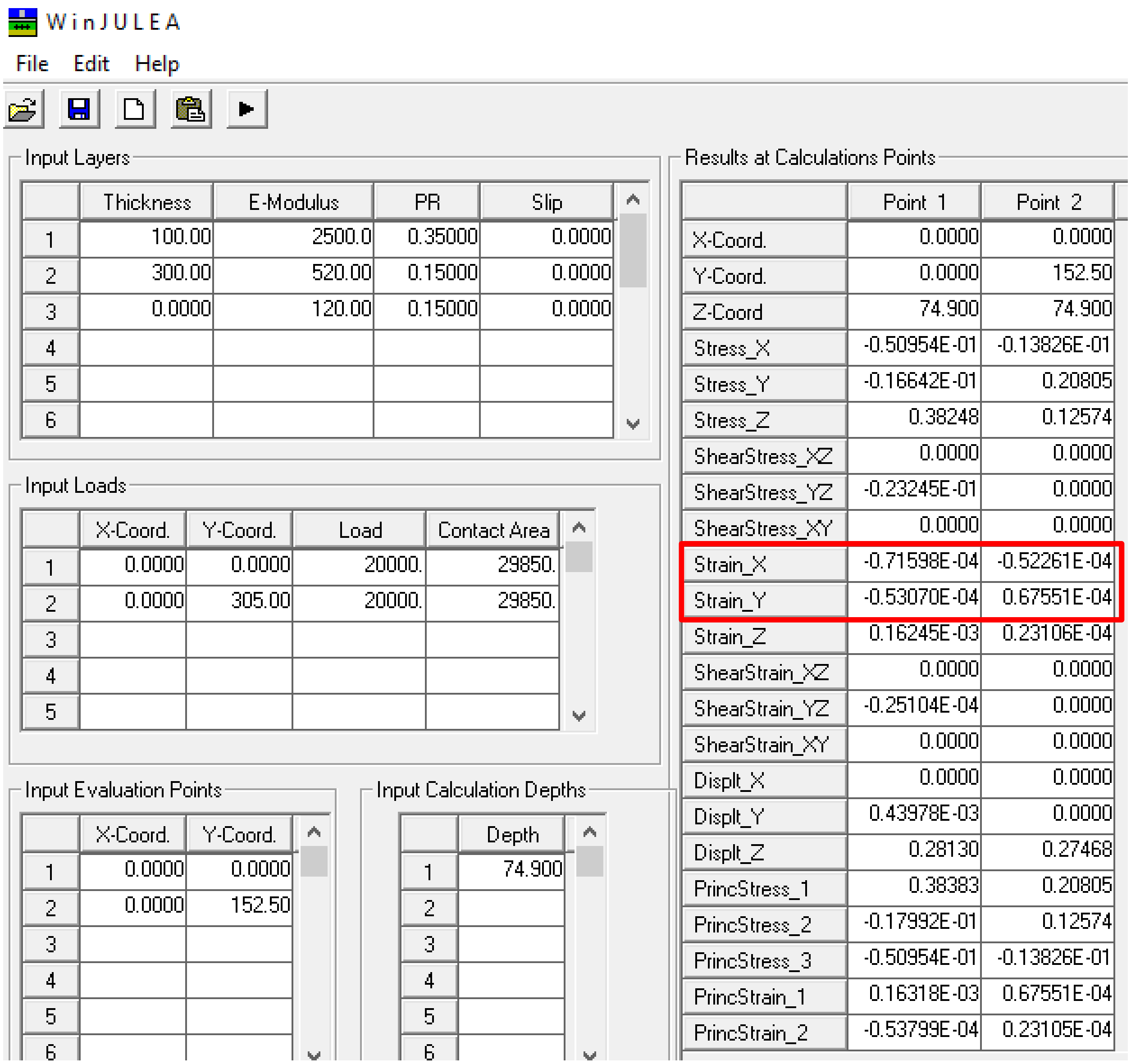

WinJULEA

File Edit Help

Input Layers

	Thickness	E-Modulus	PR	Slip
1	100.00	2500.0	0.35000	0.0000
2	300.00	520.00	0.15000	0.0000
3	0.0000	120.00	0.15000	0.0000
4				
5				
6				

Input Loads

	X-Coord.	Y-Coord.	Load	Contact Area
1	0.0000	0.0000	20000.	29850.
2	0.0000	305.00	20000.	29850.
3				
4				
5				

Input Evaluation Points

	X-Coord.	Y-Coord.
1	0.0000	0.0000
2	0.0000	152.50
3		
4		
5		
6		

Input Calculation Depths

	Depth
1	74.900
2	
3	
4	
5	
6	

Results at Calculations Points

	Point 1	Point 2
X-Coord.	0.0000	0.0000
Y-Coord.	0.0000	152.50
Z-Coord	74.900	74.900
Stress_X	-0.50954E-01	-0.13826E-01
Stress_Y	-0.16642E-01	0.20805
Stress_Z	0.38248	0.12574
ShearStress_XZ	0.0000	0.0000
ShearStress_YZ	-0.23245E-01	0.0000
ShearStress_XY	0.0000	0.0000
Strain_X	-0.71598E-04	-0.52261E-04
Strain_Y	-0.53070E-04	0.67551E-04
Strain_Z	0.16245E-03	0.23106E-04
ShearStrain_XZ	0.0000	0.0000
ShearStrain_YZ	-0.25104E-04	0.0000
ShearStrain_XY	0.0000	0.0000
Displt_X	0.0000	0.0000
Displt_Y	0.43978E-03	0.0000
Displt_Z	0.28130	0.27468
PrincStress_1	0.38383	0.20805
PrincStress_2	-0.17992E-01	0.12574
PrincStress_3	-0.50954E-01	-0.13826E-01
PrincStrain_1	0.16318E-03	0.67551E-04
PrincStrain_2	-0.53799E-04	0.23105E-04

Failure in compression at the top of the asphalt concrete

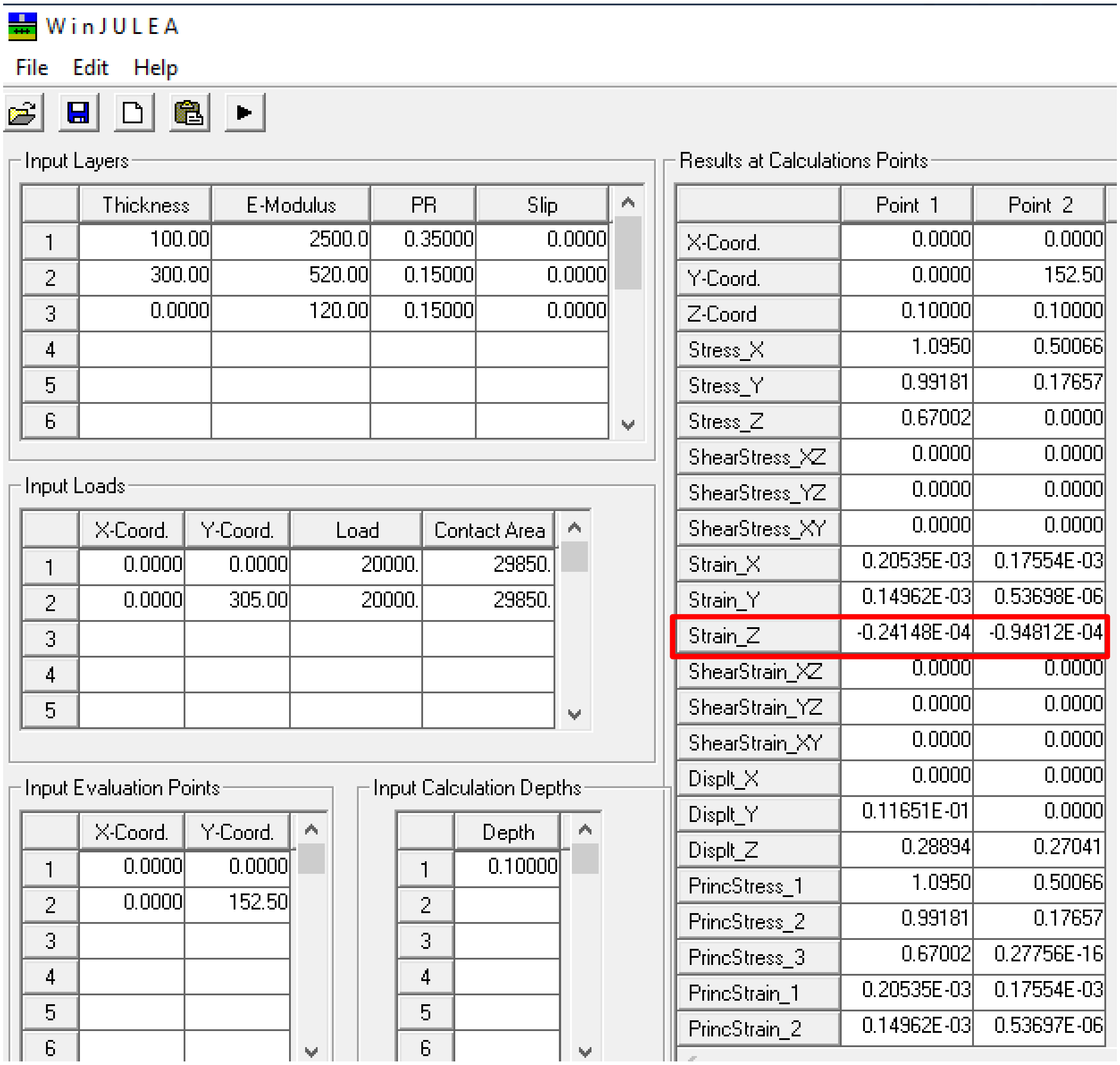

Input Layers

	Thickness	E-Modulus	PR	Slip
1	100.00	2500.0	0.35000	0.0000
2	300.00	520.00	0.15000	0.0000
3	0.0000	120.00	0.15000	0.0000
4				
5				
6				

Input Loads

	X-Coord.	Y-Coord.	Load	Contact Area
1	0.0000	0.0000	20000.	29850.
2	0.0000	305.00	20000.	29850.
3				
4				
5				

Input Evaluation Points

	X-Coord.	Y-Coord.
1	0.0000	0.0000
2	0.0000	152.50
3		
4		
5		
6		

Input Calculation Depths

	Depth
1	0.10000
2	
3	
4	
5	
6	

Results at Calculations Points

	Point 1	Point 2
X-Coord.	0.0000	0.0000
Y-Coord.	0.0000	152.50
Z-Coord	0.10000	0.10000
Stress_X	1.0950	0.50066
Stress_Y	0.99181	0.17657
Stress_Z	0.67002	0.0000
ShearStress_XZ	0.0000	0.0000
ShearStress_YZ	0.0000	0.0000
ShearStress_XY	0.0000	0.0000
Strain_X	0.20535E-03	0.17554E-03
Strain_Y	0.14962E-03	0.53698E-06
Strain_Z	-0.24148E-04	-0.94812E-04
ShearStrain_XZ	0.0000	0.0000
ShearStrain_YZ	0.0000	0.0000
ShearStrain_XY	0.0000	0.0000
Displt_X	0.0000	0.0000
Displt_Y	0.11651E-01	0.0000
Displt_Z	0.28894	0.27041
PrincStress_1	1.0950	0.50066
PrincStress_2	0.99181	0.17657
PrincStress_3	0.67002	0.27756E-16
PrincStrain_1	0.20535E-03	0.17554E-03
PrincStrain_2	0.14962E-03	0.53697E-06

Failure in compression at the top of the granular base

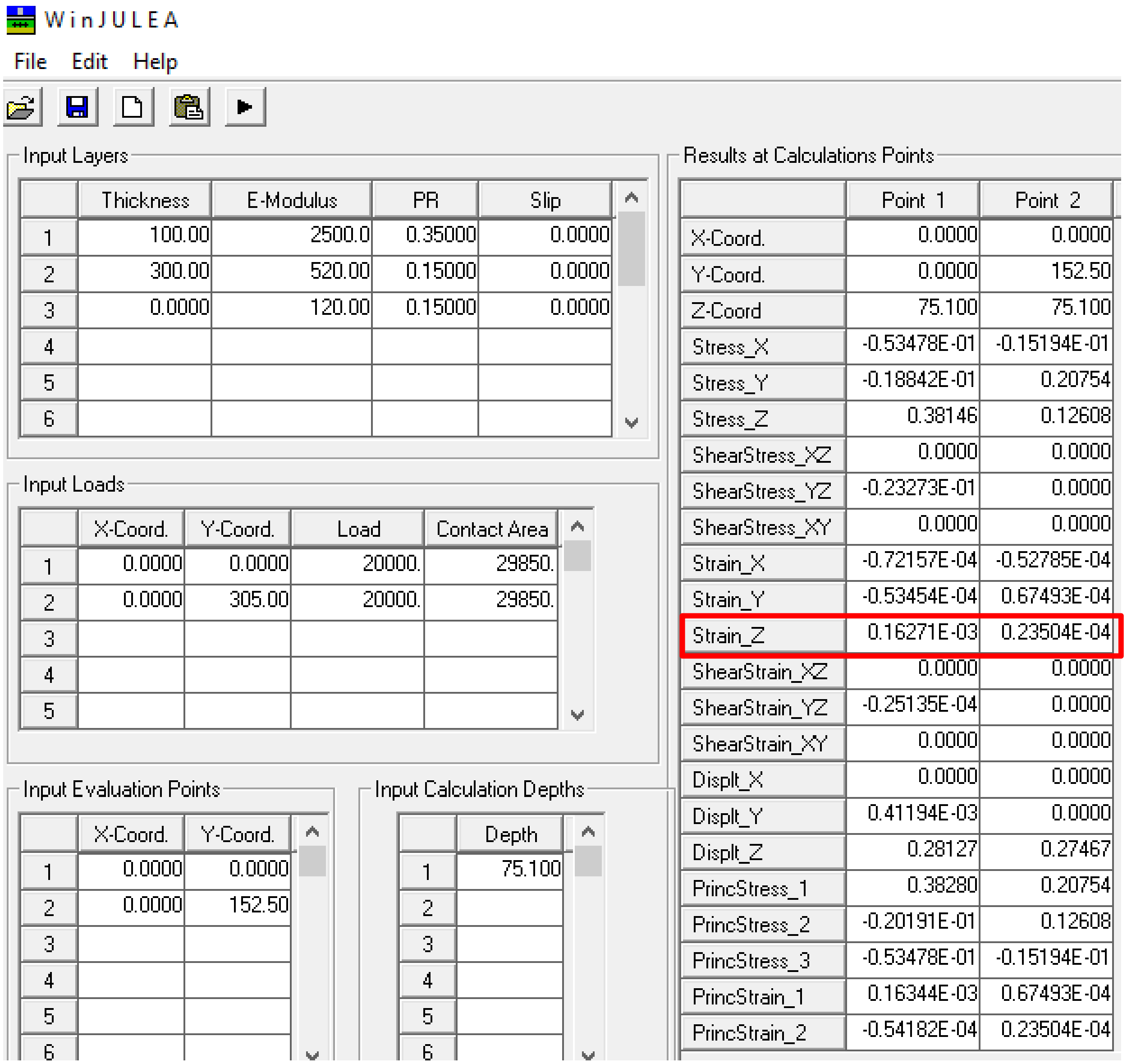

WinJULEA

File Edit Help

Input Layers

	Thickness	E-Modulus	PR	Slip
1	100.00	2500.0	0.35000	0.0000
2	300.00	520.00	0.15000	0.0000
3	0.0000	120.00	0.15000	0.0000
4				
5				
6				

Input Loads

	X-Coord.	Y-Coord.	Load	Contact Area
1	0.0000	0.0000	20000.	29850.
2	0.0000	305.00	20000.	29850.
3				
4				
5				

Input Evaluation Points

	X-Coord.	Y-Coord.
1	0.0000	0.0000
2	0.0000	152.50
3		
4		
5		
6		

Input Calculation Depths

	Depth
1	75.100
2	
3	
4	
5	
6	

Results at Calculations Points

	Point 1	Point 2
X-Coord.	0.0000	0.0000
Y-Coord.	0.0000	152.50
Z-Coord	75.100	75.100
Stress_X	-0.53478E-01	-0.15194E-01
Stress_Y	-0.18842E-01	0.20754
Stress_Z	0.38146	0.12608
ShearStress_XZ	0.0000	0.0000
ShearStress_YZ	-0.23273E-01	0.0000
ShearStress_XY	0.0000	0.0000
Strain_X	-0.72157E-04	-0.52785E-04
Strain_Y	-0.53454E-04	0.67493E-04
Strain_Z	0.16271E-03	0.23504E-04
ShearStrain_XZ	0.0000	0.0000
ShearStrain_YZ	-0.25135E-04	0.0000
ShearStrain_XY	0.0000	0.0000
Displt_X	0.0000	0.0000
Displt_Y	0.41194E-03	0.0000
Displt_Z	0.28127	0.27467
PrincStress_1	0.38280	0.20754
PrincStress_2	-0.20191E-01	0.12608
PrincStress_3	-0.53478E-01	-0.15194E-01
PrincStrain_1	0.16344E-03	0.67493E-04
PrincStrain_2	-0.54182E-04	0.23504E-04

Failure in compression at the top of the subbase

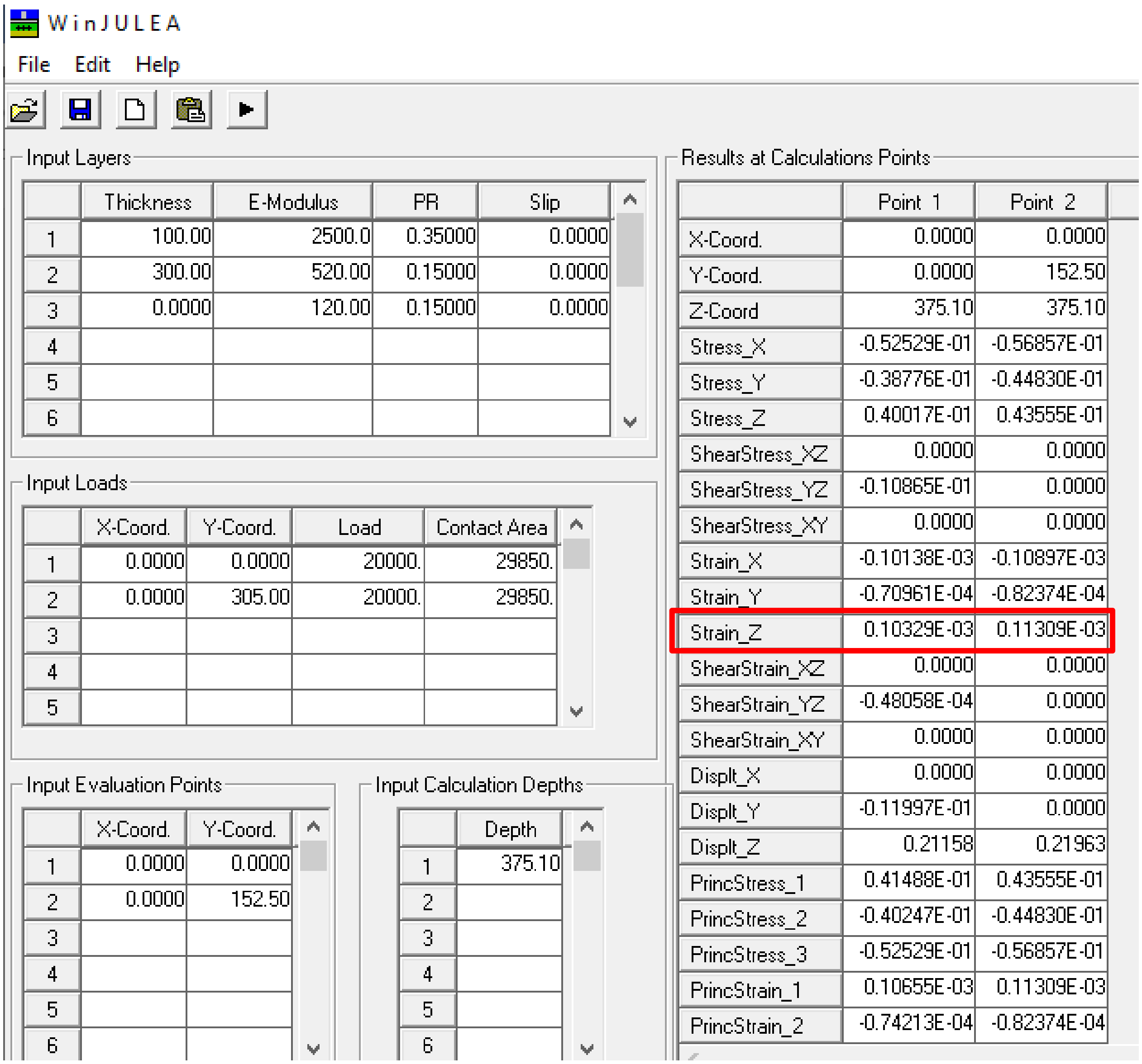
WinJULEA

File Edit Help

Input Layers

	Thickness	E-Modulus	PR	Slip
1	100.00	2500.0	0.35000	0.0000
2	300.00	520.00	0.15000	0.0000
3	0.0000	120.00	0.15000	0.0000
4				
5				
6				

Input Loads

	X-Coord.	Y-Coord.	Load	Contact Area
1	0.0000	0.0000	20000.	29850.
2	0.0000	305.00	20000.	29850.
3				
4				
5				

Input Evaluation Points

	X-Coord.	Y-Coord.
1	0.0000	0.0000
2	0.0000	152.50
3		
4		
5		
6		

Input Calculation Depths

	Depth
1	375.10
2	
3	
4	
5	
6	

Results at Calculations Points

	Point 1	Point 2
X-Coord.	0.0000	0.0000
Y-Coord.	0.0000	152.50
Z-Coord	375.10	375.10
Stress_X	-0.52529E-01	-0.56857E-01
Stress_Y	-0.38776E-01	-0.44830E-01
Stress_Z	0.40017E-01	0.43555E-01
ShearStress_XZ	0.0000	0.0000
ShearStress_YZ	-0.10865E-01	0.0000
ShearStress_XY	0.0000	0.0000
Strain_X	-0.10138E-03	-0.10897E-03
Strain_Y	-0.70961E-04	-0.82374E-04
Strain_Z	0.10329E-03	0.11309E-03
ShearStrain_XZ	0.0000	0.0000
ShearStrain_YZ	-0.48058E-04	0.0000
ShearStrain_XY	0.0000	0.0000
Displt_X	0.0000	0.0000
Displt_Y	-0.11997E-01	0.0000
Displt_Z	0.21158	0.21963
PrincStress_1	0.41488E-01	0.43555E-01
PrincStress_2	-0.40247E-01	-0.44830E-01
PrincStress_3	-0.52529E-01	-0.56857E-01
PrincStrain_1	0.10655E-03	0.11309E-03
PrincStrain_2	-0.74213E-04	-0.82374E-04

Scenario 8: 100 mm of AC + 6% cement

Failure in tension at the bottom of the asphalt concrete

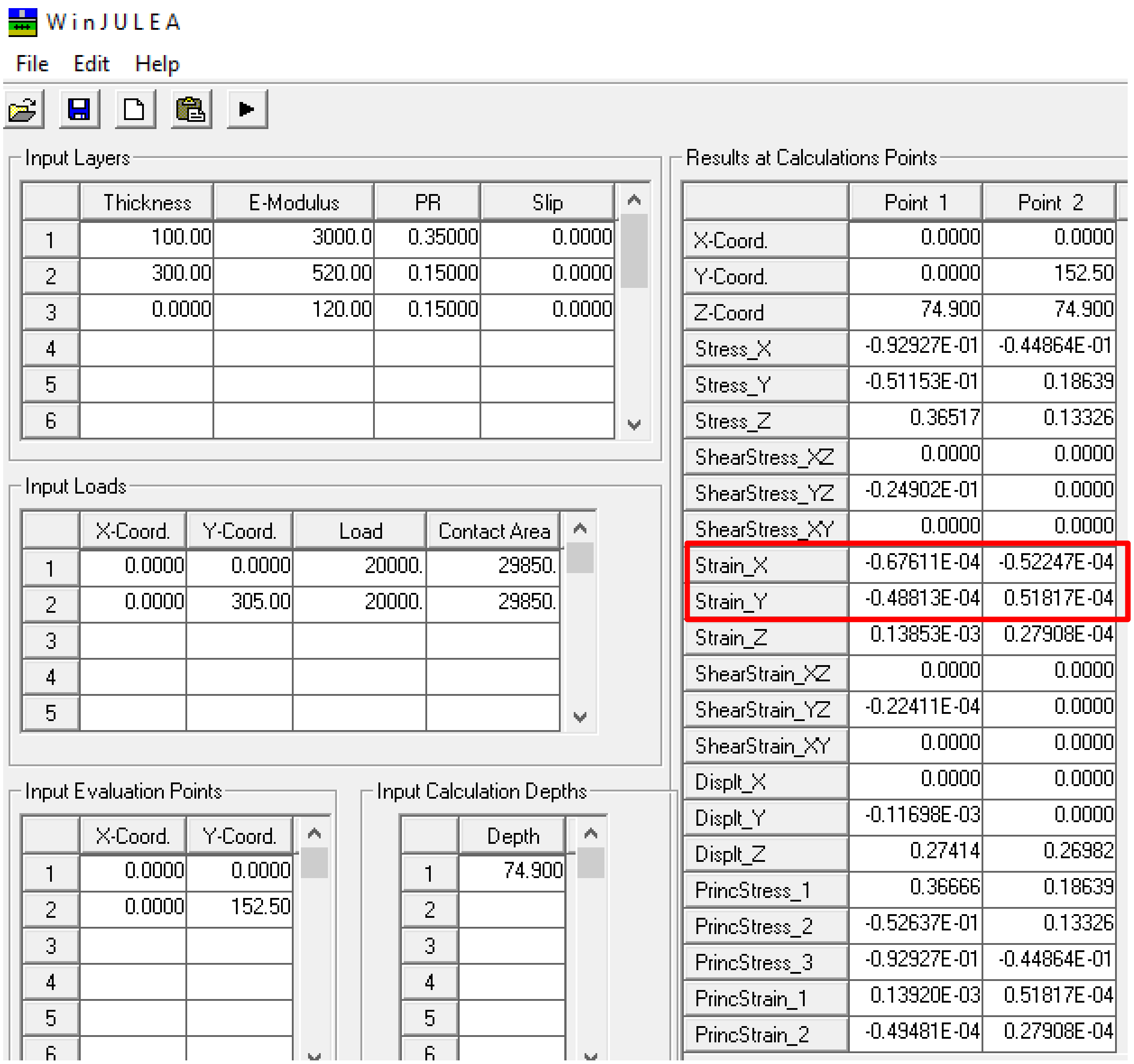

WinJULEA

File Edit Help

Input Layers

	Thickness	E-Modulus	PR	Slip
1	100.00	3000.0	0.35000	0.0000
2	300.00	520.00	0.15000	0.0000
3	0.0000	120.00	0.15000	0.0000
4				
5				
6				

Input Loads

	X-Coord.	Y-Coord.	Load	Contact Area
1	0.0000	0.0000	20000.	29850.
2	0.0000	305.00	20000.	29850.
3				
4				
5				

Input Evaluation Points

	X-Coord.	Y-Coord.
1	0.0000	0.0000
2	0.0000	152.50
3		
4		
5		
6		

Input Calculation Depths

	Depth
1	74.900
2	
3	
4	
5	
6	

Results at Calculations Points

	Point 1	Point 2
X-Coord.	0.0000	0.0000
Y-Coord.	0.0000	152.50
Z-Coord	74.900	74.900
Stress_X	-0.92927E-01	-0.44864E-01
Stress_Y	-0.51153E-01	0.18639
Stress_Z	0.36517	0.13326
ShearStress_XZ	0.0000	0.0000
ShearStress_YZ	-0.24902E-01	0.0000
ShearStress_XY	0.0000	0.0000
Strain_X	-0.67611E-04	-0.52247E-04
Strain_Y	-0.48813E-04	0.51817E-04
Strain_Z	0.13853E-03	0.27908E-04
ShearStrain_XZ	0.0000	0.0000
ShearStrain_YZ	-0.22411E-04	0.0000
ShearStrain_XY	0.0000	0.0000
Displt_X	0.0000	0.0000
Displt_Y	-0.11698E-03	0.0000
Displt_Z	0.27414	0.26982
PrincStress_1	0.36666	0.18639
PrincStress_2	-0.52637E-01	0.13326
PrincStress_3	-0.92927E-01	-0.44864E-01
PrincStrain_1	0.13920E-03	0.51817E-04
PrincStrain_2	-0.49481E-04	0.27908E-04

Failure in compression at the top of the asphalt concrete

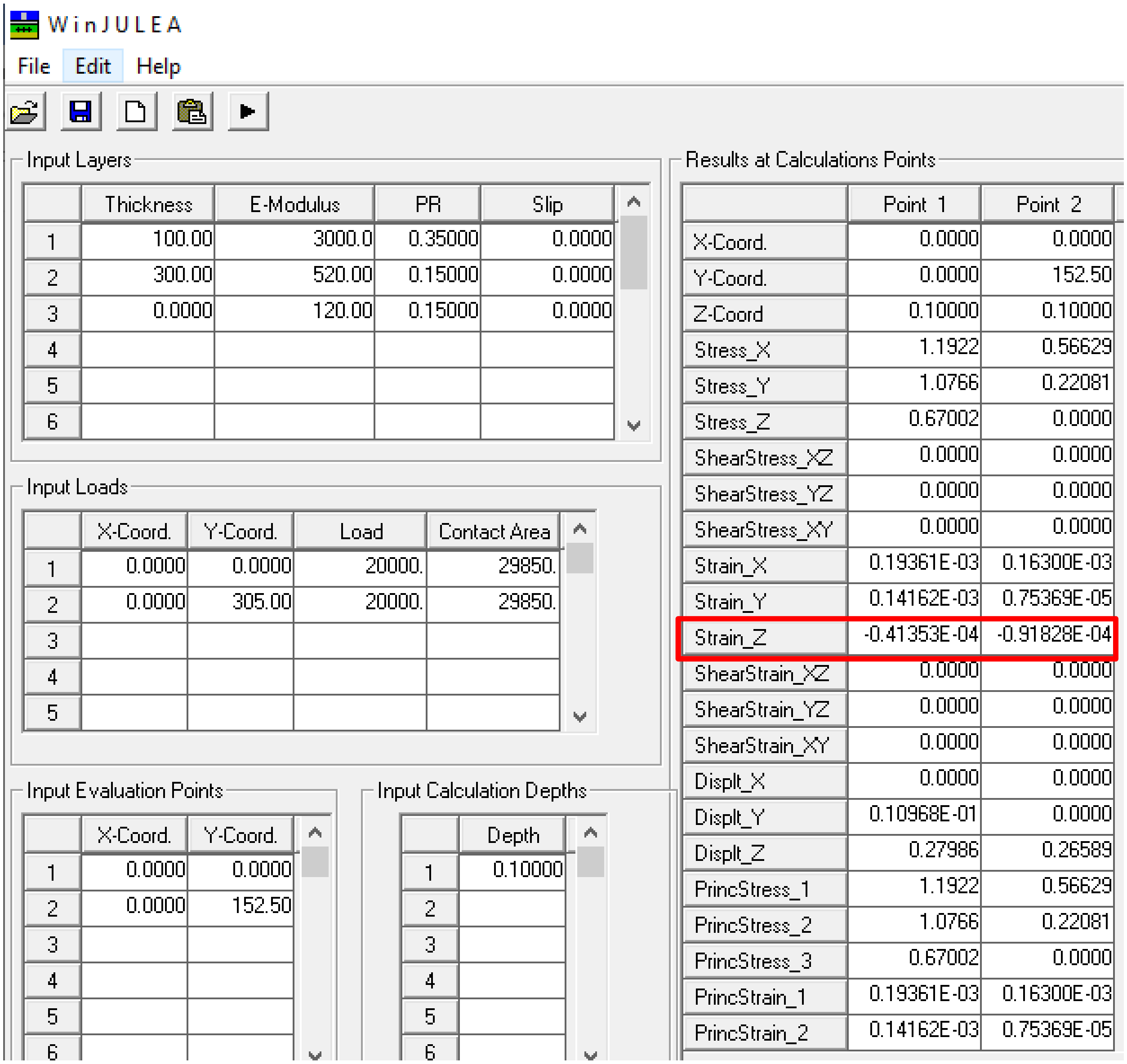
WinJULEA

File Edit Help

Input Layers

	Thickness	E-Modulus	PR	Slip
1	100.00	3000.0	0.35000	0.0000
2	300.00	520.00	0.15000	0.0000
3	0.0000	120.00	0.15000	0.0000
4				
5				
6				

Input Loads

	X-Coord.	Y-Coord.	Load	Contact Area
1	0.0000	0.0000	20000.	29850.
2	0.0000	305.00	20000.	29850.
3				
4				
5				

Input Evaluation Points

	X-Coord.	Y-Coord.
1	0.0000	0.0000
2	0.0000	152.50
3		
4		
5		
6		

Input Calculation Depths

	Depth
1	0.10000
2	
3	
4	
5	
6	

Results at Calculations Points

	Point 1	Point 2
X-Coord.	0.0000	0.0000
Y-Coord.	0.0000	152.50
Z-Coord	0.10000	0.10000
Stress_X	1.1922	0.56629
Stress_Y	1.0766	0.22081
Stress_Z	0.67002	0.0000
ShearStress_XZ	0.0000	0.0000
ShearStress_YZ	0.0000	0.0000
ShearStress_XY	0.0000	0.0000
Strain_X	0.19361E-03	0.16300E-03
Strain_Y	0.14162E-03	0.75369E-05
Strain_Z	-0.41353E-04	-0.91828E-04
ShearStrain_XZ	0.0000	0.0000
ShearStrain_YZ	0.0000	0.0000
ShearStrain_XY	0.0000	0.0000
Displt_X	0.0000	0.0000
Displt_Y	0.10968E-01	0.0000
Displt_Z	0.27986	0.26589
PrincStress_1	1.1922	0.56629
PrincStress_2	1.0766	0.22081
PrincStress_3	0.67002	0.0000
PrincStrain_1	0.19361E-03	0.16300E-03
PrincStrain_2	0.14162E-03	0.75369E-05

Failure in compression at the top of the granular base

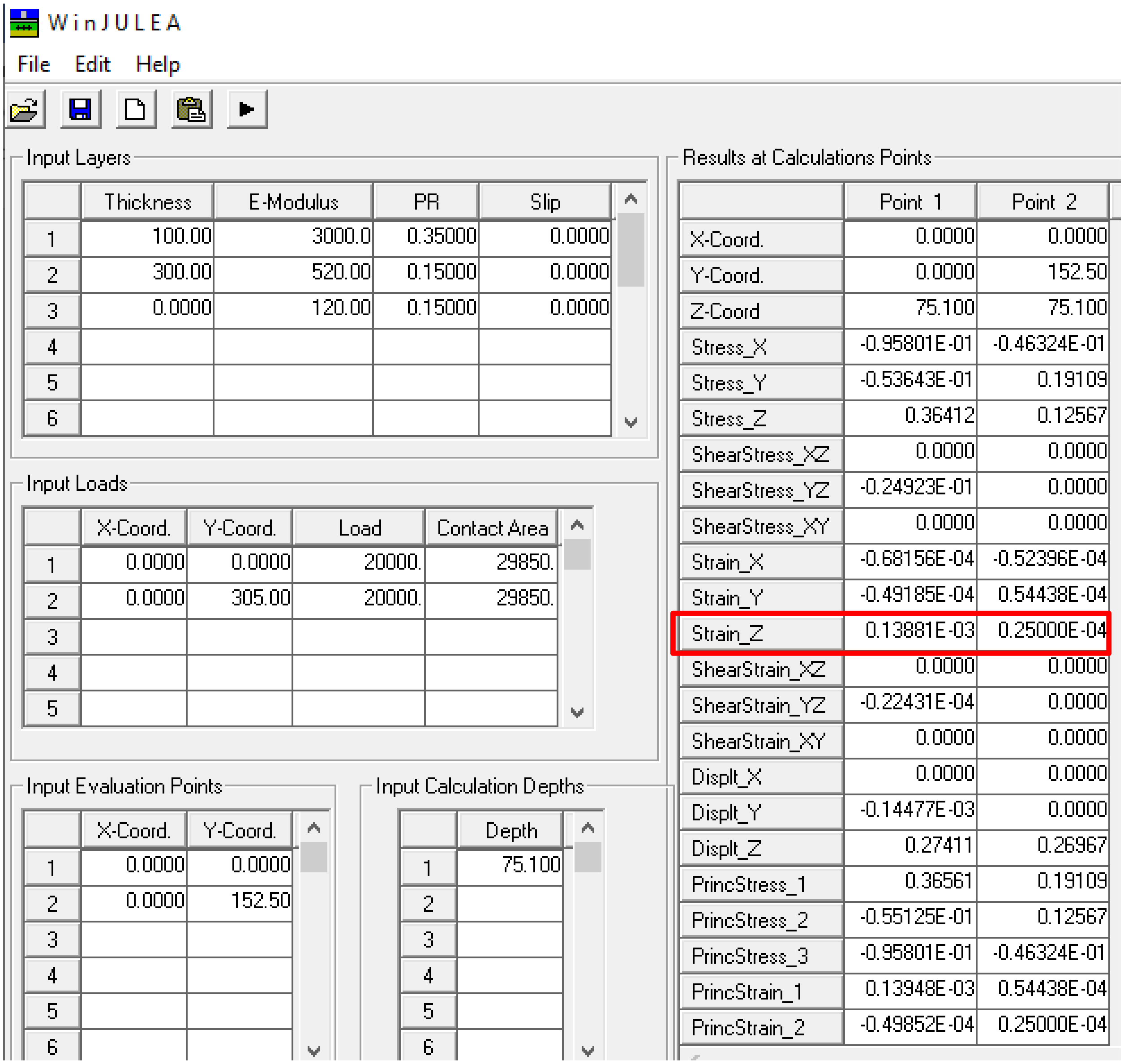

Input Layers

	Thickness	E-Modulus	PR	Slip
1	100.00	3000.0	0.35000	0.0000
2	300.00	520.00	0.15000	0.0000
3	0.0000	120.00	0.15000	0.0000
4				
5				
6				

Input Loads

	X-Coord.	Y-Coord.	Load	Contact Area
1	0.0000	0.0000	20000.	29850.
2	0.0000	305.00	20000.	29850.
3				
4				
5				

Input Evaluation Points

	X-Coord.	Y-Coord.
1	0.0000	0.0000
2	0.0000	152.50
3		
4		
5		
6		

Input Calculation Depths

	Depth
1	75.100
2	
3	
4	
5	
6	

Results at Calculations Points

	Point 1	Point 2
X-Coord.	0.0000	0.0000
Y-Coord.	0.0000	152.50
Z-Coord	75.100	75.100
Stress_X	-0.95801E-01	-0.46324E-01
Stress_Y	-0.53643E-01	0.19109
Stress_Z	0.36412	0.12567
ShearStress_XZ	0.0000	0.0000
ShearStress_YZ	-0.24923E-01	0.0000
ShearStress_XY	0.0000	0.0000
Strain_X	-0.68156E-04	-0.52396E-04
Strain_Y	-0.49185E-04	0.54438E-04
Strain_Z	0.13881E-03	0.25000E-04
ShearStrain_XZ	0.0000	0.0000
ShearStrain_YZ	-0.22431E-04	0.0000
ShearStrain_XY	0.0000	0.0000
Displt_X	0.0000	0.0000
Displt_Y	-0.14477E-03	0.0000
Displt_Z	0.27411	0.26967
PrincStress_1	0.36561	0.19109
PrincStress_2	-0.55125E-01	0.12567
PrincStress_3	-0.95801E-01	-0.46324E-01
PrincStrain_1	0.13948E-03	0.54438E-04
PrincStrain_2	-0.49852E-04	0.25000E-04

Failure in compression at the top of the subbase

WinJULEA

File Edit Help

Input Layers

	Thickness	E-Modulus	PR	Slip
1	100.00	3000.0	0.35000	0.0000
2	300.00	520.00	0.15000	0.0000
3	0.0000	120.00	0.15000	0.0000
4				
5				
6				

Input Loads

	X-Coord.	Y-Coord.	Load	Contact Area
1	0.0000	0.0000	20000.	29850.
2	0.0000	305.00	20000.	29850.
3				
4				
5				

Input Evaluation Points

	X-Coord.	Y-Coord.
1	0.0000	0.0000
2	0.0000	152.50
3		
4		
5		
6		

Input Calculation Depths

	Depth
1	375.10
2	
3	
4	
5	
6	

Results at Calculations Points

	Point 1	Point 2
X-Coord.	0.0000	0.0000
Y-Coord.	0.0000	152.50
Z-Coord	375.10	375.10
Stress_X	-0.51717E-01	-0.55905E-01
Stress_Y	-0.38503E-01	-0.44531E-01
Stress_Z	0.38907E-01	0.42374E-01
ShearStress_XZ	0.0000	0.0000
ShearStress_YZ	-0.10578E-01	0.0000
ShearStress_XY	0.0000	0.0000
Strain_X	-0.99573E-04	-0.10689E-03
Strain_Y	-0.70348E-04	-0.81732E-04
Strain_Z	0.10085E-03	0.11046E-03
ShearStrain_XZ	0.0000	0.0000
ShearStrain_YZ	-0.46786E-04	0.0000
ShearStrain_XY	0.0000	0.0000
Displt_X	0.0000	0.0000
Displt_Y	-0.11897E-01	0.0000
Displt_Z	0.20791	0.21572
PrincStress_1	0.40327E-01	0.42374E-01
PrincStress_2	-0.39922E-01	-0.44531E-01
PrincStress_3	-0.51717E-01	-0.55905E-01
PrincStrain_1	0.10399E-03	0.11046E-03
PrincStrain_2	-0.73487E-04	-0.81732E-04

BIBLIOGRAPHY

AASHTO. 1993. *AASHTO Guide for Design of Pavement Structures. American Association of State Highway and Transportation Officials*. Washington, d.c.

AASHTO. 2008. *Mechanistic-Empirical Pavement Design Guide. American Association of State HighwAy and Transportation Officials Executive Committee*.

Abdel-Wahed, Talaat A., and Naglaa K. Rashwan. 2016. "Application of Cement Dust and OPC as Mineral Filler in the Binder Hot Mix Asphalt." *15th Annual International Conference on Asphalt, Pavement Engineering/ and Infrastructure* 15(200).

Abiola, O. S., W. K. Kupolati, E. R. Sadiku, and J. M. Ndambuki. 2014. "Utilisation of Natural Fibre as Modifier in Bituminous Mixes: A Review." *Construction and Building Materials* 54:305–12. doi: 10.1016/j.conbuildmat.2013.12.037.

Adlinge, Sharad S., and Prof a K. Gupta. 2009. "Pavement Deterioration and Its Causes." *Mechanical & Civil Engineering* 9–15.

Adlinge, Sharad S., and Prof a K. Gupta. 2013. "Pavement Deterioration and Its Causes." *Mechanical & Civil Engineering* 2(4):9–15.

Ahmad, Juraidah, Nur Izzi Md Yusoff, Mohd Rosli Hainin, Mohd Yusof Abd Rahman, and Mustaque Hossain. 2014. "Evaluation on Performance Characteristics of Superpave Asphalt Mix Design under Tropical Climatic Conditions." *International Journal of Pavement Research and Technology* 7(5):331–42. doi: 10.6135/ijprt.org.tw/2014.7(5).331.

Ahmedzade, Perviz. 2013. "The Investigation and Comparison Effects of SBS and SBS with New Reactive Terpolymer on the Rheological Properties of Bitumen." *Construction and Building Materials* 38:285–91. doi: 10.1016/j.conbuildmat.2012.07.090.

Al-khateeb, Ghazi G., and Nabil M. Al-akhras. 2011. "Properties of Portland Cement-Modified Asphalt Binder Using Superpave Tests." *Construction and Building Materials* 25(2):926–

32. doi: 10.1016/j.conbuildmat.2010.06.091.

Al-Khateeb, Ghazi G., and Nabil M. Al-Akhras. 2011. "Properties of Portland Cement-Modified Asphalt Binder Using Superpave Tests." *Construction and Building Materials* 25(2):926–32. doi: 10.1016/j.conbuildmat.2010.06.091.

Al-Qaisi. 1981. "Al- Qaisi, T. A. (1981), 'The Effect of Mineral Filler on the Properties of Asphalt Paving Mixtures', M.Sc. Thesis, University of Baghdad." 1981.

Al-Suleiman, Turki I., and Adnan M. S. Shiyab. 2003. "Prediction of Pavement Remaining Service Life Using Roughness Data - Case Study in Dubai." *International Journal of Pavement Engineering* 4(2):121–29. doi: 10.1080/10298430310001634834.

Aljassar, Ahmad H., Saved Metwali, and Mohammed A. Ali. 2004. "Effect of Filler Types on Marshall Stability and Retained Strength of Asphalt Concrete." *International Journal of Pavement Engineering* 5(1):47–51. doi: 10.1080/10298430410001733491.

Almadwi, Fathi S., and Gabriel J. Assaf. 2017. "Performance Testing of Paving Mixes for Libya's Hot and Arid Conditions, Using Marshall Stability and SUPERPAVE Gyratory Compactor Methods." P. (313-323) in *In International Congress and Exhibition" Sustainable Civil Infrastructures: Innovative Infrastructure Geotechnology"*. Cham,: Springer.

Almadwi, Fathi S., and Gabriel J. Assaf. 2018. "Finding an Optimal Bitumen and Natural Sand Balance for Hot Mix Asphalt Concrete in Hot and Arid Regions." Pp. 1–12 in *Proceedings of the 5th GeoChina International Conference Civil Infrastructures Confronting Severe Weathers and Climate Changes: From Failure to Sustainability*. HangZhou, China: Springer.

Almadwi, Fathi S., and Gabriel J. Assaf. 2019. "Effects of Asphalt Binders on Pavement Mixtures Using an Optimal Balance of Desert Sand." *Construction and Building Materials* 220:415–25. doi: 10.1016/j.conbuildmat.2019.06.040.

Almadwi, Fathi S., and Gabriel J. Assaf. 2021. "Effects of Brick Powder on the Properties of

Asphalt Mixes." *Journal of Materials in Civil Engineering* 33(1):04020429. doi: 10.1061/(asce)mt.1943-5533.0003531.

Amhadi, Talal S., and Gabriel J. Assaf. 2019. "Assessment of Strength Development of Cemented Desert Soil." *International Journal of Low-Carbon Technologies* 14(4):543–49. doi: 10.1093/ijlct/ctz047.

Amhadi, Talal S, and Gabriel J. Assaf. 2019. *The Effect of Using Desert Sands and Cement to Stabilize the Base Course Layer of Roads in Libya*. Springer International Publishing.

Ankit, Gupta, Praveen Kumar, and Rajat Rastogi. 2011. "Effect of Environmental Factors on Flexible Pavement." *8th International Conference on Managing Pavement Assets* (3).

Anon. n.d. "Scholar."

Asi, Ibrahim M. 2007. "Performance Evaluation of SUPERPAVE and Marshall Asphalt Mix Designs to Suite Jordan Climatic and Traffic Conditions." *Construction and Building Materials* 21(8):1732–40. doi: 10.1016/j.conbuildmat.2006.05.036.

ASTM. 2015. "E595 − 15 Standard Test Method for Total Mass Loss and Collected Volatile Condensable Materials from Outgassing in a Vacuum Environment (E595-07)." *Astm* i(July):1–9. doi: 10.1520/E0595-07.Copyright.

Badeli, Saeed. 2018. "Evaluation of the Damage of an Asphalt Mix under Repeated Freeze-Thaw Cycles." *Thèse de Doctorat, ÉCOLE DE TECHNOLOGIE SUPÉRIEURE UNIVERSITÉ DU QUÉBEC*.

Brian D. Prowell Jingna Zhang And E. E. Ray Brown. 2005. *Aggregate Properties and the Performance of Superpave-Designed Hot-Mix Asphalt*.

Brown, S. F., and D. Needham. 2000. "A Study of Cement Modified Bitumen Emulsion Mixtures." 1–22.

Cao, Dongwei, and Jie Ji. 2011. "Evaluation of the Long-Term Properties of Sasobit Modified

Asphalt." *International Journal of Pavement Research and Technology* 4(6):384–91. doi: 10.6135/ijprt.org.tw/2011.4(6).384.

Caputo, Paolino, Abraham A. Abe, Valeria Loise, Michele Porto, Pietro Calandra, Ruggero Angelico, and Cesare Oliviero Rossi. 2020. "The Role of Additives in Warm Mix Asphalt Technology: An Insight into Their Mechanisms of Improving an Emerging Technology." *Nanomaterials* 10(6):1–17. doi: 10.3390/nano10061202.

Cardona, Diego Alejandro Ramirez, Simon Pouget, Herve Di Benedetto, and François Olard. 2015. "Viscoelastic Behaviour Characterization of a Gap-Graded Asphalt Mixture with SBS Polymer Modified Bitumen." *Materials Research* 18(2):373–81. doi: 10.1590/1516-1439.332214.

Carvalho, Regis L., and Charles W. Schwartz. 2006. "Comparisons of Flexible Pavement Designs: AASHTO Empirical versus NCHRP Project 1-37A Mechanistic-Empirical." *Transportation Research Record* (1947):167–74. doi: 10.3141/1947-16.

Castelli, Raymond J., M. Asce, Supv Geotechnical Engineer, Parsons Brinckerhoff, and N. Meridian St. 2010. "GeoFlorida 2010: Advances in Analysis, Modeling & Design (GSP 199) © 2010 ASCE 2012." *GeoFlorida 2010: Advanced in Analysis, Modeling & Design* (Gsp 199):2012–21.

Chen, Mei Zhu, Wei Wei, and Shao Peng Wu. 2009. "On Cold Materials of Pavement and High-Temperature Performance of Asphalt Concrete." *Materials Science Forum* 620 622:379–82. doi: 10.4028/www.scientific.net/MSF.620-622.379.

Chernoff, Herman. 1973. "The Use of Faces to Represent Points in K-Dimensional Space Graphically." *Journal of the American Statistical Association* 68(342):361. doi: 10.2307/2284077.

Chompoorat, T., and S. Likitlersuang. 2016. "Assessment of Shrinkage Characteristic in Blended Cement and Fly Ash Admixed Soft Clay." 311–16.

Dallas Little, Author N., Tom Scullion, Prakash BVS Kota, and Jasim Bhuiyan. 1995.

"Guidelines for Mixture Design and Thickness Design for Stabilized Bases and Subgrades." 7.

Donald Walker, T. I. C. Director. 2002. "Asphalt-PASERManual." *PASER Asphalt Roads MAnual* 32.

Doré, H. K. Zubeck and G. 2009. "Introduction to Cold Regions Pavement Engineering." *Aspectos Generales De La Planificación Tributaria En Venezuela* 2009(75):31–47.

Ekwulo, Emmanuel O., and Dennis B. Eme. 2009. "Fatigue and Rutting Strain Analysis of Flexible Pavements Designed Using CBR Methods." *African Journal of Environmental Science and Technology* 3(12):412–21.

Faheem, Ahmed F., Hussain U. Bahia, Shih Hsien Yang, and Imad Al-Qadi. 2010. "Evaluation of Rigden Fractional Voids Test Method and the Relation to Mastic Viscosity." *Asphalt Paving Technology: Association of Asphalt Paving Technologists-Proceedings of the Technical Sessions* 79:1–25.

Fattah, Mohammed Y., Hasan H. Joni, and Ahmed S. Ahmed. 2016. "Compaction and Collapse Characteristics of Dune Sand Stabilized with Lime-Silica Fume Mix." *Turkish Journal of Engineering and Environmental Sciences* 40(3):99–113. doi: 10.15446/esrj.v20n2.50724.

FH Administration. 2008. "Superpave Fundamentals - Superpave: The Future of Asphalt." *U.S. Department Of Transportation* (NHI #131053).

For, Ggregates, Oads By B. K. Majumder, and Animesh Das. 1999. *C Ement T Reated M Arginal a Ggregates*.

G. Li, Y. Zhao, S.-S. Pang, and W. Huang. 1998. "EXPERIMENTAL STUDY OF CEMENT-ASPHALT EMULSION COMPOSITE." 28(5):635–41.

Garfield, JOAN. 1992. *Design of a High-Binder–High-Modulus Asphalt Mixture*. Vol. 14.

Gopalakrishnan, Kasthurirangan, and Sunghwan Kim. 2011. “Support Vector Machines Approach to HMA Stiffness Prediction.” *Journal of Engineering Mechanics* 137(2):138–46. doi: 10.1061/(asce)em.1943-7889.0000214.

Guha, Aioub H., and Gabriel J. Assaf. 2020a. “Effect of Portland Cement as a Filler in Hot-Mix Asphalt in Hot Regions.” *Journal of Building Engineering* 28(October 2019):101036. doi: 10.1016/j.jobe.2019.101036.

Guha, Aioub H., and Gabriel J. Assaf. 2020b. “Effects of Different Fillers on Pavement Deformation of Hot Mix Asphalt in Hot Climates.” *Construction and Building Materials* 261:119898. doi: 10.1016/j.conbuildmat.2020.119898.

Haider, Syed Waqar, and Karim Chatti. 2009. “Effects of Design and Site Factors on Roughness Development in Flexible Pavements.” *Journal of Transportation Engineering* 135(3):112–20. doi: 10.1061/(ASCE)0733-947X(2009)135:3(112).

Hall, Kathleen T., Carlos E. Correa, and Amy L. Simpson. 2003. “Performance of Flexible Pavement Rehabilitation Treatments in the Long-Term Pavement Performance SPS-5 Experiment.” *Transportation Research Record* (1823):93–101. doi: 10.3141/1823-11.

Hall, Kevin, Danny Xiao, and Kelvin Wang. 2011. “Calibration of the Mechanistic-Empirical Pavement Design Guide for Flexible Pavement Design in Arkansas.” *Transportation Research Record* (2226):135–41. doi: 10.3141/2226-15.

Hamed M. H. Alani, Amjad H. Albayati and Alaa S. Abbas. 2010. “The Transition to a PG Grading System for Asphalt Cement in Iraq.” *Journal of Engineering* 16(4).

Head, R. W. 1974. “An Informal Report of Cold Mix Research Using Emulsified Asphalt as a Binder.” *Association of Asphalt Paving Technologists Proc* 110–31.

Herb, William, Raul Velasquez, Heinz Stefan, Mihai O. Marasteanu, and Tim Clyne. 2009. “Simulation and Characterization of Asphalt Pavement Temperatures.” *Road Materials and Pavement Design* 10(1):233–47. doi: 10.1080/14680629.2009.9690190.

Hoegh, Kyle, Lev Khazanovich, and Maureen Jense. 2010. "Local Calibration of Mechanistic-Empirical Pavement Design Guide Rutting Model: Minnesota Road Research Project Test Sections." *Transportation Research Record* (2180):130–41. doi: 10.3141/2180-15.

Isacsson, U., and X. Lu. 1995. "Testing and Appraisal of Polymer Modified Road Bitumens-State of the Art." *Materials and Structures* 28(3):139–59. doi: 10.1007/BF02473221.

Islam, Md Rashadul, and Rafiqul A. Tarefder. 2015. "Coefficients of Thermal Contraction and Expansion of Asphalt Concrete in the Laboratory." *Journal of Materials in Civil Engineering* 27(11):04015020. doi: 10.1061/(asce)mt.1943-5533.0001277.

Italiana, Norma. 2005. "Metodi Di Prova per Conglomerati Bituminosi a Caldo,'Test Methods for Hot Mix Asphalt ."

James, J. G., and J. A. Reid. 1969. "ROAD RESEARCH LABORATORY Ministry of Transport RRL REPORT LR 285 NOTES ON THE COSTS, LIVES & EFFECTIVENESS OF VARIOUS ROAD MARKINGS By."

Jannat, Gulfam E., Sina Varamini, and Susan L. Tighe. 2020. "Investigating the Performance of Superpave through the Ontario Highways." 961(September 2019):954–61.

Jaskuła, Piotr, Marcin Stienss, and Cezary Szydłowski. 2017. "Effect of Polymer Fibres Reinforcement on Selected Properties of Asphalt Mixtures." *Procedia Engineering* 172:441–48. doi: 10.1016/j.proeng.2017.02.026.

jenks, C. W., Jencks, C. F ., Harrigan, E. T., Adcock, M., Delaney, E. P., & Freer, H. 2011. *A Manual for Design of Hot-Mix Asphalt with Commentary*.

Kakrasul, Jamal. 2015. "The Superpave System." *Newsletter*.

Kandhal, Prithvi S., Cynthia Y. Lynn, and Frazier Parker. 1998. "Characterization Tests for Mineral Fillers Related to Performance of Asphalt Paving Mixtures." *Transportation Research Record* (1638):101–10. doi: 10.3141/1638-12.

Kanitpong, Kunnawee, and Hussain Bahia. 2005. “Relating Adhesion and Cohesion of Asphalts to the Effect of Moisture on Laboratory Performance of Asphalt Mixtures.” *Transportation Research Record* (1901):33–43. doi: 10.3141/1901-05.

Kasperick, Taylor, and Khaled Ksaibati. 2015. “Calibration of the Mechanistic-Empirical Pavement Design Guide for Local Paved Roads in Wyoming.”

Kök, Baha Vural, and Hakan Çolak. 2011. “Laboratory Comparison of the Crumb-Rubber and SBS Modified Bitumen and Hot Mix Asphalt.” *Construction and Building Materials* 25(8):3204–12. doi: 10.1016/j.conbuildmat.2011.03.005.

Kucukvar, Murat, Mehdi Noori, Gokhan Egilmez, and Omer Tatari. 2014. “Stochastic Decision Modeling for Sustainable Pavement Designs.” *International Journal of Life Cycle Assessment* 19(6):1185–99. doi: 10.1007/s11367-014-0723-4.

Lesueur, Didier, Joëlle Petit, and Hans Josef Ritter. 2013. “The Mechanisms of Hydrated Lime Modification of Asphalt Mixtures: A State-of-the-Art Review.” *Road Materials and Pavement Design* 14(1):1–16. doi: 10.1080/14680629.2012.743669.

Likitlersuang, Suched, and Thanakorn Chompoorat. 2016. “Laboratory Investigation of the Performances of Cement and Fly Ash Modified Asphalt Concrete Mixtures.” *International Journal of Pavement Research and Technology* 9(5):337–44. doi: 10.1016/j.ijprt.2016.08.002.

Lytton, Robert L. 2000. “Pavements for Performance BASE COURSE STIFFNESS.” (00):5–16.

Madwi, Fathi. 2020. “Sand-Asphalt Mix Design with Available Materials for Hot and Arid Environments By.”

McDaniel, Rebecca S. 2015. *Fiber Additives in Asphalt Mixtures*.

Montanelli, Eng. Filippo, and Iterchimica srl. 2013. “Fiber/Polymeric Compound for High Modulus Polymer Modified Asphalt (PMA).” *Procedia - Social and Behavioral Sciences*

104:39–48. doi: 10.1016/j.sbspro.2013.11.096.

MTQ. 2016. “Ministère Des Transports, Québec (MTQ).”

Nega, Ainalem. 2015. “Development and Validation of Characterization Method Using Finite Element Numerical Modeling and Advance Laboratory Methods for Western Australia Asphalt Mixes.” *Development and Validation of Characterization Method Using Finite Element Numerical Modeling and Advance Laboratory Methods for Western Australia Asphalt Mixes* (December).

Nega, Ainalem, Hamid Nikraz, and Colin Leek. 2013. “Engineering Characterization of Hot-Mix Asphalt in Western Australia.” *Airfield and Highway Pavement 2013: Sustainable and Efficient Pavements - Proceedings of the 2013 Airfield and Highway Pavement Conference* 987–98. doi: 10.1061/9780784413005.082.

Obadat, Mohammad. 2021. “Marshall Mix Design Mohammad Obadat, 2021-03 The University of Tennessee at Martin. Department of Engineering Https://Www.Utm.Edu/Staff/Mobadat/Courses/Pavement%20Design%20and%20Analysis/Superp.Html.” 2021.

Olard, François. 2012. “GB5 Mix Design: High-Performance and Cost-Effective Asphalt Concretes by Use of Gap-Graded Curves and SBS Modified Bitumens.” *Road Materials and Pavement Design* 13(SUPPL. 1):234–59. doi: 10.1080/14680629.2012.657074.

Oruc, S., M. Bostancioglu, and B. Yilmaz. 2013. “Effect of Residual Asphalt Content on Creep Strain of Cement Modified Emulsified Asphalt Mixtures.” *Journal of Civil Engineering and Urbanism* 3(3):122–27.

Oruc, Seref, Fazil Celik, and Atakan Aksoy. 2006a. “Performance of Cement Modified Dense Graded Cold-Mix Asphalt and Establishing Mathematical Model.” *Indian Journal of Engineering and Materials Sciences* 13(6):512–19.

Oruc, Seref, Fazil Celik, and Atakan Aksoy. 2006b. “Performance of Cement Modified Dense Graded Cold-Mix Asphalt and Establishing Mathematical Model.” *Indian Journal of*

Engineering and Materials Sciences 13(6):512–19.

Pais, J. C., S. I. R. Amorim, and M. J. C. Minhoto. 2013. "Impact of Traffic Overload on Road Pavement Performance." *Journal of Transportation Engineering* 139(9):873–79. doi: 10.1061/(ASCE)TE.1943-5436.0000571.

Pereira, Raul, Ana Almeida-Costa, Cátia Duarte, and Agostinho Benta. 2018. "Warm Mix Asphalt: Chemical Additives' Effects on Bitumen Properties and Limestone Aggregates Mixture Compactibility." *International Journal of Pavement Research and Technology* 11(3):285–99. doi: 10.1016/j.ijprt.2017.10.005.

Portland Cement Association (PCA). 2003. "Reflective Cracking in Cement Stabilized Pavements." *Soil-Cement Information,* 1–4.

Pouliot, Nadia, Jacques Marchand, and Michel Pigeon. 2003. "Hydration Mechanisms, Microstructure, and Mechanical Properties of Mortars Prepared with Mixed Binder Cement Slurry-Asphalt Emulsion." *Journal of Materials in Civil Engineering* 15(1):54–59. doi: 10.1061/(asce)0899-1561(2003)15:1(54).

Preciado, Jaime, Gilberto Martínez Arguelles, Margareth Dugarte, Alessandra Bonicelli, Julio Cantero, Daniela Vega, and Yennis Barros. 2017. "Improving Mechanical Properties of Hot Mix Asphalt Using Fibres and Polymers in Developing Countries." *IOP Conference Series: Materials Science and Engineering* 245(2). doi: 10.1088/1757-899X/245/2/022013.

Von Quintus, Harold L., Ahmed Eltahan, and Amber Yau. 2001. "Smoothness Models for Hot-Mix Asphalt-Surfaced Pavements: Developed from Long-Term Pavement Performance Program Data." *Transportation Research Record* (1764):139–56. doi: 10.3141/1764-15.

Raymond, Christopher M., Susan L. Tighe, Ralph Haas, and Leo Rothenburg. 2003. "Analysis of Influences on As-Built Pavement Roughness in Asphalt Overlays." *International Journal of Pavement Engineering* 4(4):181–92. doi: 10.1080/10298430310001653077.

Rohan w, Perera. Starr D, Kohn. 2006. "Ride Quality Performance of Asphalt Concrete

Pavements Subjected to Different Rehabilitation Strategies.” *Proceedings of the 2000 CSCE Annual Conference, London Pp. 7-10 (2000)* 486–97.

Salem, Hassan Awadat, Djordje Uzelac, and Bojan Matic. 2014. “Temperature Zoning of Libya Desert for Asphalt Mix Design.” Pp. 1414–26 in Vols. 638–640. Trans Tech Publications Ltd.

Schmidt, R J; Graf, P. E. 1974. “EFFECT OF WATER ON RESILIENT MODULUS OF ASPHALT- TREATED MIXES OF ASPHALT-TREATED SPECIMENS IN THE PRESENCE OF MOISTURE INCREASES WITH AN INCREASE IN EXPOSURE TEMPERATURE . THE FOLLOWING ARE AMONG THE STEPS.” 1973–76.

SHRP. 1994. *SHRP-A-379 “The SUPERPAVE Mix Design System Manual of Specifications , Test Methods , and Practices.”*

Smith, James T., and Susan L. Tighe. 2004. “Assessment of Overlay Roughness in Long-Term Pavement Performance Test Sites: Canadian Case Study.” *Transportation Research Record* (1869):126–35. doi: 10.3141/1869-15.

Sol-Sánchez, Miguel, Fernando Moreno-Navarro, Gema García-Travé, and Ma Carmen Rubio-Gámez. 2015. “Laboratory Study of the Long-Term Climatic Deterioration of Asphalt Mixtures.” *Construction and Building Materials* 88:32–40. doi: 10.1016/j.conbuildmat.2015.03.090.

Song, Hun, Jeongyun Do, and Yangseob Soh. 2006. “Feasibility Study of Asphalt-Modified Mortars Using Asphalt Emulsion.” *Construction and Building Materials* 20(5):332–37. doi: 10.1016/j.conbuildmat.2005.01.027.

Sterling, VA. 2011. *A Manual for Design of Hot-Mix Asphalt with Commentary*.

Swami, B. L., Y. A. Mehta, and S. Bose. 2004. “A Comparison of the Marshall and Superpave Design Procedure for Materials Sourced in India.” *International Journal of Pavement Engineering* 5(3):163–73. doi: 10.1080/10298430412331309115.

Tayebali, Akhtarhusein A., Glen A. Malpass, and N. Paul Khosla. 1998. "Effect of Mineral Filler Type and Amount on Design and Performance of Asphalt Concrete Mixtures." *Transportation Research Record* 117(1609):36–43. doi: 10.3141/1609-05.

Tighe, S., Haas, R., Ningyuan, L. 2000. "Roughness Progression of Asphalt Overlays in the C- SHRP ' s LTPP Study." Pp. 7–10 in *Proceedings of the 2000 CSCE Annual Conference, London,*.

Tighe, S., Haas, R., Ningyuan, L. 2003. "Acceptability of Pavement Roughness on Urban Highways by Driving Public." *Proceedings of the 2000 CSCE Annual Conference, London Pp. 7-10 (2000)* (1860):187–93. doi: 10.3141/1860-21.

Uemura, T., and Y. Nakamori. 1993. "Stabilization Process of Cement-Asphalt Emulsion in Japan." *First World Congress on Emulsion* 4–13.

Visintine, Beth A., Gary R. Hicks, Ding Xin Cheng, Gary E. Elkins, and Jonathan Groeger. 2015. "Factors Affecting the Performance of Pavement Preservation Treatments." *9th International Conference on Managing Pavement Assets* 23.

Wahhab, H. I. Al-abdul, M. N. Fatani, A. S. Noureldin, and A. Bubshait. 1995. "National Study of Asphalt Pavement Rutting in Saudi Arabia." *Transportation Research Record* (1473).

Wang, Hao, Imad L. Al-Qadi, Ahmed F. Faheem, Hussain U. Bahia, Shih Hsien Yang, and Gerald H. Reinke. 2011. "Effect of Mineral Filler Characteristics on Asphalt Mastic and Mixture Rutting Potential." *Transportation Research Record* (2208):33–39. doi: 10.3141/2208-05.

Wang, Kelvin C. P., Qiang Li, Kevin D. Hall, and Robert P. Elliott. 2007. "Experimentation with Gray Theory for Pavement Smoothness Prediction." *Transportation Research Record* (1990):3–13. doi: 10.3141/1990-01.

Wang, Zhenjun, and Aimin Sha. 2010. "Micro Hardness of Interface between Cement Asphalt Emulsion Mastics and Aggregates." *Materials and Structures/Materiaux et Constructions* 43(4):453–61. doi: 10.1617/s11527-009-9502-2.

Watson, Donald, and David Jared. 1998. “Georgia Department of Transportation’s Experience with Microsurfacing.” *Transportation Research Record* (1616):42–46. doi: 10.3141/1616-07.

Willway, T., L. Baldachin, S. Reeves, and M. Harding. 2008. “The Effects of Climate Change on Highway Pavements and How to Minimise Them : Technical Report.” *Department for Transport, Local Transport Strategy and Funding Division, UK* 1–124.

With, Nduction, Pplications By, Yonas B. Dibike, Slavco Velickov, Dimitri Solomatine, and Michael B. Abbott. 2001. “M i s v M : I A.” 15(July):208–16.

Xiao, Yuan. 2009. “Evaluation of Engineering Properties of Hot Mix Asphalt Concrete for the Mechanistic-Empirical Pavement Design.” *Chemical Information and Modeling.*

Zhou, G., Wang, L. 2009. “Analysis of Flexible Pavement Distresses on IRI Model Guoqing Zhou 1 and Linbing Wang 2 1 2.” 150–60.

Zhou, Joseph G. Spinelli and Yu. 2004. “Mapping Quality of Life with Chernoff Faces Joseph G. Spinelli and Yu Zhou.” *Proceedings of Twenty-Fourth ESRI International User Conference* (Figure 1):2–7.

Zhu, Jiqing, Björn Birgisson, and Niki Kringos. 2014. “Polymer Modification of Bitumen: Advances and Challenges.” *European Polymer Journal* 54(1):18–38. doi: 10.1016/j.eurpolymj.2014.02.005.

Zumrawi, Magdi M. E., and Samir A. Sheikh Edrees. 2016. “Comparison of Marshall and Superpave Asphalt Design Methods for Sudan Pavement Mixes.” *International Journal of Scientific and Technical Advancements* 2(1):29–35.